Response to interactive comments on “Global impacts of tropospheric halogens (Cl, Br, I) on oxidants and composition in GEOS-Chem” by T. Sherwen et al.

General response from authors:

We thank anonymous reviewers #1 and #2 for their positive reviews and constructive comments on our paper. We have updated the manuscript following these comments and addressed all points raised. We feel that the reviewers have improved our manuscript and are grateful for their time and contributions.

Two errors in the code have been identified following submission to ACPD (The calculation of cloud surface area and a typographic error in the representation of a bromine and VOC reaction). The conclusions of the paper are unaffected, but the magnitude of the impacts of halogen chemistry has increased slightly. For instance, the reported decrease in tropospheric ozone burden has increased (18.6% instead of ~15 %) and tropospheric OH has also decreased (8.2 % instead of 6.5 %). We have also extended the definition of the chemical lifetime of Cly and Bry to include cloud processes which was not included in the previous version. The numbers and figures throughout the paper have been updated accordingly.

In addition to reviewer’s comments, a few minor updates were made. The formatting of subscripts for chemical species (e.g. Cl_y, HO_x) has been updated. Figures have updated with improved formatting and any repetition of labeling were removed. Finally, a link has been made in the introduction to a companion paper, which considers halogen effects in the preindustrial atmosphere.

Anonymous Referee #1:
Received and published: 3 July 2016

This manuscript presents a comprehensive model study of halogen chemistry; using an updated version of the global model GEOS-Chem, the authors examine the impact of halogens on the composition of the troposphere. It is a very interesting paper and it adds to the growing corpus of studies that try to assess the global impact of halogen chemistry. The manuscript is well written and the material clearly presented and discussed. I recommend publication in Atmos. Chem. Phys., with minor corrections.

We thank reviewer #1 for the positive comments about our manuscript and we respond to the minor corrections raised below.

GENERAL COMMENTS
In the introduction it should be noted that some halogen chemistry actually leads to increased O3 formation, due to increased oxidation of VOC and recycling of NOx. Especially since ClNO2 chemistry is highlighted later in the paper.

This content has been added to the introduction.

A few clarifications about the chemical mechanism are needed. In particular: is nucleation included for IxOy species? Or are the only losses for these species photolysis and heterogeneous uptake? Release of Cl and Br is described as only via uptake of N2O5 (page 4, line 30) which seems to contrast with the description of acid catalysed release described earlier in the same section (page 3, line 31). This (apparent?) contradiction should be clarified.

The manuscript has been updated to improve the clarity of the explanation of which processed are included.

The importance of aqueous-phase chemistry is briefly mentioned in Section 3.4.3 as a possible explanation for the disagreement between modelled and measured chlorine, but is probably an issue for bromine, and maybe iodine, as well. Given that this is likely the main uncertainty in the model (with regard to halogen chemistry) more discussion seems warranted.

A referenced sentence has been added to conclusions to highlight these uncertainties and to direct readers to reviews where this discussion has already happened in depth (Saiz-Lopez et al. 2012b, Simpson et al. 2015) and modeling work that has considered this (Sherwen et al. 2016a, Schmidt et al. 2016)

The section on the impact of halogens on ozone concentration should be expanded. While it is true that halogens generally improve the agreement with ozone, this is not always the case (eg, Mace Head, Mont Cimone, Neumayer in Figure 12, Lindenberg, Marambio in Fig 13). It is also quite clear that the model often fails to reproduce ozone at higher altitudes. These discrepancies should be discussed.

We accept the model does not completely reproduce the observations, but would argue that it does a reasonable job considering the complexities of O_3 sources, chemistry, and transport. There are two sonde sites in Fig. 13 that are now outside the quartiles of the observations. To make the comparison comparably fair to the sonde comparison, the surface plot has been updated to display the 5th to 95th percentile of the observations. Adding these observations highlights that for the majority of sites there is a significant improvement on inclusions of halogens. However, the simulation of ozone clearly degrades at Neumayer and the South pole and a statement has been added to highlight this.

MINOR COMMENTS
It may not be clear to everybody where the measurements were taken. I suggest either a map indicating the location of the sites and of the campaigns or an expansion of Table 3 to include all the measurements used in the paper.

A figures has been added to show locations Ozone measurements and another to show locations of halogen measurements.

Section 4.2: is HO2 increased in the model with halogen chemistry? If so by how much.

As HO_x is mainly consists of HO_2, the numbers are essentially the same as for HO_x and therefore are not included separately. Both HO_x and HO_2 decrease, as seen in that section for HO_x and in Figure 17 for HO_2.

Page 8, Line 2: higher

Updated.

Page 8, Line 12: dominated

Updated.

Page 10, Line 27: suggested

Updated.

Anonymous Referee #2

Received and published: 18 July 2016

This manuscript describes modeling of the global impacts of tropospheric halogens on oxidants (ozone and its photoproducts). The manuscript is well written and expands upon prior modeling work that examined one or two halogens by including all three atmospherically relevant halogens (Cl, Br, and I). The coupling of these species is of interest because cross reactions between the halogens could have significant impacts on the chemistry. The results of the modeling are compared to available observations. The paper nicely summarizes the results of the modeling efforts in figures and tables. The paper is appropriate for ACP and I recommend publication following minor revisions.

We thank reviewer #2 for the positive comments about our manuscript and we respond to the minor corrections raised below.

Minor comments:
On page 3, near the bottom, the photolysis of I2Ox species is discussed. The section is not very clear with regard to "recent work". This phrase seems to refer to work other than the present ACPD paper. If so, please indicate what "recent work" is and where the "unpublished spectrum" is from.

The citation for this is Saiz-Lopez et al. (2014), which has been moved within the sentence to make the link clearer.

On page 6, the discussion of general lifetimes reads well. It might be valuable to add a bit more detail on the relative XOx lifetimes. Specifically, which reaction is the major control on the XOx lifetime would be of interest. The lifetime variation (short for IOx, longer for BrOx, and then very short for ClOx) would also be interesting to be discussed in terms of chemical principles.

The discussion of XO_x lifetime has been expanded in the manuscript as requested by the reviewer. Elsewhere the lifetimes and controls on lifetime of iodine (Sherwen et al. 2016a) and bromine (Parrella et al. 2012, Schmidt et al. 2016) have previously been discussed.

Page 7, line 10, Tropospheric repeats twice int he same sentence.

Updated.

Page 8, line 12, hihjer misspelled

Updated.

Page 8, line 23, "is dominate" needs rewording

Updated.

Page 9, line 14, "at the surface concentrations" maybe "at" is the wrong word?

Updated.

Page 9, line 26, With regard to ozone as a greenhouse gas, it seems like a discussion of the free tropospheric loss of ozone should be put in the context of the altitude range where ozone is greenhouse active.

A sentence has been added to this effect and a link made to the companion paper (Sherwen et al 2016c), which explores impact of tropospheric O3 change in more detail and in terms of climatic implications from preindustrial to present day.

Page 10, line 5, it is interesting to note that coupling of halogens (cross reactions) appear unimportant. In some literature, they point to fast rates of cross reactions, but I think the cross rates differ between measurements / evaluations; could this be discussed more fully.

A sentence has been added to the manuscript to explain the difference between previous studies (in localized regions with high XO concentrations) and the global picture considered here.

Global impacts of tropospheric halogens (Cl, Br, I) on oxidants and composition in GEOS-Chem

T. Sherwen[1], J. A. Schmidt[2], M. J. Evans[1,3], L. J. Carpenter[1], K. Großmann[4,a], S. D. Eastham[5], D. J. Jacob[5], B. Dix[6], T. K. Koenig[6,7], R. Sinreich[6], I. Ortega[6,7], R. Volkamer[6,7], A. Saiz-Lopez[8], C. Prados-Roman[8,b], A. S. Mahajan[9], and C. Ordóñez[10]

[1]Wolfson Atmospheric Chemistry Laboratories (WACL), Department of Chemistry,University of York, York, YO10 5DD, UK
[2]Department of Chemistry, University of Copenhagen, Universitetsparken, DK-2100 Copenhagen O, Denmark
[3]National Centre for Atmospheric Science (NCAS), University of York, York, YO10 5DD, UK
[4]Institute of Environmental Physics, University of Heidelberg, Heidelberg, Germany
[5]School of Engineering and Applied Sciences, Harvard University, Cambridge, MA, USA
[6]Department of Chemistry and Biochemistry, University of Colorado, Boulder, CO 80309-0215, USA
[7]Cooperative Institute for Research in Environmental Sciences, University of Colorado, Boulder, CO 80309-021, USA
[8]Department of Atmospheric Chemistry and Climate, Institute of Physical Chemistry Rocasolano, CSIC, Madrid, 28006, Spain
[9]Indian Institute of Tropical Meteorology, Maharashtra, 411008, India
[10]Dpto. Física de la Tierra II, Facultad de Ciencias Físicas, Universidad Complutense de Madrid, 28040 Madrid, Spain
[a]Now at: Joint Institute For Regional Earth System Science and Engineering (JIFRESSE), University of California Los Angeles, Los Angeles, CA, 90095, USA
[b]Now at: Atmospheric Research and Instrumentation Branch, National Institute for Aerospace Technology (INTA), Madrid, Spain

Correspondence to: Tomás Sherwen (tomas.sherwen@york.ac.uk)

Abstract. We present a simulation of the global present-day composition of the troposphere which includes the chemistry of halogens (Cl, Br, I). Building on previous work within the GEOS-Chem model we include emissions of inorganic iodine from the oceans, anthropogenic and biogenic sources of halogenated gases, gas phase chemistry, and a parameterised approach to heterogeneous halogen chemistry. Consistent with ~~Schmidt et al. (2016)~~ Schmidt et al. (2016) we do not include sea-salt debromination. Observations of halogen radicals (BrO, IO) are sparse but the model has some skill in reproducing these. Modelled IO shows both high and low biases ~~in~~ when compared to different datasets, BrO concentrations though appear to be modelled low. Comparisons to the very sparse observations dataset of reactive Cl species suggests the model represents a lower limit ~~on impacts due to likely~~ of the impacts of these species, likely due to underestimates in emissions and therefore burdens. Inclusion of Cl, Br, and I results in a general improvement in simulation of ozone (O_3) concentrations, except in polar regions where the model now underestimates O_3 concentrations. Halogen chemistry reduces the global tropospheric O_3 burden by ~~$\sim$15~~ 18.6 %, with the O_3 lifetime reducing from 26 days to 22 days. Global mean OH concentrations of ~~1.34~~ 1.28 x10^6 molecules cm^{-3} are ~~4.5~~ 8.2 % lower than in a simulation without halogens, leading to an increase in the CH_4 lifetime (~~6.5~~ 10.8 %) due to OH oxidation from ~~7.48 years to 7.96~~ 7.47 years to 8.28 years. Oxidation of CH_4 by Cl is small ($\sim$~~1~~ 2 %) but Cl oxidation of other VOCs (ethane, acetone, and propane) can be significant ($\sim$~~9-18~~ 15-27 %). Oxidation of VOCs by Br is smaller, representing ~~2.1~~3.9 %of the loss of acetaldehyde and ~~0.6~~0.9 % of the loss of formaldehyde.

1 Introduction

To address problems such as air quality degradation and climate change, we need to understand the composition of the troposphere and its oxidative capacity. A complicated relationship exists between key chemical families and species such as ozone ($\mathrm{O_3}$), $\mathrm{HO_x}$ ($\mathrm{HO_2}$+OH), $\mathrm{NO_x}$ ($\mathrm{NO_2}$+NO) and organic compounds which include carbon monoxide (CO), methane ($\mathrm{CH_4}$), hydrocarbons and oxygenated volatile organic compounds (VOCs) (~~see for example Monks et al. (2015)~~for example see Monks et al. 2015). The most important ~~of tropospheric oxidants~~ tropospheric oxidant is OH, which is itself produced indirectly through photolysis of $\mathrm{O_3}$. Oxidants control the concentrations of key climate and air-quality gases and aerosols (including $\mathrm{O_3}$, methane, sulfate aerosol, and secondary organic aerosols) (Monks et al., 2009; Prather et al., 2012; Unger et al., 2006). $\mathrm{O_3}$ itself is not directly emitted, and ~~it's~~ its tropospheric burden is controlled by its sources through chemical ~~productions from~~ production from $\mathrm{NO_x}$ and organic compounds, transport from the stratosphere, and loss via deposition and chemical reactions (Monks et al., 2015).

Halogens (Cl, Br, I) are known to destroy $\mathrm{O_3}$ through catalytic cycles, such as that shown in reactions 1-3 (Chameides and Davis, 1980). Tropospheric halogens have also been shown to change OH concentrations (Bloss et al., 2005) and perturb OH to $\mathrm{HO_2}$ ratios towards OH (Chameides and Davis, 1980). Halogens perturb the NO to $\mathrm{NO_2}$ ratio and reduce $\mathrm{NO_x}$ concentrations by hydrolysis of $\mathrm{XNO_3}$. These perturbations also indirectly decrease $\mathrm{O_3}$ formation (von Glasow et al., 2004). Halogens directly oxidise organics species, with Cl radical reactions proceeding the fastest (Atkinson et al., 2006; Sander et al., 2011). ~~They~~ This can cause significant $\mathrm{O_3}$ formation through increased $\mathrm{RO_2}$ concentrations (Knipping and Dabdub, 2003), notably in regions with elevated $\mathrm{ClNO_2}$ (Sarwar et al., 2014). Halogens also play an important role in determining the chemistry of mercury (Holmes et al., 2009; Parrella et al., 2012; Wang et al., 2015; Coburn et al., 2016). The literature on tropospheric halogens has been the topic of several recent reviews, which cover the background in more detail (Simpson et al., 2015; Saiz-Lopez et al., 2012b). However, many uncertainties still exist, notably with heterogeneous halogen chemistry ~~(Abbatt et al., 2012)~~(Abbatt et al., 2012; Simpson et al., 2015), and gas-phase iodine chemistry (Saiz-Lopez et al., 2014; Sommariva and von Glasow, 2012).

$$\mathrm{O_3} + \cancel{X}\mathrm{X} \rightarrow \mathrm{XO} + \mathrm{O_2} \tag{1}$$

$$\mathrm{HO_2} + \mathrm{XO} \rightarrow \mathrm{HOX} + \mathrm{O_2} \tag{2}$$

$$\mathrm{HOX} + h\nu \rightarrow \mathrm{OH} + \mathrm{X} \tag{3}$$

~~Net: $\mathrm{HO_2} + \mathrm{O_3} \rightarrow 2\mathrm{O_2} + \mathrm{OH}$~~

$$Net: \mathrm{HO_2} + \mathrm{O_3} \rightarrow 2\mathrm{O_2} + \mathrm{OH} \tag{4}$$

Tropospheric halogen chemistry has been studied in box model studies (see Simpson et al. 2015 and citations within) and more recently in global models (e.g. ~~Parrella et al. 2012; Saiz-Lopez et al. 2012a, 2014; Schmidt et al. 2016; **?**~~Parrella et al. 2012; Saiz-Lo
Modelling has sought to quantify emissions budgets and evaluate these on a global scale (Bell et al., 2002; Ziska et al.,

2013; Hossaini et al., 2013; Ordóñez et al., 2012). Global studies have considered impacts of halogens in the troposphere ~~(Parrella et al., 2012; Saiz-Lopez et al., 2012a, 2014; Schmidt et al., 2016; ?)~~ (Parrella et al., 2012; Saiz-Lopez et al., 2012a, 2014; Schmi reported reductions in the tropospheric O_3 burden by up to ∼15 %. However, this field of research is quickly evolving, with new halogen sources such as inorganic ocean iodine (Carpenter et al., 2013; MacDonald et al., 2014) and $ClNO_2$ produced from N_2O_5 hydrolysis on sea-salt (Roberts et al., 2009; Bertram and Thornton, 2009; Sarwar et al., 2014) now appearing to be globally important.

Previous studies of halogen chemistry within the GEOS-Chem (www.geos-chem.org) model have focussed on either bromine or iodine chemistry. Parrella et al. (2012) presented a bromine scheme and its effects on oxidants in the past and present atmosphere. Eastham et al. (2014) presented the Unified tropospheric-stratospheric Chemistry eXtension (UCX), which added a stratospheric bromine and chlorine scheme. This chlorine scheme was then employed in the troposphere with an updated heterogeneous bromine and chlorine scheme by Schmidt et al. (2016). An iodine scheme was employed in the troposphere to consider present day impacts of iodine on oxidants ~~(?)~~(Sherwen et al., 2016a), which used the representation of bromine chemistry from Parrella et al. (2012). Up to this point, ~~however,~~ the coupling of chlorine, bromine, and iodine in the GEOS-Chem model and its subsequent impact on the simulated present-day composition of the atmosphere ~~has~~ have not been described.

Here we present such a coupled halogen ~~scheme within~~ model built within the GEOS-Chem ~~and consider~~ framework and consider the present-day tropospheric impacts of halogens. ~~This simulation~~ The model presented here includes recent updates to chlorine (Eastham et al., 2014; Schmidt et al., 2016), bromine (Parrella et al., 2012; Schmidt et al., 2016), and iodine ~~(?)~~ (Sherwen et al., 2016a) chemistry with further updates and additions described in Section 2. In Section 3 we describe the modelled distribution of inorganic halogens (Section 3.1-3.3), and compare with observations (Section 3.4). We then outline the impact on oxidants (Section 4.1-4.2), organic compounds (Section 4.3), and other species (Section 4.4).

2 Model Description

This work uses the GEOS-Chem chemical transport model (www.geos-chem.org, version 10) run at 4°x5° spatial resolution. The model is forced by assimilated meteorological and surface fields from NASA's Global Modelling and Assimilation Office (GEOS-5) . The model chemistry scheme includes ~~, ,~~ O_x, HO_x, NO_x, and VOC chemistry as described in Mao et al. (2013). Dynamic and chemical time-step are 30 and 60 minutes, respectively. Stratospheric chemistry is modelled using a linearised mechanism as described by Murray et al. (2012).

We update the standard model chemistry to give a representation of chlorine, bromine and iodine chemistry. We describe this version of the model as "Cl+Br+I" in this paper. It is based on the iodine chemistry described in ~~?~~ Sherwen et al. (2016a) with updates to the bromine and chlorine scheme described by Schmidt et al. (2016) and Eastham et al. (2014). We have made a range of updates beyond these. Updated or new reactions not included in ~~?~~Sherwen et al. (2016a), Schmidt et al. (2016), or Eastham et al. (2014) are given in Table 1 with a full description of the halogen chemistry scheme used given in Appendix Tables 6-9.

For the photolysis of I_2O_X (X=2,3,4) we have adopted the absorption cross-sections reported by Gómez Martín et al. (2005) and Spietz et al. (2005) and used the I_2O_2 cross-section for I_2O_4. A quantum yield of unity was assumed for all I_2O_X species. It is noted that recent work has used an unpublished spectrum for I_2O_4 that is much lower ~~that~~ than that of I_2O_3 ~~Saiz-Lopez et al. (2014)~~(Saiz-Lopez et al., 2014), but this is not expected to have a large effect on conclusions presented here.

The parameterisation for oceanic iodide concentration was changed from Chance et al. (2014), as used in Sherwen et al. (2016a), to MacDonald et al. (2014) as the latter resulted in an improved comparison with observations (see Section 7.5 of ~~?~~Sherwen et al. 2016a).

The product of acid catalysed di-halogen release following I^+ (HOI, INO_2, INO_3) uptake was updated from I_2 as ~~?~~ in Sherwen et al. (2016a) to yield IBr and ICl following McFiggans et al. (2002). Acidity is calculated online through titration of sea salt aerosol by uptake of ~~sulfate~~ sulfur dioxide (SO_2), nitric acid (HNO_3) and sulfuric acid (H_2SO_4) as described by Alexander (2005). Re-release of IX (X=Cl,Br) is only permitted to proceed if the sea salt is acidic (Alexander, 2005). Thus aerosol cycling of IX in the model is not a net source of I_y (and may be a net sink on non-acid aerosol) but alters the speciation ~~(?)~~(Sherwen et al., 2016a). The ratio between IBr and ICl was set to be 0.15:0.85 (IBr:ICl), instead of the 0.5:0.5 used previously (Saiz-Lopez et al., 2014; McFiggans et al., 2000). A ratio of 0.5:0.5 gives a large overestimate of BrO with respect to the observations used in Section 3.4.2 (Read et al., 2008; Volkamer et al., 2015). We attributed this reduction to the de-bromination of sea-salt which we do not consider here, and the potential for the model to over estimate the ~~BrOx~~ BrO_x lifetime. This is discussed further in the next section but future laboratory and field studies of these heterogenous process are needed to help constrain these parameters.

Iodine on aerosol is represented in the model with separate tracers based on the aerosol on which irreversible uptake occurs (see Table 8). We include ~~3~~ three iodine aerosol tracers to represent iodine on accumulation and coarse mode sea-salt and on sulfate aerosol. The physical properties of the iodine aerosol tracers are assumed to be the same as its parent aerosol as previously described for sulfate (Alexander et al., 2012) and sea-salt aerosol (Jaeglé et al., 2011). As in Sherwen et al. (2016a), no nucleation of iodine species is considered in this work, with only photolytic and heterogeneous loss being treated.

We have added to the chlorine chemistry scheme described by Eastham et al. (2014) to include more tropospheric relevant reactions based on the JPL 10-6 compilation (Sander et al., 2011) and IUPAC (Atkinson et al., 2006). The heterogenous reaction of N_2O_5 on aerosols was updated to yield products of $ClNO_2$ and HNO_3 (Bertram and Thornton, 2009; Roberts et al., 2009) on sea salt, and $2HNO_3$ on other aerosol types. Reaction probabilities are unchanged (Evans and Jacob, 2005).

Deposition and photolysis of ~~inter-halogen~~ di-halogen species (ICl, BrCl, IBr) and the reaction between ClO and IO were also included (Sander et al., 2011).

3 Model results

We run the model for two years (1/1/2004 to 1/1/2006), discarding the first year as a “spin-up” period and using the second year (2005) for analysis. Non-halogen emissions are described in ~~?~~Sherwen et al. (2016a). A reference simulation without any halogens (“NOHAL”) was also performed. Where comparisons with observations are shown, the model is run for the appropriate year with a 3 months “spin-up” before the observational dates, unless explicitly stated otherwise. The appropriate month from the 2005 simulation is used as the initialisation for these observational comparisons to account for inter-annual variations. The model is sampled at the nearest timestamp and grid box. The model only calculates chemistry in the troposphere. To avoid confusion we do not show results above the tropopause (lapse rate of temperature falls below 2 K/km).

3.1 Emissions

The emissions fluxes of chlorine, bromine, and iodine species are shown in Figure 1 with global totals in Table 2. We do not consider the Cl and Br contained within sea-salt as emitted in our simulation, following Schmidt et al. (2016) until a chemical process liberates them into the gas-phase. These liberation processes are the uptake of N_2O_5 on sea-salt and uptake of I^+ species on sea-salt. We do not include explicit sea-salt de-bromination for reasons described in ~~Schmidt et al. (2016)~~Schmidt et al. (2016).

The organic iodine (CH_3I, CH_2I_2, CH_2ICl, CH_2IBr) emissions are from Ordóñez et al. (2012) as described in ~~?~~Sherwen et al. (2016a). Inorganic iodine emissions (HOI, I_2) (Carpenter et al., 2013; MacDonald et al., 2014) are ~~28~~ 30 % lower here than reported by ~~?~~Sherwen et al. (2016a), due to use of the MacDonald et al. (2014) parameterisation for ocean surface iodide rather than that of Chance et al. (2014). Heterogeneous iodine aerosol chemistry (Section 2 and Appendix Section B1) does not lead to a net release of iodine, instead just recycling it from less active forms (INO_2, INO_3, HOI) into more active forms (ICl/IBr).

The organic bromine (CH_3Br, $CHBr_3$, CH_2Br_2) emissions have been reported previously (Parrella et al., 2012; Schmidt et al., 2016) and our simulation is consistent with this work. A further source of 0.031 Tg Br yr^{-1} (~~3.4~~ 3.5 % of total) is included here from CH_2IBr photolysis. The heterogeneous cycling for Br_y (defined in footnote below[1]) has been updated here from Schmidt et al. (2016), as described in Section 2/Appendix B1. An additional Br_y source not considered by Schmidt et al. (2016) is iodine activated IBr release from sea salt, which amounts to ~~0.31~~ 0.30 Tg Br yr^{-1} and the majority (67 %) of this is tropical (22°N-22°S). ~~With all these updates, the tropospheric mean daytime (07:00-19:00) BrO concentration is 1.1 pmol mol^{-1} (0.64 pmol mol^{-1} 24 hr average), which is 13 % higher than reported in Schmidt et al. (2016).~~

The organic chlorine emission (CH_3Cl, $CHCl_3$, CH_2Cl_2) for this simulation (Table 2) has been described previously Schmidt et al. (2016) and set using fixed surface concentrations. An additional source of 0.046 Tg Cl yr^{-1}(~~0.94~~ 0.96 % of total) is present from CH_2ICl photolysis ~~(?)~~(Sherwen et al., 2016a). $ClNO_2$ production from the heterogeneous uptake of N_2O_5 provides a source of 0.66 Tg Cl yr^{-1} (14 % of total) with the vast majority (95 %) being in the northern hemisphere, with strongest sources in coastal regions north of 20^oN. For June we calculate a global source of 21 Gg Cl $month^{-1}$ which is substantially less than the 62 Gg Cl $month^{-1}$ (Pers. com. Sarwar Golam 2016) calculated in a previous study (Sarwar et al., 2014). The difference in N_2O_5 concentrations due to differences in model resolution ~~probably~~ may contributes to this. Uptake of HOI, INO_2 and INO_3 to sea-salt aerosol leads to the emission of ICl, giving an additional source of ~~0.78~~ 0.76 Tg Cl yr^{-1} (~~17.6~~ 15.7 % of total) mostly (67 %) in tropical (22°N-22°S) locations.

---

[1] Here X_y (X=Cl,Br,I) is the sum of gas-phase inorganic species of a given halogen in units of that halogen . I_y=$2I_2 + HOI + IO + OIO + HI + INO + INO_2 + INO_3 + 2I_2O_2 + 2I_2O_3 + 2I_2O_4$; Br_y=Br+2Br_2+HOBr+BrO+HBr+$BrNO_2$+$BrNO_3$+IBr+BrCl; and Cl_y=Cl+2Cl_2+HOCl+ClO+HCl+$ClNO_2$+$ClNO_3$+ICl+BrCl+ClOO+OClO+2Cl_2O_2

Most of the emissions of Br and I species in our simulation occur in the tropics. It is notable that the chlorine emissions are more widely distributed ~~.~~ (Fig. 1). This is as a result of longer lifetimes of chlorine precursor gases which moves their destruction further from their emissions and that the $ClNO_2$ source is primarily in the northern extra tropics.

3.2 Deposition of halogens

Figure 2 shows the global annual integrated wet and dry deposition of inorganic X_y (X=Cl, Br,I). Much of the deposition of the halogens occurs over the oceans (~~69 %, 83~~ 70 %, 73 %, and 90 % for ~~, and~~ Cl_y, Br_y and I_y respectively). It is high over regions of significant tropical precipitation (~~ITCZ~~Intertropical Convergence Zone, Maritime continents, Indian Ocean) and much lower at the poles reflecting lower precipitation and emissions.

We find that the the major Cl_y depositional sink is HCl (~~85~~ 94 %), with HOCl contributing ~~11~~ 5.1 % and $ClNO_3$ ~~3.2~~ 1.1 %. The Br_y sink is split between HBr, HOBr and $BrNO_3$ with fractional contributions of ~~38~~33, 30 and ~~24~~ 28 % respectively. The major I_y sink is HOI deposition which represents 59 % of the depositional flux. The two next largest sinks are deposition of INO_3 and iodine aerosol (22 % and 15 %).

3.3 Halogen species concentrations

Figure 3 shows the surface and zonal concentration of annual mean ~~, ,~~ I_y, Br_y, Cl_y, with Figure 4 showing the same for IO, BrO and Cl, key halogen compounds in the atmosphere. Figure 5 ~~showing~~ shows the global molecule weighted mean vertical profile of the halogen speciation.

Inorganic iodine concentrations are highest in the tropical marine boundary layer consistent with their dominant ~~emissions~~ emission regions. The highest concentrations are calculated in the coastal tropical regions, where enhanced O_3 concentrations from industrial areas flow over high predicted oceanic iodide concentrations and lead to increased oceanic inorganic iodine emissions. Within the vertical there is an average of ~0.5-1 pmol mol^{-1} of I_y consistent with previous model studies ~~(Saiz-Lopez et al., 2014; ?)~~(Saiz-Lopez et al., 2014; Sherwen et al., 2016a). The lowest concentrations of I_y are seen just above the marine boundary layer where I_y loss via wet deposition is most favourable due to partitioning towards water soluble HOI. At higher altitudes, lower temperature and high photolysis rates push the I_y speciation to less water soluble compounds (IO, INO_3) and hence the I_y lifetime is longer. IO concentrations (Figure 4) follow ~~the concentrations of I_y with high concentrations~~ those of I_y, with high values in the tropical marine boundary layer. ~~The IO concentration~~ IO increases into the upper troposphere reflecting a partitioning of ~~I_y~~ I_y in this region towards IO (and ~~$IONO_2$~~INO_3) and away from HOI. The global mean tropospheric lifetimes of ~~and are 2.3~~ I_y and IO_x (IO+I) are 2.2 days and 1.3 minutes, respectively. IO_x loss proceeds predominately via reaction of IO with HO_2 (78 %), with smaller losses via IO+BrO (7.9 %) and IO+NO_2 (7.4 %).

Total reactive bromine is more equally spread through the atmosphere than iodine. This reflects the longer lifetime of source species with respect to photolysis which gives a more significant source higher in the atmosphere. The highest concentrations are still found in the tropics. Unlike ~~,~~ I_y, Br_y increases significantly with altitude, with $BrNO_3$ and HOBr being the two most dominant species. BrO concentrations (Figure 4) follows ~~the concentration~~ those of inorganic bromine. In the boundary layer the highest concentrations are found in the ~~tropical marine boundary layer concentrations are in the tropical marine~~

~~boundary~~tropics. BrO and IO do not strongly correlate in the tropical marine boundary layer reflecting their differing sources. BrO concentrations increase towards the upper troposphere associated with the increase in total ~~Br_y~~Br_y. The global annual average (molecule weighted) tropospheric BrO mixing ratio in our simulation is ~~0.64~~ 0.49 pmol mol^{-1} (~~Bry~~Br_y=~~4.5~~ 3.25 pmol mol^{-1}). When previous implementations (Parrella et al., 2012; Schmidt et al., 2016) are run for the same year and model version as this work (GEOS-Chem v10), the modelled BrO concentrations are found to be ~~12 % lower than Schmidt et al. (2016) , but 17~~ 11 % higher than Schmidt et al. (2016) and 33 % higher than Parrella et al. (2012). We calculate ~~a tropospheric lifetime of of 17 days and a lifetime of 15 minutes .~~ tropospheric lifetimes of 18 days for Br_y and 8.1 minutes for BrO_x (BrO+Br). Similarly to IO_x, BrO_x loss proceeds predominately via reaction of BrO with HO_2 (71 %) and NO_2 (18 %).

Total inorganic chlorine has a highly non-uniform distribution at the surface reflecting the ~~dominance of the~~ $ClNO_2$ source from N_2O_5 uptake on sea-salt. At the surface $ClNO_2$, HCl, BrCl and HOCl represent around 25 % of the total Cl_y each. Away from the surface the $ClNO_2$ concentrations drop off rapidly due to the short lifetime of sea salt. HCl concentrations increase significantly into the middle and upper troposphere and ~~dominate the~~ dominates the Cl_y distribution. This suggests that stratospheric chlorine freed from CFCs and organic chlorine strongly contributes to free tropospheric concentrations of ~~. However modelled is likely a lower limit on the concentrations in the uppermost troposphere (Froidevaux et al., 2008).~~ Cl_y. Cl mixing ratios are very low ($\sim$0.075 fmol mol^{-1} or $\sim$2000 cm^{-3}) in the marine boundary layer. Reactive Cl (~~ie not HCl) drop~~ i.e. Cl_y excluding HCl) drops from the surface to around ~~10km~~ 10 km where it then increases again towards ~~to~~ the stratosphere. Cl shows a wider distrbution than IO and BrO reflecting the source wider distribution of ~~Cl_y~~Cl_y. We calculate ~~a tropospheric lifetime of of 15 days , a lifetime of 2 seconds, and a~~ tropospheric lifetimes of 5 days for Cl_y and 3.8 hours for ClO_x (Cl+ClO+ClOO+2Cl_2O_2). A global tropospheric mean inorganic chlorine (Cl_y) concentration of ~~70~~ 71 pmol mol^{-1} in seen in our simulation. ClO_x loss proceeds through reaction of Cl with CH_4 (27 %), ClO reaction with HO_2 (21 %), and ClO reaction with NO_2 (10 %). The longer XO_x lifetime of ClO_x, compared to BrO_x and IO_x, can be explain through the importance of the relatively slow dominant loss route through reaction with CH_4.

The chemistry of halogens and sea-salt is highly uncertain (Simpson et al., 2015; Saiz-Lopez et al., 2012b; Abbatt et al., 2012). Estimates for sea-salt de-bromination range from 0.51 Tg yr^{-1} (Parrella et al. 2012 implemented in GEOS-Chem v10 and v9-2) to 2.9 Tg yr^{-1} (Fernandez et al., 2014). ~~Some studies have also~~ Other studies have not included sea-salt de-bromination (von Glasow et al., 2004; Schmidt et al., 2016) as we do not in this work. Schmidt et al. (2016) found that including debromination of sea-salt aerosol improved the simulation of the BrO and HOBr observations reported during the “Combined Airborne Studies in the Tropics” (CAST, Harris et al. 2016) campaign, but resulted in over-prediction of the “Tropical Ocean tRoposphere Exchange of Reactive halogen and Oxygenated VOC” campaign (TORERO; Volkamer et al. 2015; Wang et al. 2015) BrO observations. Arguably this work ~~therefore~~ provides a lower estimate of bromine and chlorine sources in the troposphere, with further work needed to understand the Br_y budget.

The difference in lifetimes of inorganic halogen families (X_y) can be understood from the change in loss routes, which shifts HX to HOX following the order of group 17 in the periodic table (Cl→Br→I).

Figure 6 shows column integrated BrO and IO, which are the major halogen species for which we have observations (see Section 3.4). Tropospheric ClO concentrations ~~within the troposphere~~ are small (see Figure 5) and are therefore not shown in Fig 6. Tropical maxima are seen for both BrO and IO, with BrO concentrations decreasing towards the equator. For IO a localised maximum is seen in the Arabian Sea. The IO maximum in Antarctica reported from satellite retrievals (Schönhardt et al., 2008) is not reproduced in our model potentially reflecting the lack of polar specific processes in the model.

3.4 Comparison with halogen observations

The observational dataset of tropospheric halogen compounds is sparse. Previous studies that this work is based on have shown comparisons for the oceanic precursors for chlorine (Eastham et al., 2014; Schmidt et al., 2016), bromine (Parrella et al., 2012; Schmidt et al., 2016), and iodine ~~(Bell et al., 2002; ?; Ordóñez et al., 2012)~~(Bell et al., 2002; Sherwen et al., 2016a; Ordóñez et al., 2012). The model performance in simulating these compounds has not changed since these previous publications so we focus here on the available observations of concentrations of IO, BrO, and some inorganic chlorine species ($ClNO_3$, HCl and Cl_2).

3.4.1 Iodine monoxide (IO)

A comparison of IO to a suite of recent remote surface observations is shown in Fig 7. The model shows an overall negative bias of ~~21~~ 23 %. This compares with the 90 % positive bias previously reported in ~~(?)~~(Sherwen et al., 2016a). This reduction in bias is due to the use of the MacDonald et al. (2014) iodide parameterisation over that of Chance et al. (2014) which has reduced the inorganic emission of iodine, along with the restriction of iodine recycling to acidic aerosol.

Figure 8 shows a comparison between modelled IO with altitude against observations in the eastern Pacific (Volkamer et al., 2015; Wang et al., 2015). In general, the model agreement with observations is good. There is an average bias of +~~40~~ 37 % in the free troposphere (350 hPa<p<900 hPa), which increases to +~~58~~ 54 % in the upper troposphere (350 hPa>p>tropopause). As with the surface measurements, the model bias when comparing to IO observations (Volkamer et al., 2015; Wang et al., 2015) in the free and upper troposphere is decreased from previously reported positive biases of 73 % and 96 %, respectively ~~(?)~~(Sherwen et al., 2016a).

3.4.2 Bromine monoxide (BrO)

Comparisons of BrO against seasonal satellite tropospheric BrO observations from GOME-2 (Theys et al., 2011) are shown in Figure 9. As shown previously (Parrella et al., 2012; Schmidt et al., 2016) the model has some skill in capturing both the latitudinal and monthly variations in tropospheric BrO columns. However it underestimates the column BrO in the lower southern latitudes (60°S-90°S), and to a smaller degree also in lower northern latitudes (60°N-90°N) which may reflect the lack of bromine from polar (blown snow, frost flowers etc.) sources and sea-salt de-bromination processes.

As shown in Fig. 10, comparisons between the model and observations of BrO made at Cape Verde (Read et al., 2008; Mahajan et al., 201 a negative bias of 22 %. We attribute this to the high local sea-salt loadings at this site (Carpenter et al., 2010), which is situated in the surf zone. This may locally increase the BrO concentrations. The model concentrations of $\sim$1 pmol mol^{-1} are however consistent with other ship borne observations made in the region (Leser et al., 2003).

Figure 11 shows modelled vertical BrO concentrations against observations in the eastern Pacific (Volkamer et al., 2015; Wang et al., 2015). We find a reasonable agreement within the free troposphere (350 hPa$<p<$900 hPa) in both the tropics and subtropics, with an average ~~negative bias of 15 and 34~~ bias of -3.5 and +4.2 %, respectively. A similar ~~comparisons~~ comparison is seen in the upper troposphere (350 hPa$>p>$tropopause) ~~show similar~~ with negative biases for the tropics and subtropics, of ~~20 and 24 % ,~~ 6.3 and 9.7 % respectively. The decrease in agreement seen in the TORERO comparison (Fig. 11) relative to that previously presented in Schmidt et al. (2016) is due to reduced BrCl and BrO production from slower cloud multiphase chemistry (see ~~Sections~~ appendix sections B1-B3). We model ~~hihjer~~ higher BrO concentrations in the tropical marine boundary layer which are above those observed (Volkamer et al., 2015). Our modelled concentrations are lower than those reported previously (Miyazaki et al., 2016; Long et al., 2014; Pszenny et al., 2004; Keene et al., 2009).

~~As shown in Fig. 10, comparisons between the model and observations of BrO made at Cape Verde (Read et al., 2008; Mahajan et al., 201 a negative bias of 50 %. We attribute this to the high local sea-salt loadings at this site (Carpenter et al., 2010), which is situated in the surf zone. This may locally increase the BrO concentrations. The model concentrations of $\sim$1 pmol mol^{-1} are however consistent with other ship borne observations made in the region (Leser et al., 2003).~~

Our model does not include sea-salt de-bromination and yet calculated roughly the correct concentrations of BrO. Inclusion of sea-salt de-bromination leads to excessively high BrO concentration in the model (Schmidt et al., 2016). Sea-salt de-bromination is well ~~observed~~established, thus the success of the model despite the lack of inclusion of this process ~~suggest~~ suggests model failure in other areas. The BrO_x lifetime may be too long. ~~This is dominate~~ The conversion of BrO_x to HBr is dominated by the reaction between Br and organics to produce HBr. Oceanic sources of VOCs such as acetaldehyde have been proposed (Millet et al., 2010; Volkamer et al., 2015) and a significant increase in the concentration of these species would lead to lower BrO_x concentrations. Alternatively, a reduction in the efficiency of cycling of Br_y through aerosol would also have a similar effect. The aerosol phase chemistry is complex and the parameterisations used here may be too simple or fail to capture key processes (e.g. pH, organics). These all require further study in order to help reconcile models with the rapidly growing body of observation of both gas and aerosol phase bromine in the atmosphere~~with models~~.

3.4.3 Nitryl chloride ($ClNO_2$), hydrochloric acid (HCl), hypochlorous acid (HOCl) and molecular chlorine (Cl_2)

Very few constraints on the concentration of tropospheric chlorine species are available~~.~~

~~An~~ , however an increasing number of $ClNO_2$ observations are ~~available (Table 3)~~becoming available. Table 3 shows a comparison between the model an available observations. We find that the model does reasonably well in coastal regions, but does not reproduce observations in continental regions or regions with very high ~~.~~ NO_x.

Lawler et al. (2011) reports measurements of HOCl and Cl_2 at Cape Verde for a week in June 2009. For the first 4 days of the campaign, HOCl concentrations were higher and peaked at $\sim$100 pmol mol^{-1} with Cl_2 concentrations peaking at $\sim$30 pmol mol^{-1}. For the later days, HOCl concentrations dropped to around 20 pmol mol^{-1} and Cl_2 concentrations to $\sim$0-10 pmol mol^{-1}. We calculate much lower concentrations of Cl_2 (~~-~~$\sim$1x10^{-3} pmol mol^{-1}) and slightly lower HOCl (~~-~~$\sim$10 pmol mol^{-1})~~throughout the same days of the year in our analysis year (2005)~~. This is similar to findings of Long et al. (2014), who also found better comparisons with the ~~cleaner~~ later period of observations. Similar to the comparison with observed $ClNO_2$, our simulation underestimates HOCl and Cl_2.

The model does not include many sources of reactive chlorine. The failure to reproduce continental $ClNO_2$ is likely due to a lack of representation of sources such as salt plains, direct emission from power station and swimming pools, and HCl acid displacement. The inability to reproduce the very high $ClNO_2$ found in some cities (Pasadena) and industrialised regions(Texas) may be due to the coarse resolution of the model compared to the spatial inhomogeneity of these observations. The failure to reproduce the Cape Verde observations may be due to the very simple aerosol phase chlorine chemistry included in the model. Overall we suggest that the model provides a lower limit estimate of the chlorine emissions and therefore burdens within the troposphere, but constraints ~~at the~~ of surface concentrations are limited and vertical profiles are not available. Further laboratory work to better define aerosol processes and observations will be necessary to investigate the role of chlorine on tropospheric chemistry.

4 Impact of halogens

We now investigate the impact of the halogen chemistry on the composition of the troposphere. We start with O_3 and OH and then move onto other components of the troposphere.

4.1 Ozone (O_3)

Figure 12 shows changes in column, surface and zonal O_3 both in absolute and fractional terms between simulations with and without halogen emissions (“Cl+Br+I” vs “NOHAL”). Globally the mass-weighted, annual-average mixing ratio is reduced by ~~7.4~~ 9.4 pmol mol^{-1} ~~(14.6%)~~ with the inclusion of halogens and tropospheric burden decreases by 18.6 % (“Cl+Br+I”-“NOHAL”)/ “NOHAL”*100). A much larger percentage decrease of ~~25.0 % (7.2~~ 30.0 % (8.5 pmol mol^{-1}) is seen over the ocean surface. Large percentage losses are seen in the oceanic southern hemisphere as reported previously ~~(Long et al., 2014; Schmidt et al.~~ the significant ocean-atmosphere exchange in this regions. The majority (65 %) of the change in O_3 mass due to halogens occurs in the free troposphere (350 hPa<p<900 hPa). The location of O_3 concentration decreases is noteworthy as the climate effect of O_3 is highly spatial and vertically variable (Myhre et al., 2013). Effects of halogens on tropospheric O_3 from pre-industrial to present-day are explored elsewhere (Sherwen et al., 2016b).

Comparisons of the model and observed surface and sonde O_3 concentrations are given in Figures 13 and 14. In the tropics the fidelity of the simulation improves with the inclusion of halogens~~(Schmidt et al., 2016; ?)~~, as shown previously by Schmidt et al. (2016) and Sherwen et al. (2016a). Sonde and surface comparisons north of ∼50°N and south of ∼60°S however show that the model now underestimates O_3. This is clearly the case for Neumayer and the South Pole (Fig. 13).

The global odd oxygen budget (O_x, as defined in the ~~footnote below~~Footnote below[2]) in the troposphere with (“Cl+Br+I”) and without halogens (“NOHAL”) is shown in Table 4. The O_x loss through chlorine, bromine, and iodine represents ~~0.46, 5.8 and 12~~ 0.8, 8.4 and 12.2 % of the total O_x loss respectively, thus halogens constitute ~~18.2~~ 21.4 % of the overall O_3 loss. The sum of halogen driven ~~loss is 900 Tg~~ O_x loss is 1036 Tg O_x yr^{-1}, which is similar to the magnitude of loss via reaction of O_3 with HO_2 of ∼1100 Tg O_x yr^{-1} (~~23~~ 21.9 % of total). Halogen cross-over reactions (BrO+IO, BrO+ClO, IO+ClO) contribute little to the overall O_3 loss. This number compares with ∼930 Tg O_x yr^{-1} reported in GEOS-Chem previously by ~~?~~Sherwen et al. (2016a). Saiz-Lopez et al. (2014) found that, between 50°~~S-50~~S and 50°N and the over ocean only, halogens are responsible for the loss of 640 Tg O_x yr^{-1}. We find a ~~comparable value of 670~~ higher value of 827 O_x yr^{-1} with our model.

~~The majority of the halogen driven loss (58.1 %) occurs in the free troposphere (350 hPa<p<900 hPa). Halogens represent 34.9 and 31.0 % of~~ Halogens represent 39.6 and 33.0 % of O_x loss in the upper troposphere (350 hPa>p>tropopause) and marine boundary layer (900 hPa<p) respectively as shown in Figure 15. The marine boundary layer O_x loss attributable to halogens is ~~equal~~ comparable to the 31 % reported by Prados-Roman et al. (2015a) previously, and it is ~~slightly higher than that~~ higher than the 26 % reported solely for iodine ~~of 26 % (?).~~(Sherwen et al., 2016a). The inter-reaction of halogen monoxide species is found to less important here than previous studies (e.g. Read et al. 2008) which has been basis in locations of higher halogen monoxide concentrations. Inclusion of sea-salt, which would increase BrO in the marine boundary layer would increase the magnitude of contribution of theses routes to total halogen driven O_x loss.

Although the partitioning ~~between the~~ of the O_x loss processes is significantly different between the simulations with ~~halogens and without~~ and without halogens (Table 4), the overall annual O_x loss only increases by ~~2.2 % (4933~~ ∼0.25 % (4841 vs 4829 Tg yr^{-1}). The O_x production term decreases by ~~1.0~~ 3.4 %. This decrease is due to a reduction in ~~concentrations due to~~ NO_x concentrations via hydrolysis of XNO_3 (X=Cl, Br, I). Our tropospheric NO_x burden decreases by ~~1.7 % to 168~~ 3.1 % to 167 Gg N (see table 10) on inclusion of halogens consistent with ~~observations and~~ previous model studies (Long et al., 2014; von Glasow et al., 2004; Parrella et al., 2012; Schmidt et al., 2016). Globally ~~loss~~ NO_x losses through $ClNO_3$ and $BrNO_3$ hydrolysis ~~is~~ are approximately equal (1:~~0.86~~0.88), and overall ~~proceeds~~ proceed at a rate of ∼10 % of the NO_x loss through the NO_2+OH pathway. Iodine nitrite and nitrate (INO_2, INO_3) hydrolysis is much less significant (∼~~0.25~~ 0.2 % of rate of NO_2+OH). Net O_x is the difference between the production and loss terms and the change here is much greater leading to an overall decrease in net production of tropospheric O_3 (PO_x-~~) of 26 % (159~~ LO_x) of 32 % (194 Tg yr^{-1}), and a resultant ~~in decrease~~ decrease in O_3 lifetime of ~~14 %.~~ 16 %.

4.2 HO_x ($OH+HO_2$)

We find that global molecule weighted average HO_x ($OH+HO_2$) concentrations are reduced by ~~8.5~~ 10.2 % with the inclusion of halogens, with OH decreasing by ~~4.5~~ 8.2 % from 1.40x10^6 to ~~1.34~~1.28x10^6 molecules cm^{-3}. Lower O_3 concentrations

---

[2] Here O_x is defined as $O_3 + NO_2 + 2NO_3 + PAN + PMN + PPN + HNO_4 + 3N_2O_5 + HNO_3 + MPN + XO + HOX + XNO_2 + 2XNO_3 + 2OIO + 2I_2O_2 + 3I_2O_3 + 4I_2O_4 + 2Cl_2O_2 + 2OClO$, where X=Cl, Br, I; PAN = peroxyacetyl nitrate; PPN = peroxypropionyl nitrate; MPN = methyl peroxy nitrate; and PMN = peroxymethacryloyl nitrate.

~~decrease~~ decreases the primary OH source ($O_3 \xrightarrow{h\nu} 2OH$) by ~~15.5~~ 17.4 %, and the secondary OH source ~~from~~ (HO_2+NO~~by 2.2~~) by 4.7 %.

The reduction in the sources of OH is buffered by an additional OH source from the photolysis of HOX (X=Cl, Br, I) which acts to increase the conversion of HO_2 to OH. Previously, ~~?~~ Sherwen et al. (2016a) showed an increase of 1.8 % in global OH concentrations on inclusion of iodine. However, increased ~~and reduced~~ Br_y and reduced I_y concentrations in the simulations described here mean that the increased OH source from HOX photolysis does not compensate fully for the reduced primary source, resulting in an overall ~~4.5~~ 8.2 % reduction in global mean OH. This buffering contributes to a ~~smaller~~ change in OH ~~than report previously by Schmidt et al. (2016) of~~ smaller than the 11 % reported previously (Schmidt et al., 2016). As reported previously (Long et al., 2014; Schmidt et al., 2016), we also find the net effect of halogens on the OH:HO_2 ratio is a small increase (~~4.4~~ 2.3 %).

4.3 Organic Compounds

The oxidation of volatile organic compounds (VOCs) by halogens is included in this simulation (see Table 6 for reactions). The global fractional loss due to OH, Cl, Br, NO_3, and photolysis ($h\nu$) for a range of organics is shown in Figure 16.

Globally, Br oxidation is small in our simulation and contributes ~~2.0~~ 3.9 % to the loss of acetaldehyde (CH_3CHO), ~~0.6~~ 0.8 % of the loss of formaldehyde (CH_2O), ~~0.26~~ 0.63 % of the loss of $\geqslant$C4 alkenes, and <0.001 % of the loss of other compounds. Recent work has ~~suggests~~ suggested a significant source of oceanic oxygenated VOCs ~~(Millet et al., 2010; Coburn et al., 2014; Sinreich et al.,~~ (Coburn et al., 2014; Lawson et al., 2015; Mahajan et al., 2014; Millet et al., 2010; Myriokefalitakis et al., 2008; Sinreich et al., 2010; Vol we do not include in this simulation. Furthermore although our modelled Br_y is broadly comparable to some previous work ~~(Schmidt et al., 2016; Parrella et al., 2012)~~(Parrella et al., 2012; Schmidt et al., 2016), it is lower in the marine boundary layer than in other recent work (Long et al., 2014). The combination of these two factors suggest that our model provides a lower bounds of impacts of bromine on VOCs. Significantly higher concentrations of oVOC would decrease the ~~BrO~~ BrO_x concentrations in the model and might then allow an increased sea-salt source of reactive bromine.

The oxidation of ~~Volatile Organic Compounds (VOCs)~~ VOCs by chlorine is more significant. In our simulation chlorine accounts for ~~18, 9, and 9~~ 27, 15, and 14 % of the global loss of ethane (C_2H_6), propane (C_3H_8), and acetone ($CH_3C(O)CH_3$)~~)~~, respectively. Loss of other VOCs is globally small. This increased loss due to Cl is to some extent compensated for by the reduction in the OH concentrations that we calculate. Thus the overall lifetime of ethane, propane, and acetone changes from 131, 38, 85 days in the simulation without halogens to ~~120~~113, 37, ~~82~~ 80 in the simulation with halogens. Notably the ethane lifetime without halogens is ~~10% longerthan it is with~~16 % longer. Given that we consider the chlorine in the model to be a lower limit, ethane oxidation by chlorine may in reality be more significant than found here.

Methane is a significant climate gas, as it has the second highest forcing amongst well-mixed greenhouse gases from preindustrial to present day (Myhre et al., 2013). In our simulation without halogens we calculate a tropospheric chemical lifetime due to OH of ~~7.48~~ 7.47 years. With the inclusion of halogen chemistry the OH concentration drops, extending the methane lifetime due to OH ~~of become to 7.96~~ to 8.28 years (an increase of ~~6.5~~ 10.8 %). However, in our halogen simulations, chlorine radicals also oxidise methane (~~∼1~~ 2.0 % of the total loss) shortening the lifetime to ~~7.89 years (0.85~~ 8.16 years (1.52 %). As noted previously, the model's chlorine concentrations appear to be underestimated. Allan et al. (2007) estimate a 25 Tg yr^{-1} sink for methane from Cl (∼4 %), significantly higher than our estimate (4 Tg). Overall the model's CH$_4$ lifetime still appears to be short compared to the observationally based estimation of 9.1 ± 0.9 from Prather et al. (2012), but halogens decrease this bias.

In our simulations, halogens (essentially chlorine) have a significant but not overwhelming role in the concentrations of hydrocarbons (from ∼1 % of ~~methane~~ methanol loss to ∼~~18~~ 27 % of ethane loss). However, as discussed earlier the low biases seen with the very limited observational dataset of chlorine compounds would suggest that the impacts calculated here are probably lower limits.

4.4 Other species

With the inclusion of halogens in the troposphere there are a large number of changes in the composition of the troposphere. Figure 17 illustrates the fractional global change in burden by species (for abbreviation see ~~footnote~~Footnote[3]). The spatial and zonal distribution of these changes by species family (~~, ,~~ HO$_x$, NO$_x$, SO$_x$ as defined in ~~footnote~~the Footnote[4]) are shown in Figure 18 and for a few VOCs (C$_3$H$_8$, C$_2$H$_6$, acetone, and ⩾C4 alkanes) in Figure 19. A tabulated form of these changes is given within the Appendix (Table 10)

As discussed in ~~section 4.1 and 4.1~~Sections 4.1 and 4.2, a clear decrease in oxidants (O$_3$, OH, HO$_2$, H$_2$O$_2$) is seen. This drives an increase in the concentrations of some VOCs (~~2.1~~ 4.5 % on a per carbon basis), including CO (~~2.8~~ 6.1 %) and ~~Isoprene (3.4~~ isoprene (6.2 %). However, as discussed, it also adds an additional Cl sink term which leads to an overall decrease in some species (e.g. C$_2$H$_6$, (CH$_3$)$_2$CO, C$_3$H$_8$) particularly in the northern hemisphere oceanic regions. The SO$_x$ burden increases slightly (~~0.7~~ 0.5 %), which can be attributed to decreases in oxidants.

5 Summary and Conclusions

We have presented a model of tropospheric composition which has attempted to include the major routes of halogen chemistry impacts. Assessment of the model performance is limited as observations of halogen species are extremely sparse. However, given the available observations we conclude that the model has some useful skill in predicting the concentration of iodine and bromine species and appears to underestimate the concentrations of chlorine species.

Consistent with previous studies, our model shows significant halogen driven changes in the concentrations of oxidants. The tropospheric O$_3$ burden and global mean OH ~~decreased by 14.6~~ decreases by 18.6 %, and ~~4.5~~ 8.2 % respectively, on inclusion of halogens. The methane lifetime increases by ~~6.5~~ 10.8 %, improving agreement with observations.

---

[3] Abbreviated species names are defined in the GEOS-Chem manual (http://acmg.seas.harvard.edu/geos/doc/man/appendix_6.html) and here: MOH=~~Methanol~~methanol, EOH=~~Ethanol~~ethanol, ALD2=~~Acetaldehyde~~acetaldehyde, ISOP=~~Isoprene~~isoprene, ALK4=≥C4 alkanes, CH$_3$O$_2$~~,~~=~~Methylperoxy~~ methylperoxy radical, A3O2=primary RO$_2$ from C$_3$H$_8$, B3O2=secondary RO$_2$ from C$_3$H$_8$, ATO2=RO$_2$ from ~~Acetone~~acetone, R4O2=RO$_2$ from ≥C4 alkanes, RIO2=RO$_2$ from ~~Acetone~~ acetone

[4] Here we define families of HO$_x$, NO$_x$ and SO$_x$ as follows. ~~:~~HO$_x$=OH + HO$_2$, ~~:~~NO$_x$=NO+NO$_2$, ~~:~~SO$_x$= SO$_2$ + SO$_4$ + SO$_4$ on sea salt.

There are a range of changes in the concentrations of other species. Direct reaction with Cl atoms leads to enhanced oxidation of hydrocarbons with ethane showing a significant response. Given the model appears to provide a lower limit for atomic Cl concentrations this suggests a major missing oxidation pathway for ethane which is currently not considered. NO$_x$ concentrations are reduced by aerosol hydrolysis of the halogen nitrates which leads to reduced global O$_3$ production. Our simulation of BrO appears to be relatively consistent with ~~those observed~~observations, however we do not include a sea-salt de-bromination mechanism. This would suggest that either the cycling of bromine in our model is generally too fast, or that we do not have sufficiently large BrO$_x$ sinks (potentially oVOCs). Both ~~hypothesis~~ hypotheses warrant further research.

Significant uncertainties however remain in our understanding of halogens in the troposphere. The gas phase chemistry and photolysis parameters of iodine compounds are uncertain, together with the emissions of their organic and inorganic precursors ~~(?)~~(Sherwen et al., 2016a). For chlorine, bromine and iodine heterogeneous chemistry, little experimental data exists and suitable parameterisations for the complex aerosols found in the atmosphere are unavailable ~~(Abbatt et al., 2012; Saiz-Lopez et al., 2012b; Sim~~ (Abbatt et al., 2012). The uncertainties of this have been discussed in recent reviews (Saiz-Lopez et al., 2012b; Simpson et al., 2015), considered in previous model studies (Schmidt et al., 2016; Sherwen et al., 2016a), and still warrant further exploration.

Understanding fully the impact of halogens on tropospheric composition will require significant development of new experimental techniques and more field observations, new laboratory studies and models which are able to exploit these developments.

Appendix A: Tabulated Burden Changes on inclusion of halogens

Table 10 gives the burdens with and without halogens and the fractional change.

Appendix B: Gas phase Chemistry Scheme

Here is described the full halogen chemistry scheme as presented in previous work ~~(Bell et al., 2002; Eastham et al., 2014; Parrella et al., 20~~ with updates as detailed in section 2 and Table 1. The complete gas phase photolysis, bimolecular and termolecular reactions are described in Tables 5, 6, and 7 .

B1 Heterogenous reactions

The halogen multiphase chemistry mechanism is based on the iodine mechanism ("Br+I") described in ~~?~~ Sherwen et al. (2016a) and the coupled (Cl, Br) mechanism of Schmidt et al. (2016). The heterogenous reactions in the scheme are shown in Table 8 and with further detail individual detail on certain reactions below. The loss rate of a molecule X due to multiphase processing on aerosol is calculated following Jacob (2000).

$$\frac{dn_X}{dt} = -\left(\frac{r}{D_g} + \frac{4}{c\gamma}\right)^{-1} A n_X, \tag{B1}$$

where r is the aerosol effective radius, D_g is the gas phase diffusion coefficient of X, c is the average thermal velocity of X, γ is the reactive uptake coefficient, A is the aerosol surface area concentration, and n_X is the gas phase concentration of X.

B2 Aerosols

We consider halogen reactions on sulfate aerosols, sea salt aerosols, and liquid and ice cloud droplets. The implementation of sulfate type aerosols in GEOS-Chem is described by ~~?~~ Park et al. (2004) and Pye et al. (2009). Sulfate aerosols are assumed to be acidic with pH=0.

The GEOS-Chem sea salt aerosol simulation is as described by Jaeglé et al. (2011). The transport and deposition of sea salt bromide follows that of the parent aerosol. Oxidation of bromide on sea-salt produces volatile forms of bromine that are released to the gas phase. Sea salt aerosol is emitted alkaline, but the alkalinity can be titrated in GEOS-Chem by uptake of $\mathrm{HNO_3}$, $\mathrm{SO_2}$, $\mathrm{H_2SO_4}$ (Alexander, 2005). Sea salt aerosol with no remaining alkalinity is assumed to have pH=5. We assume no halide oxidation on alkaline sea salt aerosol.

The liquid cloud droplet surface area is modelled using cloud liquid water content from GEOS-FP (Lucchesi, 2013) and assuming effective cloud droplet radii of 10 μm and 6 μm for marine and continental clouds, respectively. The ice cloud droplet surface area is modelled in a similar manner assuming effective ice droplet radii of 75 µm. We assume that ice cloud chemistry is confined to an unfrozen overlayer surrounding the ice crystal, see Schmidt et al. (2016) for details. Cloud water pH (typically between 4 and 6) is calculated locally in GEOS-Chem following (Alexander et al., 2012).

The reactive uptake coefficients depend on the aerosol halide concentration. For sea salt aerosol, the bromide concentration is calculated directly from the bromide content and the aerosol mass. Sea salt aerosol chloride is assumed to be in excess (see below). For clouds and sulfate aerosol, the bromide and chloride concentration is estimated assuming equilibrium between gas phase HX and aerosol phase $\mathrm{X^-}$.

B3 Reactive uptake coefficients

B3.1 $\mathbf{HOBr + Cl^-/Br^-}$

The reactive uptake coefficient is calculated as

$$\gamma = \left(\Gamma^{-1} + \alpha^{-1}\right)^{-1}, \tag{B2}$$

where the mass accomodation coefficient for HOBr is $\alpha = 0.6$ and

$$\Gamma = \frac{4H_{\mathrm{HOBr}}RTk_{\mathrm{HOBr+X^-}}[\mathrm{X^-}][\mathrm{H^+}]l_r f(r,l_r)}{c}, \tag{B3}$$

with $k_{\mathrm{HOBr+Cl^-}} = 5.9\times10^{9}\,\mathrm{M^{-2}s^{-1}}$ and $k_{\mathrm{HOBr+Br^-}} = 1.6\times10^{10}\,\mathrm{M^{-2}s^{-1}}$. In the equation above c is the average thermal velocity of HOBr, and $f(l_r,r)$ is a reacto-diffusive correction factor,

$$f(l_r,r) = \coth\left(\frac{r}{l_r}\right) - \frac{l_r}{r}, \tag{B4}$$

with r being the radius of the aerosol. For sea salt aerosol $\mathrm{HOBr + Cl^-}$ is assumed to be limited by mass accommodation, i.e. $\Gamma \gg \alpha$, due to high concentration of $\mathrm{Cl^-}$ in sea salt aerosol. The reacto-diffusive length scale is

$$l_r = \sqrt{\frac{D_l}{k_{\mathrm{HOBr+X^-}}[\mathrm{X^-}][\mathrm{H^+}]}}, \tag{B5}$$

where $D_l = 1.4 \times 10^{-5}\,\mathrm{cm^2 s^{-1}}$ is the aqueous phase diffusion coefficient for HOBr. The listed parameters are taken from Ammann et al. (2013), and $k_{\mathrm{HOBr+Br^-}}$ is from Beckwith et al. (1996).

B3.2 $\mathbf{ClNO_3 + Br^-}$

The reactive uptake coefficient is calculated as

$$\gamma = \left(\Gamma^{-1} + \alpha^{-1}\right)^{-1}, \tag{B6}$$

where the mass accomodation coefficient for $\mathrm{ClNO_3}$ is $\alpha = 0.108$ and

$$\Gamma = \frac{4WRT\sqrt{[\mathrm{Br^-}]D_l}}{c}, \tag{B7}$$

where c is the average thermal velocity of $\mathrm{ClNO_3}$, $D_l = 5.0 \times 10^{-6}\,\mathrm{cm^2 s^{-1}}$ is the aqueous phase diffusion coefficient for $\mathrm{ClNO_3}$, and $W = 10^6\,\sqrt{\mathrm{Ms}}\,\mathrm{bar^{-1}}$.

B3.3 $\mathbf{O_3 + Br^-}$

The reactive uptake coefficient is calculated as

$$\gamma = \Gamma_b + \Gamma_s, \tag{B8}$$

where Γ_b is the bulk reaction coefficient,

$$\Gamma_b = \frac{4H_{\mathrm{O_3}}RTk_{\mathrm{O_3+Br^-}}[\mathrm{Br^-}]l_r f(r,l_r)}{c}, \tag{B9}$$

with $k_{\mathrm{O_3+Br^-}} = 6.8 \times 10^8\,\exp(-4450\,\mathrm{K}/T)\,\mathrm{M^{-1}s^{-1}}$. In the equation above c is the average thermal velocity of $\mathrm{O_3}$, and $f(l_r,r)$ is a reacto-diffusive correction factor,

$$f(l_r,r) = \coth\left(\frac{r}{l_r}\right) - \frac{l_r}{r}, \tag{B10}$$

with r being the radius of the aerosol. The reacto-diffusive length scale is

$$l_r = \sqrt{\frac{D_l}{k_{\mathrm{O_3+Br^-}}[\mathrm{Br^-}]}}, \tag{B11}$$

where $D_l = 8.9 \times 10^{-6}\,\mathrm{cm^2 s^{-1}}$ is the aqueous phase diffusion coefficient for $\mathrm{O_3}$.

The surface reaction coefficient is calculated as,

$$\Gamma_s = \frac{4k_s[\mathrm{Br^-(surf)}]K_{\mathrm{LangC}}N_{\mathrm{max}}}{c(1 + K_{\mathrm{LangC}}[\mathrm{O_3(g)}])}, \tag{B12}$$

where the surface reaction rate constant is $k_s = 10^{-16}\,\mathrm{cm^2 s^{-1}}$, the equilibrium constant for $\mathrm{O_3}$ is $K_{\mathrm{LangC}} = 10^{-13}\,\mathrm{cm^3}$, and the maximum number of available sites is taken as $N_{\mathrm{max}} = 3 \times 10^{14}\,\mathrm{cm^{-2}}$. The surface bromide concentration is estimated as,

$$[\mathrm{Br^-(surf)}] = \min(3.41 \times 10^{14}\,\mathrm{cm^{-2}M^{-1}}\,[\mathrm{Br^-}], N_{\mathrm{max}}). \tag{B13}$$

Acknowledgements. This work was funded by NERC quota studentship NE/K500987/1 with support from the NERC BACCHUS and CAST projects NE/L01291X/1, NE/J006165/1.

J. A. Schmidt acknowledges funding through a Carlsberg Foundation post-doctoral fellowship (CF14-0519)

R. Volkamer acknowledges funding from US National Science Foundation CAREER award ATM-0847793, AGS-1104104, and AGS-1452317. The involvement of the NSF-sponsored Lower Atmospheric Observing Facilities, managed and operated by the National Center for Atmospheric Research (NCAR) Earth Observing Laboratory (EOL), is acknowledged.

T. Sherwen would like to acknowledge constructive comments and input from GEOS-Chem Support Team ~~.~~at Harvard Univeristy. We also acknowledge constructive input from Qianjie Chen and Becky Alexander of the University of Washington.

References

Abbatt, J. P. D., Lee, A. K. Y., and Thornton, J. A.: Quantifying trace gas uptake to tropospheric aerosol: recent advances and remaining challenges, Chem. Soc. Rev., 41, 6555–6581, doi:10.1039/c2cs35052a, 2012.

Alexander, B.: Sulfate formation in sea-salt aerosols: Constraints from oxygen isotopes, J. Geophys. Res., 110, D10 307, doi:10.1029/2004JD005659, 2005.

Alexander, B., Allman, D. J., Amos, H. M., Fairlie, T. D., Dachs, J., Hegg, D. A., and Sletten, R. S.: Isotopic constraints on the formation pathways of sulfate aerosol in the marine boundary layer of the subtropical northeast Atlantic Ocean, J. Geophys. Res., 117, D06 304, doi:10.1029/2011JD016773, 2012.

Allan, W., Struthers, H., and Lowe, D. C.: Methane carbon isotope effects caused by atomic chlorine in the marine boundary layer: Global model results compared with Southern Hemisphere measurements, J Geophys. Res-Atmos., 112, doi:10.1029/2006JD007369, 2007.

Ammann, M., Cox, R. A., Crowley, J. N., Jenkin, M. E., Mellouki, A., Rossi, M. J., Troe, J., and Wallington, T. J.: Evaluated kinetic and photochemical data for atmospheric chemistry: Volume VI – heterogeneous reactions with liquid substrates, Atmos. Chem. Phys., 13, 8045–8228, doi:10.5194/acp-13-8045-2013, 2013.

Atkinson, R., Baulch, D. L., Cox, R. A., Crowley, J. N., Hampson, R. F., Hynes, R. G., Jenkin, M. E., Rossi, M. J., Troe, J., and IUPAC Subcommittee: Evaluated kinetic and photochemical data for atmospheric chemistry: Volume II – gas phase reactions of organic species, Atmos. Chem. Phys., 6, 3625–4055, doi:10.5194/acp-6-3625-2006, 2006.

Atkinson, R., Baulch, D. L., Cox, R. A., Crowley, J. N., Hampson, R. F., Hynes, R. G., Jenkin, M. E., Rossi, M. J., and Troe, J.: Evaluated kinetic and photochemical data for atmospheric chemistry: Volume III - gas phase reactions of inorganic halogens, Atmos. Chem. Phys., 7, 981–1191, 2007.

Atkinson, R., Baulch, D. L., Cox, R. A., Crowley, J. N., Hampson, R. F., Hynes, R. G., Jenkin, M. E., Rossi, M. J., Troe, J., and Wallington, T. J.: Evaluated kinetic and photochemical data for atmospheric chemistry: Volume IV - gas phase reactions of organic halogen species, J. Phys. Chem. Ref. Data, 8, 4141–4496, 2008.

Bannan, T. J., Booth, A. M., Bacak, A., Muller, J. B. A., Leather, K. E., Le Breton, M., Jones, B., Young, D., Coe, H., Allan, J., Visser, S., Slowik, J. G., Furger, M., Prévôt, A. S. H., Lee, J., Dunmore, R. E., Hopkins, J. R., Hamilton, J. F., Lewis, A. C., Whalley, L. K., Sharp, T., Stone, D., Heard, D. E., Fleming, Z. L., Leigh, R., Shallcross, D. E., and Percival, C. J.: The first UK measurements of nitryl chloride using a chemical ionization mass spectrometer in central London in the summer of 2012, and an investigation of the role of Cl atom oxidation, J Geophys. Res-Atmos., 120, 5638–5657, doi:10.1002/2014JD022629, 2015.

Beckwith, R. C., Wang, T. X., and Margerum, D. W.: Equilibrium and Kinetics of Bromine Hydrolysis, Inorg. Chem., 35, 995–1000, doi:10.1021/ic950909w, 1996.

Bedjanian, Y., Le Bras, G., and Poulet, G.: Kinetic study of the Br + IO, I + BrO and Br + I2 reactions. Heat of formation of the BrO radical, Chem. Phys. lett., 266, 233–238, doi:http://dx.doi.org/10.1016/S0009-2614(97)01530-3, 1997.

Bell, N., Hsu, L., Jacob, D. J., Schultz, M. G., Blake, D. R., Butler, J. H., King, D. B., Lobert, J. M., and Maier-Reimer, E.: Methyl iodide: Atmospheric budget and use as a tracer of marine convection in global models, J. Geophys. Res-Atmos., 107, ACH 8–1–ACH 8–12, doi:10.1029/2001jd001151, 2002.

Bertram, T. H. and Thornton, J. A.: Toward a general parameterization of N2O5 reactivity on aqueous particles: the competing effects of particle liquid water, nitrate and chloride, Atmos. Chem. Phys., 9, 8351–8363, doi:10.5194/acp-9-8351-2009, 2009.

Bloss, W. J., Evans, M. J., Lee, J. D., Sommariva, R., Heard, D. E., and Pilling, M. J.: The oxidative capacity of the troposphere: Coupling of field measurements of OH and a global chemistry transport model, Faraday Discuss., 130, 425–436, doi:10.1039/b419090d, 2005.

Carpenter, L. J., Fleming, Z. L., Read, K. A., Lee, J. D., Moller, S. J., Hopkins, J. R., Purvis, R. M., Lewis, A. C., Muller, K., Heinold, B., Herrmann, H., Fomba, K. W., van Pinxteren, D., Muller, C., Tegen, I., Wiedensohler, A., Muller, T., Niedermeier, N., Achterberg, E. P., Patey, M. D., Kozlova, E. A., Heimann, M., Heard, D. E., Plane, J. M. C., Mahajan, A., Oetjen, H., Ingham, T., Stone, D., Whalley, L. K., Evans, M. J., Pilling, M. J., Leigh, R. J., Monks, P. S., Karunaharan, A., Vaughan, S., Arnold, S. R., Tschritter, J., Pohler, D., Friess, U., Holla, R., Mendes, L. M., Lopez, H., Faria, B., Manning, A. J., and Wallace, D. W. R.: Seasonal characteristics of tropical marine boundary layer air measured at the Cape Verde Atmospheric Observatory, J. Atmos. Chem., 67, 87–140, doi:10.1007/s10874-011-9206-1, 2010.

Carpenter, L. J., MacDonald, S. M., Shaw, M. D., Kumar, R., Saunders, R. W., Parthipan, R., Wilson, J., and Plane, J. M. C.: Atmospheric iodine levels influenced by sea surface emissions of inorganic iodine, Nature Geosci., 6, 108–111, doi:10.1038/ngeo1687, 2013.

Chameides, W. L. and Davis, D. D.: Iodine: Its possible role in tropospheric photochemistry, J Geophys. Res-Oceans, 85, 7383–7398, doi:10.1029/JC085iC12p07383, 1980.

Chance, R., Baker, A. R., Carpenter, L., and Jickells, T. D.: The distribution of iodide at the sea surface, Environ. Sci.: Processes Impacts, 16, 1841–1859, doi:10.1039/C4EM00139G, 2014.

Coburn, S., Ortega, I., Thalman, R., Blomquist, B., Fairall, C. W., and Volkamer, R.: Measurements of diurnal variations and eddy covariance (EC) fluxes of glyoxal in the tropical marine boundary layer: description of the Fast LED-CE-DOAS instrument, Atmospheric Measurement Techniques, 7, 3579–3595, doi:10.5194/amt-7-3579-2014, 2014.

Coburn, S., Dix, B., Edgerton, E., Holmes, C. D., Kinnison, D., Liang, Q., ter Schure, A., Wang, S., and Volkamer, R.: Mercury oxidation from bromine chemistry in the free troposphere over the southeastern US, Atmospheric Chemistry and Physics, 16, 3743–3760, doi:10.5194/acp-16-3743-2016, http://www.atmos-chem-phys.net/16/3743/2016/acp-16-3743-2016.html, 2016.

Dean, J. A.: Lange's Handbook of Chemistry, McGraw-Hill, Inc., 1992.

Deiber, G., George, C., Le Calvé, S., Schweitzer, F., and Mirabel, P.: Uptake study of ClONO2 and BrONO2 by Halide containing droplets, Atmos. Chem. Phys., 4, 1291–1299, doi:10.5194/acp-4-1291-2004, 2004.

Eastham, S. D., Weisenstein, D. K., and Barrett, S. R. H.: Development and evaluation of the unified tropospheric–stratospheric chemistry extension (UCX) for the global chemistry-transport model GEOS-Chem, Atmos. Environ., 89, 52–63, doi:http://dx.doi.org/10.1016/j.atmosenv.2014.02.001, 2014.

Evans, M. J. and Jacob, D. J.: Impact of new laboratory studies of N2O5 hydrolysis on global model budgets of tropospheric nitrogen oxides, ozone, and OH, Geophys. Res. Lett., 32, L09 813, doi:10.1029/2005GL022469, 2005.

Faxon, C. B., Bean, J. K., and Ruiz, L. H.: Inland Concentrations of Cl2 and ClNO2 in Southeast Texas Suggest Chlorine Chemistry Significantly Contributes to Atmospheric Reactivity, Atmosphere, 6, 1487, doi:10.3390/atmos6101487, 2015.

Fernandez, R. P., Salawitch, R. J., Kinnison, D. E., Lamarque, J.-F., and Saiz-Lopez, A.: Bromine partitioning in the tropical tropopause layer: implications for stratospheric injection, Atmospheric Chemistry and Physics, 14, 13 391–13 410, doi:10.5194/acp-14-13391-2014, 2014.

Frenzel, A., Scheer, V., Sikorski, R., George, C., Behnke, W., and Zetzsch, C.: Heterogeneous Interconversion Reactions of BrNO2, ClNO2, Br2, and Cl2, J. Phys. Chem. A, 102, 1329–1337, doi:10.1021/jp973044b, 1998.

Froidevaux, L., Jiang, Y. B., Lambert, A., Livesey, N. J., Read, W. G., Waters, J. W., Fuller, R. A., Marcy, T. P., Popp, P. J., Gao, R. S., Fahey, D. W., Jucks, K. W., Stachnik, R. A., Toon, G. C., Christensen, L. E., Webster, C. R., Bernath, P. F., Boone, C. D., Walker, K. A., Pumphrey, H. C., Harwood, R. S., Manney, G. L., Schwartz, M. J., Daffer, W. H., Drouin, B. J., Cofield, R. E., Cuddy, D. T., Jarnot, R. F., Knosp, B. W., Perun, V. S., Snyder, W. V., Stek, P. C., Thurstans, R. P., and Wagner, P. A.: Validation of Aura Microwave Limb Sounder HCl measurements, Journal of Geophysical Research: Atmospheres, 113, doi:10.1029/2007JD009025, 2008.

Gómez Martín, J. C., Spietz, P., and Burrows, J. P.: Spectroscopic studies of the I2/O3 photochemistry: Part 1: Determination of the absolute absorption cross sections of iodine oxides of atmospheric relevance, J Photoch. Photobio. A, 176, 15–38, doi:http://dx.doi.org/10.1016/j.jphotochem.2005.09.024, 2005.

Gómez Martín, J. C., Spietz, P., and Burrows, J. P.: Kinetic and Mechanistic Studies of the I2/O3 Photochemistry, J. Phys. Chem. A, 111, 306–320, doi:10.1021/jp061186c, 2007.

Großmann, K., Frieß, U., Peters, E., Wittrock, F., Lampel, J., Yilmaz, S., Tschritter, J., Sommariva, R., von Glasow, R., Quack, B., Krüger, K., Pfeilsticker, K., and Platt, U.: Iodine monoxide in the Western Pacific marine boundary layer, Atmos. Chem. Phys., 13, 3363–3378, doi:10.5194/acp-13-3363-2013, 2013.

Harris, N. R. P., Carpenter, L. J., Lee, J. D., Vaughan, G., Filus, M. T., Jones, R. L., OuYang, B., Pyle, J. A., Robinson, A. D., Andrews, S. J., Lewis, A. C., Minaeian, J., Vaughan, A., Dorsey, J. R., Gallagher, M. W., Breton, M. L., Newton, R., Percival, C. J., Ricketts, H. M. A., Baugitte, S. J.-B., Nott, G. J., Wellpott, A., Ashfold, M. J., Flemming, J., Butler, R., Palmer, P. I., Kaye, P. H., Stopford, C., Chemel, C., Boesch, H., Humpage, N., Vick, A., MacKenzie, A. R., Hyde, R., Angelov, P., Meneguz, E., and Manning, A. J.: Co-ordinated Airborne Studies in the Tropics (CAST), Bulletin of the American Meteorological Society, 0, doi:10.1175/BAMS-D-14-00290.1, http://dx.doi.org/10.1175/BAMS-D-14-00290.1, 2016.

Holmes, C. D., Jacob, D. J., Mason, R. P., and Jaffe, D. A.: Sources and deposition of reactive gaseous mercury in the marine atmosphere, Atmospheric Environment, 43, 2278–2285, doi:10.1016/j.atmosenv.2009.01.051, 2009.

Hossaini, R., Mantle, H., Chipperfield, M. P., Montzka, S. A., Hamer, P., Ziska, F., Quack, B., Krüger, K., Tegtmeier, S., Atlas, E., Sala, S., Engel, A., Bönisch, H., Keber, T., Oram, D., Mills, G., Ordóñez, C., Saiz-Lopez, A., Warwick, N., Liang, Q., Feng, W., Moore, F., Miller, B. R., Marécal, V., Richards, N. A. D., Dorf, M., and Pfeilsticker, K.: Evaluating global emission inventories of biogenic bromocarbons, Atmos. Chem. Phys., 13, 11 819–11 838, doi:10.5194/acp-13-11819-2013, 2013.

Jacob, D. J.: Heterogeneous chemistry and tropospheric ozone, Atmos. Environ., 34, 2131–2159, doi:http://dx.doi.org/10.1016/S1352-2310(99)00462-8, 2000.

Jaeglé, L., Quinn, P. K., Bates, T. S., Alexander, B., and Lin, J. T.: Global distribution of sea salt aerosols: new constraints from in situ and remote sensing observations, Atmos. Chem. Phys., 11, 3137–3157, doi:10.5194/acp-11-3137-2011, 2011.

Kaltsoyannis, N. and Plane, J. M. C.: Quantum chemical calculations on a selection of iodine-containing species (IO, OIO, INO3, (IO)2, I2O3, I2O4 and I2O5) of importance in the atmosphere, Phys. Chem. Chem. Phys., 10, 1723–1733, 2008.

Keene, W. C., Long, M. S., Pszenny, A. A. P., Sander, R., Maben, J. R., Wall, A. J., O'Halloran, T. L., Kerkweg, A., Fischer, E. V., and Schrems, O.: Latitudinal variation in the multiphase chemical processing of inorganic halogens and related species over the eastern North and South Atlantic Oceans, Atmospheric Chemistry and Physics, 9, 7361–7385, doi:10.5194/acp-9-7361-2009, 2009.

King, K. D., Golden, D. M., and Benson, S. W.: Kinetics of the gas-phase thermal bromination of acetone. Heat of formation and stabilization energy of the acetonyl radical, J. Am. Chem. Soc, 92, 5541–5546, doi:10.1021/ja00722a001, 1970.

Knipping, E. M. and Dabdub, D.: Impact of Chlorine Emissions from Sea-Salt Aerosol on Coastal Urban Ozone, Environmental Science & Technology, 37, 275–284, doi:10.1021/es025793z, http://dx.doi.org/10.1021/es025793z, 2003.

Lawler, M. J., Sander, R., Carpenter, L. J., Lee, J. D., von Glasow, R., Sommariva, R., and Saltzman, E. S.: HOCl and Cl2 observations in marine air, Atmos. Chem. Phys., 11, 7617–7628, doi:10.5194/acp-11-7617-2011, 2011.

Lawson, S. J., Selleck, P. W., Galbally, I. E., Keywood, M. D., Harvey, M. J., Lerot, C., Helmig, D., and Ristovski, Z.: Seasonal in situ observations of glyoxal and methylglyoxal over the temperate oceans of the Southern Hemisphere, Atmospheric Chemistry and Physics, 15, 223–240, doi:10.5194/acp-15-223-2015, 2015.

Leser, H., Hönninger, G., and Platt, U.: MAX-DOAS measurements of BrO and NO2 in the marine boundary layer, Geophys. Res. Lett., 30, 1537, doi:10.1029/2002GL015811, http://dx.doi.org/10.1029/2002GL015811, 2003.

Long, M. S., Keene, W. C., Easter, R. C., Sander, R., Liu, X., Kerkweg, A., and Erickson, D.: Sensitivity of tropospheric chemical composition to halogen-radical chemistry using a fully coupled size-resolved multiphase chemistry–global climate system: halogen distributions, aerosol composition, and sensitivity of climate-relevant gases, Atmos. Chem. Phys., 14, 3397–3425, doi:10.5194/acp-14-3397-2014, 2014.

Lucchesi, R.: No TitleFile Specification for GEOS-5 FP. GMAO Office Note No. 4 (Version 1.0), Tech. rep., NASA GMAO, 2013.

MacDonald, S. M., Gómez Martín, J. C., Chance, R., Warriner, S., Saiz-Lopez, A., Carpenter, L. J., and Plane, J. M. C.: A laboratory characterisation of inorganic iodine emissions from the sea surface: dependence on oceanic variables and parameterisation for global modelling, Atmos. Chem. Phys., 14, 5841–5852, doi:10.5194/acp-14-5841-2014, 2014.

Mahajan, A. S., Plane, J. M. C., Oetjen, H., Mendes, L., Saunders, R. W., Saiz-Lopez, A., Jones, C. E., Carpenter, L. J., and McFiggans, G. B.: Measurement and modelling of tropospheric reactive halogen species over the tropical Atlantic Ocean, Atmos. Chem. Phys., 10, 4611–4624, doi:10.5194/acp-10-4611-2010, 2010.

Mahajan, A. S., Gómez Martín, J. C., Hay, T. D., Royer, S.-J., Yvon-Lewis, S., Liu, Y., Hu, L., Prados-Roman, C., Ordóñez, C., Plane, J. M. C., and Saiz-Lopez, A.: Latitudinal distribution of reactive iodine in the Eastern Pacific and its link to open ocean sources, Atmos. Chem. Phys., 12, 11 609–11 617, doi:10.5194/acp-12-11609-2012, 2012.

Mahajan, A. S., Prados-Roman, C., Hay, T. D., Lampel, J., Pöhler, D., Groβmann, K., Tschritter, J., Frieß, U., Platt, U., Johnston, P., Kreher, K., Wittrock, F., Burrows, J. P., Plane, J. M. C., and Saiz-Lopez, A.: Glyoxal observations in the global marine boundary layer, Journal of Geophysical Research: Atmospheres, 119, 6160–6169, doi:10.1002/2013JD021388, 2014.

Mao, J., Paulot, F., Jacob, D. J., Cohen, R. C., Crounse, J. D., Wennberg, P. O., Keller, C. A., Hudman, R. C., Barkley, M. P., and Horowitz, L. W.: Ozone and organic nitrates over the eastern United States: Sensitivity to isoprene chemistry, J Geophys. Res-Atmos., 118, 11,256–11,268, doi:10.1002/jgrd.50817, 2013.

McFiggans, G., Plane, J. M. C., Allan, B. J., Carpenter, L. J., Coe, H., and O'Dowd, C.: A modeling study of iodine chemistry in the marine boundary layer, J Geophys. Res-Atmos., 105, 14 371–14 385, doi:10.1029/1999JD901187, 2000.

McFiggans, G., Cox, R. A., Mossinger, J. C., Allan, B. J., and Plane, J. M. C.: Active chlorine release from marine aerosols: Roles for reactive iodine and nitrogen species, J Geophys. Res-Atmos., 107, doi:10.1029/2001jd000383, 2002.

McGrath, M. P. and Rowland, F. S.: Ideal Gas Thermodynamic Properties of HOBr, J Phys Chem-US, 98, 4773–4775, doi:10.1021/j100069a001, 1994.

Mielke, L. H., Furgeson, A., and Osthoff, H. D.: Observation of ClNO2 in a Mid-Continental Urban Environment, Environ. Sci. Technol., 45, 8889–8896, doi:10.1021/es201955u, 2011.

Mielke, L. H., Stutz, J., Tsai, C., Hurlock, S. C., Roberts, J. M., Veres, P. R., Froyd, K. D., Hayes, P. L., Cubison, M. J., Jimenez, J. L., Washenfelder, R. A., Young, C. J., Gilman, J. B., de Gouw, J. A., Flynn, J. H., Grossberg, N., Lefer, B. L., Liu, J., Weber, R. J., and Osthoff, H. D.: Heterogeneous formation of nitryl chloride and its role as a nocturnal NOx reservoir species during CalNex-LA 2010, J Geophys. Res-Atmos., 118, 10,610–638,652, doi:10.1002/jgrd.50783, 2013.

Millet, D. B., Guenther, A., Siegel, D. A., Nelson, N. B., Singh, H. B., de Gouw, J. A., Warneke, C., Williams, J., Eerdekens, G., Sinha, V., Karl, T., Flocke, F., Apel, E., Riemer, D. D., Palmer, P. I., and Barkley, M.: Global atmospheric budget of acetaldehyde: 3-D model analysis and constraints from in-situ and satellite observations, Atmospheric Chemistry and Physics, 10, 3405–3425, doi:10.5194/acp-10-3405-2010, 2010.

Miyazaki, Y., Coburn, S., Ono, K., Ho, D. T., Pierce, R. B., Kawamura, K., and Volkamer, R.: Contribution of dissolved organic matter to submicron water-soluble organic aerosols in the marine boundary layer over the eastern equatorial Pacific, Atmospheric Chemistry and Physics Discussions, 2016, 1–24, doi:10.5194/acp-2016-164, 2016.

Monks, P. S., Granier, C., Fuzzi, S., Stohl, A., Williams, M. L., Akimoto, H., Amann, M., Baklanov, A., Baltensperger, U., Bey, I., Blake, N., Blake, R. S., Carslaw, K., Cooper, O. R., Dentener, F., Fowler, D., Fragkou, E., Frost, G. J., Generoso, S., Ginoux, P., Grewe, V., Guenther, A., Hansson, H. C., Henne, S., Hjorth, J., Hofzumahaus, A., Huntrieser, H., Isaksen, I. S. A., Jenkin, M. E., Kaiser, J., Kanakidou, M., Klimont, Z., Kulmala, M., Laj, P., Lawrence, M. G., Lee, J. D., Liousse, C., Maione, M., McFiggans, G., Metzger, A., Mieville, A., Moussiopoulos, N., Orlando, J. J., O'Dowd, C. D., Palmer, P. I., Parrish, D. D., Petzold, A., Platt, U., Pöschl, U., Prévôt, A. S. H., Reeves, C. E., Reimann, S., Rudich, Y., Sellegri, K., Steinbrecher, R., Simpson, D., ten Brink, H., Theloke, J., van der Werf, G. R., Vautard, R., Vestreng, V., Vlachokostas, C., and von Glasow, R.: Atmospheric composition change – global and regional air quality, Atmos. Environ., 43, 5268–5350, doi:http://dx.doi.org/10.1016/j.atmosenv.2009.08.021, 2009.

Monks, P. S., Archibald, A. T., Colette, A., Cooper, O., Coyle, M., Derwent, R., Fowler, D., Granier, C., Law, K. S., Mills, G. E., Stevenson, D. S., Tarasova, O., Thouret, V., von Schneidemesser, E., Sommariva, R., Wild, O., and Williams, M. L.: Tropospheric ozone and its precursors from the urban to the global scale from air quality to short-lived climate forcer, Atmos. Chem. Phys., 15, 8889–8973, doi:10.5194/acp-15-8889-2015, 2015.

Murray, L. T., Jacob, D. J., Logan, J. A., Hudman, R. C., and Koshak, W. J.: Optimized regional and interannual variability of lightning in a global chemical transport model constrained by LIS/OTD satellite data, J Geophys. Res-Atmos., 117, D20 307, doi:10.1029/2012JD017934, 2012.

Myhre, G., Shindell, D., Bréon, F.-M., Collins, W., Fuglestvedt, J., Huang, J., Koch, D., Lamarque, J.-F., Lee, D., Mendoza, B., Nakajima, T., Robock, A., Stephens, G., Takemura, T., and H. Zhang, .: Anthropogenic and Natural Radiative Forcing. In: Climate Change 2013: The Physical Science Basis. Contribution of Working Group I to the Fifth Assessment Report of the Intergovernmental Panel on Climate Change, Tech. rep., IPCC, 2013.

Myriokefalitakis, S., Vrekoussis, M., Tsigaridis, K., Wittrock, F., Richter, A., Brühl, C., Volkamer, R., Burrows, J. P., and Kanakidou, M.: The influence of natural and anthropogenic secondary sources on the glyoxal global distribution, Atmospheric Chemistry and Physics, 8, 4965–4981, doi:10.5194/acp-8-4965-2008, 2008.

Ordóñez, C., Lamarque, J. F., Tilmes, S., Kinnison, D. E., Atlas, E. L., Blake, D. R., Santos, G. S., Brasseur, G., and Saiz-Lopez, A.: Bromine and iodine chemistry in a global chemistry-climate model: description and evaluation of very short-lived oceanic sources, Atmos. Chem. Phys., 12, 1423–1447, doi:10.5194/acp-12-1423-2012, 2012.

Orlando, J. J. and Tyndall, G. S.: Rate Coefficients for the Thermal Decomposition of BrONO2 and the Heat of Formation of BrONO2, J Phys Chem-US, 100, 19 398–19 405, doi:10.1021/jp9620274, 1996.

Osthoff, H. D., Roberts, J. M., Ravishankara, A. R., Williams, E. J., Lerner, B. M., Sommariva, R., Bates, T. S., Coffman, D., Quinn, P. K., Dibb, J. E., Stark, H., Burkholder, J. B., Talukdar, R. K., Meagher, J., Fehsenfeld, F. C., and Brown, S. S.: High levels of nitryl chloride in the polluted subtropical marine boundary layer, Nature Geosci, 1, 324–328, doi:http://www.nature.com/ngeo/journal/v1/n5/suppinfo/ngeo177_S1.html, 2008.

Park, R. J., Jacob, D. J., Field, B. D., Yantosca, R. M., and Chin, M.: Natural and transboundary pollution influences on sulfate-nitrate-ammonium aerosols in the United States: Implications for policy, J Geophys. Res-Atmos., 109, n/a—-n/a, doi:10.1029/2003JD004473, 2004.

Parrella, J. P., Jacob, D. J., Liang, Q., Zhang, Y., Mickley, L. J., Miller, B., Evans, M. J., Yang, X., Pyle, J. A., Theys, N., and Van Roozendael, M.: Tropospheric bromine chemistry: implications for present and pre-industrial ozone and mercury, Atmos. Chem. Phys., 12, 6723–6740, doi:10.5194/acp-12-6723-2012, 2012.

Phillips, G. J., Tang, M. J., Thieser, J., Brickwedde, B., Schuster, G., Bohn, B., Lelieveld, J., and Crowley, J. N.: Significant concentrations of nitryl chloride observed in rural continental Europe associated with the influence of sea salt chloride and anthropogenic emissions, Geophys. Res. Lett., 39, doi:10.1029/2012GL051912, 2012.

Prados-Roman, C., Cuevas, C. A., Fernandez, R. P., Kinnison, D. E., Lamarque, J.-F., and Saiz-Lopez, A.: A negative feedback between anthropogenic ozone pollution and enhanced ocean emissions of iodine, Atmos. Chem. Phys., 15, 2215–2224, doi:10.5194/acp-15-2215-2015, 2015a.

Prados-Roman, C., Cuevas, C. A., Hay, T., Fernandez, R. P., Mahajan, A. S., Royer, S.-J., Galí, M., Simó, R., Dachs, J., Großmann, K., Kinnison, D. E., Lamarque, J.-F., and Saiz-Lopez, A.: Iodine oxide in the global marine boundary layer, Atmos. Chem. Phys., 15, 583–593, doi:10.5194/acp-15-583-2015, 2015b.

Prather, M. J., Holmes, C. D., and Hsu, J.: Reactive greenhouse gas scenarios: Systematic exploration of uncertainties and the role of atmospheric chemistry, Geophys. Res. Lett., 39, n/a—-n/a, doi:10.1029/2012GL051440, 2012.

Pszenny, A. A. P., Moldanová, J., Keene, W. C., Sander, R., Maben, J. R., Martinez, M., Crutzen, P. J., Perner, D., and Prinn, R. G.: Halogen cycling and aerosol pH in the Hawaiian marine boundary layer, Atmospheric Chemistry and Physics, 4, 147–168, doi:10.5194/acp-4-147-2004, 2004.

Pye, H. O. T., Liao, H., Wu, S., Mickley, L. J., Jacob, D. J., Henze, D. K., and Seinfeld, J. H.: Effect of changes in climate and emissions on future sulfate-nitrate-ammonium aerosol levels in the United States, J. Geophys. Res., 114, D01 205, doi:10.1029/2008JD010701, 2009.

Read, K. A., Mahajan, A. S., Carpenter, L. J., Evans, M. J., Faria, B. V. E., Heard, D. E., Hopkins, J. R., Lee, J. D., Moller, S. J., Lewis, A. C., Mendes, L., McQuaid, J. B., Oetjen, H., Saiz-Lopez, A., Pilling, M. J., and Plane, J. M. C.: Extensive halogen-mediated ozone destruction over the tropical Atlantic Ocean, Nature, 453, 1232–1235, doi:10.1038/nature07035, 2008.

Riedel, T. P., Bertram, T. H., Crisp, T. A., Williams, E. J., Lerner, B. M., Vlasenko, A., Li, S.-M., Gilman, J., de Gouw, J., Bon, D. M., Wagner, N. L., Brown, S. S., and Thornton, J. A.: Nitryl Chloride and Molecular Chlorine in the Coastal Marine Boundary Layer, Environ. Sci. Technol., 46, 10 463–10 470, doi:10.1021/es204632r, 2012.

Riedel, T. P., Wagner, N. L., Dubé, W. P., Middlebrook, A. M., Young, C. J., Öztürk, F., Bahreini, R., VandenBoer, T. C., Wolfe, D. E., Williams, E. J., Roberts, J. M., Brown, S. S., and Thornton, J. A.: Chlorine activation within urban or power plant plumes: Vertically resolved ClNO2 and Cl2 measurements from a tall tower in a polluted continental setting, J Geophys. Res-Atmos., 118, 8702–8715, doi:10.1002/jgrd.50637, http://dx.doi.org/10.1002/jgrd.50637, 2013.

Riffault, V., Bedjanian, Y., and Poulet, G.: Kinetic and mechanistic study of the reactions of OH with IBr and HOI, J Photoch. Photobio. A, 176, 155–161, doi:http://dx.doi.org/10.1016/j.jphotochem.2005.09.002, 2005.

Roberts, J. M., Osthoff, H. D., Brown, S. S., Ravishankara, A. R., Coffman, D., Quinn, P., and Bates, T.: Laboratory studies of products of N2O5 uptake on Cl containing substrates, Geophys. Res. Lett., 36, doi:10.1029/2009GL040448, 2009.

Saiz-Lopez, A., Lamarque, J. F., Kinnison, D. E., Tilmes, S., Ordonez, C., Orlando, J. J., Conley, A. J., Plane, J. M. C., Mahajan, A. S., Santos, G. S., Atlas, E. L., Blake, D. R., Sander, S. P., Schauffler, S., Thompson, A. M., and Brasseur, G.: Estimating the climate significance of halogen-driven ozone loss in the tropical marine troposphere, Atmos. Chem. Phys., 12, 3939–3949, doi:10.5194/acp-12-3939-2012, 2012a.

Saiz-Lopez, A., Plane, J. M. C., Baker, A. R., Carpenter, L. J., von Glasow, R., Martin, J. C. G., McFiggans, G., and Saunders, R. W.: Atmospheric Chemistry of Iodine, Chem. Rev., 112, 1773–1804, doi:10.1021/cr200029u, 2012b.

Saiz-Lopez, A., Fernandez, R. P., Ordóñez, C., Kinnison, D. E., Gómez Martín, J. C., Lamarque, J.-F., and Tilmes, S.: Iodine chemistry in the troposphere and its effect on ozone, Atmos. Chem. Phys.., 14, 19 985–20 044, doi:10.5194/acpd-14-19985-2014, 2014.

Sander, R.: Compilation of Henry's law constants (version 4.0) for water as solvent, Atmos. Chem. Phys., 15, 4399–4981, doi:10.5194/acp-15-4399-2015, 2015.

Sander, S. P., Golden, D. M., Kurylo, M. J., Moortgat, G. K., Wine, P. H., Ravishankara, A. R., Kolb, C. E., Molina, M. J., Finlayson-Pitts, B. J., Huie, R. E., and Orkin, V. L.: Chemical kinetics and photochemical data for use in Atmospheric Studies Evaluation Number 15, 2006.

Sander, S. P., Friedl, R. R., Abbatt, J. P. D., Barker, J. R., Burkholder, J. B., Golden, D. M., Kolb, C. E., Kurylo, M. J., Moortgat, G. K., Wine, P. H., Huie, R. E., and Orkin, V. L.: Chemical kinetics and photochemical data for use in atmospheric studies, Evaluation Number 17, Tech. rep., NASA Jet Propulsion Laboratory, Pasadena, 2011.

Sarwar, G., Simon, H., Xing, J., and Mathur, R.: Importance of tropospheric ClNO2 chemistry across the Northern Hemisphere, Geophys. Res. Lett., 41, 4050–4058, doi:10.1002/2014GL059962, 2014.

Schmidt, J. A., Jacob, D. J., Horowitz, H. M., Hu, L., Sherwen, T., Evans, M. J., Liang, Q., Suleiman, R. M., Oram, D. E., Breton, M. L., Percival, C. J., Wang, S., Dix, B., and Volkamer, R.: Modeling the observed tropospheric BrO background: Importance of multiphase chemistry and implications for ozone, OH, and mercury, J Geophys. Res-Atmos., doi:10.1002/2015JD024229, 2016.

Schönhardt, A., Richter, A., Wittrock, F., Kirk, H., Oetjen, H., Roscoe, H. K., and Burrows, J. P.: Observations of iodine monoxide columns from satellite, Atmos. Chem. Phys., 8, 637–653, doi:10.5194/acp-8-637-2008, 2008.

Schweitzer, F., Mirabel, P., and George, C.: Uptake of Hydrogen Halides by Water Droplets, J Phys Chem A, 104, 72–76, doi:10.1021/jp992621o, http://dx.doi.org/10.1021/jp992621o, 2000.

Seakins, P. W., Pilling, M. J., Niiranen, J. T., Gutman, D., and Krasnoperov, L. N.: Kinetics and thermochemistry of R + HBr <=> RH + Br reactions : determinations of the heat of formation of C2H5, i-C3H7, sec-C4H9, and t-C4H9, J. Phys. Chem., 96, 9847–9855, 1992.

Sherwen, T., Evans, M. J., Carpenter, L. J., Andrews, S. J., Lidster, R. T., Dix, B., Koenig, T. K., Sinreich, R., Ortega, I., Volkamer, R., Saiz-Lopez, A., Prados-Roman, C., Mahajan, A. S., and Ordóñez, C.: Iodine's impact on tropospheric oxidants: a global model study in GEOS-Chem, Atmos. Chem. Phys., 16, 1161–1186, doi:10.5194/acp-16-1161-2016, 2016a.

Sherwen, T., Evans, M. J., Carpenter, L. J., Schmidt, J. A., and Mickely, L. J.: Halogen chemistry reduces tropospheric O3 radiative forcing, Atmospheric Chemistry and Physics Discussions, pp. 1–18, doi:10.5194/acp-2016-688, http://www.atmos-chem-phys-discuss.net/acp-2016-688/, 2016b.

Simpson, W. R., Brown, S. S., Saiz-Lopez, A., Thornton, J. A., and von Glasow, R.: Tropospheric Halogen Chemistry: Sources, Cycling, and Impacts, Chemical Reviews, 115, 4035–4062, doi:10.1021/cr5006638, 2015.

Sinreich, R., Coburn, S., Dix, B., and Volkamer, R.: Ship-based detection of glyoxal over the remote tropical Pacific Ocean, Atmospheric Chemistry and Physics, 10, 11 359–11 371, doi:10.5194/acp-10-11359-2010, 2010.

Sofen, E. D., Bowdalo, D., Evans, M. J., Apadula, F., Bonasoni, P., Cupeiro, M., Ellul, R., Galbally, I. E., Girgzdiene, R., Luppo, S., Mimouni, M., Nahas, A. C., Saliba, M., and Tørseth, K.: Gridded global surface ozone metrics for atmospheric chemistry model evaluation, Earth Syst Sci Data, 8, 41–59, doi:10.5194/essd-8-41-2016, 2016.

Sommariva, R. and von Glasow, R.: Multiphase halogen chemistry in the tropical Atlantic Ocean, Environ. Sci. Technol., 46, 10 429–10 437, doi:10.1021/es300209f, 2012.

Spietz, P., Gómez Martín, J. C., and Burrows, J. P.: Spectroscopic studies of the I2/O3 photochemistry: Part 2. Improved spectra of iodine oxides and analysis of the IO absorption spectrum, J Photoch. Photobio. A, 176, 50–67, doi:http://dx.doi.org/10.1016/j.jphotochem.2005.08.023, 2005.

Tham, Y. J., Yan, C., Xue, L., Zha, Q., Wang, X., and Wang, T.: Presence of high nitryl chloride in Asian coastal environment and its impact on atmospheric photochemistry, Chin. Sci. Bull, 59, 356–359, doi:10.1007/s11434-013-0063-y, 2014.

Theys, N., Van Roozendael, M., Hendrick, F., Yang, X., De Smedt, I., Richter, A., Begoin, M., Errera, Q., Johnston, P. V., Kreher, K., and De Mazière, M.: Global observations of tropospheric BrO columns using GOME-2 satellite data, Atmos. Chem. Phys., 11, 1791–1811, doi:10.5194/acp-11-1791-2011, 2011.

Thornton, J. A., Kercher, J. P., Riedel, T. P., Wagner, N. L., Cozic, J., Holloway, J. S., Dubé, W. P., Wolfe, G. M., Quinn, P. K., Middlebrook, A. M., Alexander, B., and Brown, S. S.: A large atomic chlorine source inferred from mid-continental reactive nitrogen chemistry, Nature, 464, 271–274, 2010.

Unger, N., Shindell, D. T., Koch, D. M., and Streets, D. G.: Cross influences of ozone and sulfate precursor emissions changes on air quality and climate, Proc. Natl. Acad. Sci. U.S.A., 103, 4377–4380, doi:10.1073/pnas.0508769103, 2006.

Vogt, R., Sander, R., Von Glasow, R., and Crutzen, P. J.: Iodine chemistry and its role in halogen activation and ozone loss in the marine boundary layer: A model study, J Atmos. Chem., 32, 375–395, doi:10.1023/a:1006179901037, 1999.

Volkamer, R., Baidar, S., Campos, T., Coburn, S., DiGangi, J., Dix, B., Eloranta, E., Koenig, T., Moley, B., Ortega, I., Pierce, B., Reeves, M., Sinreich, R., Wang, S.-Y., Zondlo, M., and Romashkin, P.: Aircraft measurements of BrO, IO, glyoxal, NO2, H2O, O2-O2 and aerosol extinction profiles in the tropics: Comparison with aircraft-/ship-based in situ and lidar measurements, Atmos. Meas. Tech., 8, 623–687, doi:10.5194/amt-8-2121-2015, 2015.

von Glasow, R., von Kuhlmann, R., Lawrence, M. G., Platt, U., and Crutzen, P. J.: Impact of reactive bromine chemistry in the troposphere, Atmos. Chem. Phys., 4, 2481–2497, doi:10.5194/acp-4-2481-2004, 2004.

Wang, S.-Y., Schmidtd, J., Baidar, S., Coburn, S., Dix, B., Koenig, T., Apel, E., Bowdalo, D., Campos, T., Eloranta, E., Evans, M., DiGangii, J., Zondlo, M., Gao, R.-S., Haggerty, J., Hall, S., Hornbrook, R., Jacob, D., Morley, B., Pierce, B., Reeves, M., Romashkin, P., ter Schure, A., and Volkamer, R.: Active and widespread halogen chemistry in the tropical and subtropical free troposphere, Proc. Natl. Acad. Sci. U.S.A., 112, 9281–9286, doi:10.1073/pnas.1505142112, 2015.

WOUDC: WOUDC Ozone Monitoring Community, World Meteorological Organization-Global Atmosphere Watch Program (WMO-GAW)/World Ozone and Ultraviolet Radiation Data Centre (WOUDC) [Data]., doi:10.14287/10000001, http://www.woudc.org, 2014.

Young, P. J., Archibald, A. T., Bowman, K. W., Lamarque, J. F., Naik, V., Stevenson, D. S., Tilmes, S., Voulgarakis, A., Wild, O., Bergmann, D., Cameron-Smith, P., Cionni, I., Collins, W. J., Dalsøren, S. B., Doherty, R. M., Eyring, V., Faluvegi, G., Horowitz, L. W., Josse, B., Lee, Y. H., MacKenzie, I. A., Nagashima, T., Plummer, D. A., Righi, M., Rumbold, S. T., Skeie, R. B., Shindell, D. T., Strode, S. A., Sudo, K., Szopa, S., and Zeng, G.: Pre-industrial to end 21st century projections of tropospheric ozone from the Atmospheric Chemistry and Climate Model Intercomparison Project (ACCMIP), Atmos. Chem. Phys., 13, 2063–2090, doi:10.5194/acp-13-2063-2013, 2013.

Ziska, F., Quack, B., Abrahamsson, K., Archer, S. D., Atlas, E., Bell, T., Butler, J. H., Carpenter, L. J., Jones, C. E., Harris, N. R. P., Hepach, H., Heumann, K. G., Hughes, C., Kuss, J., Krüger, K., Liss, P., Moore, R. M., Orlikowska, A., Raimund, S., Reeves, C. E., Reifenhäuser, W., Robinson, A. D., Schall, C., Tanhua, T., Tegtmeier, S., Turner, S., Wang, L., Wallace, D., Williams, J., Yamamoto, H., Yvon-Lewis, S., and Yokouchi, Y.: Global sea-to-air flux climatology for bromoform, dibromomethane and methyl iodide, Atmos. Chem. Phys., 13, 8915–8934, doi:10.5194/acp-13-8915-2013, 2013.

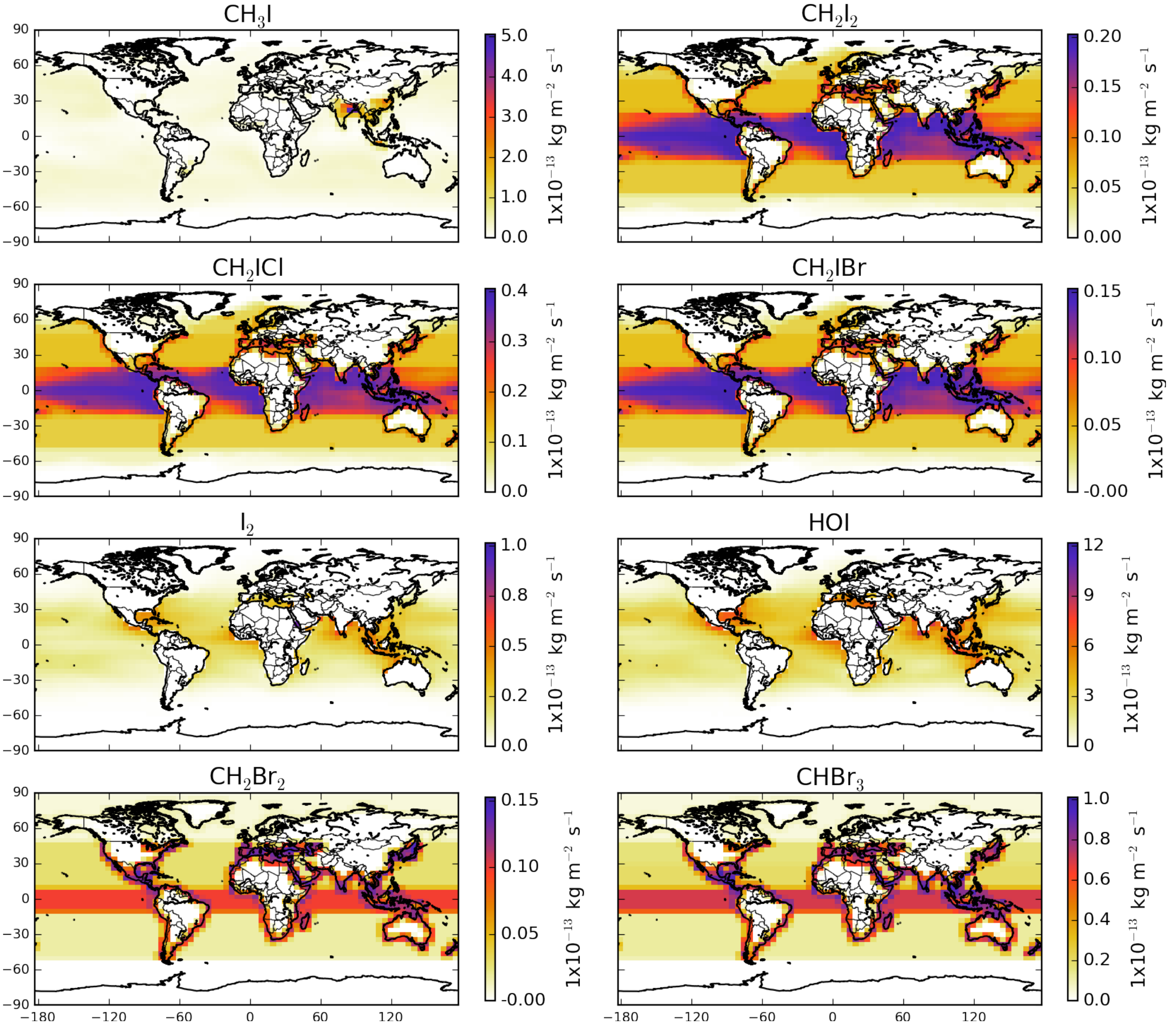

Figure 1. Average annual halogen surface emission of species and column integrated fluxes for species that have fixed surface concentrations in the model (CH_3Cl, CH_3Cl_2, $CHCl_3$, $CHBr_3$) or those with vertically variable sources ($ClNO_2$ from N_2O_5 uptake on sea-salt and IX (X=Cl,Br) production from HOI, lNO_2, and lNO_3 uptake). Values are given in kg X m^{-2} s^{-1} (X=Cl,Br,I).

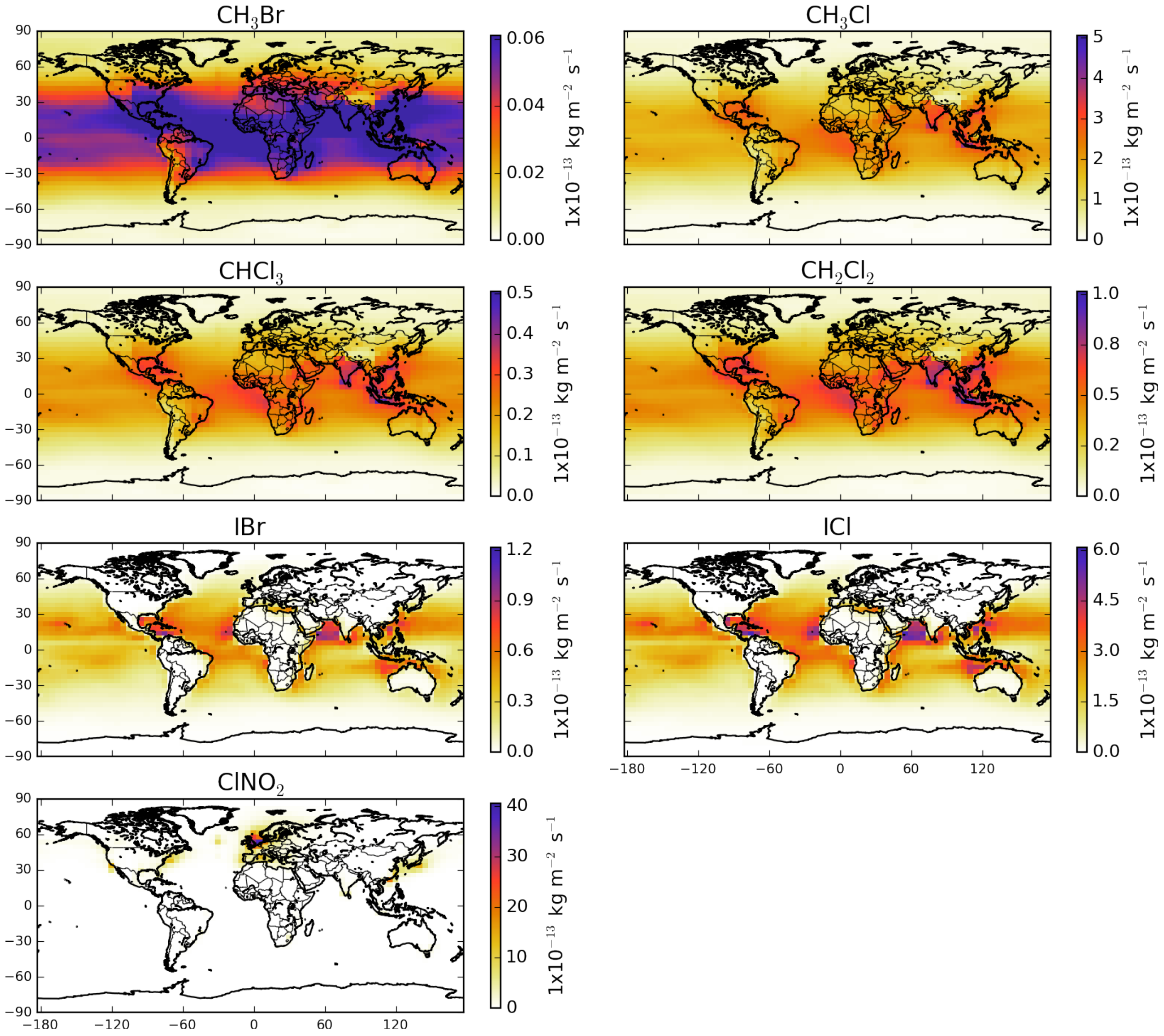

Figure 1. Continued.

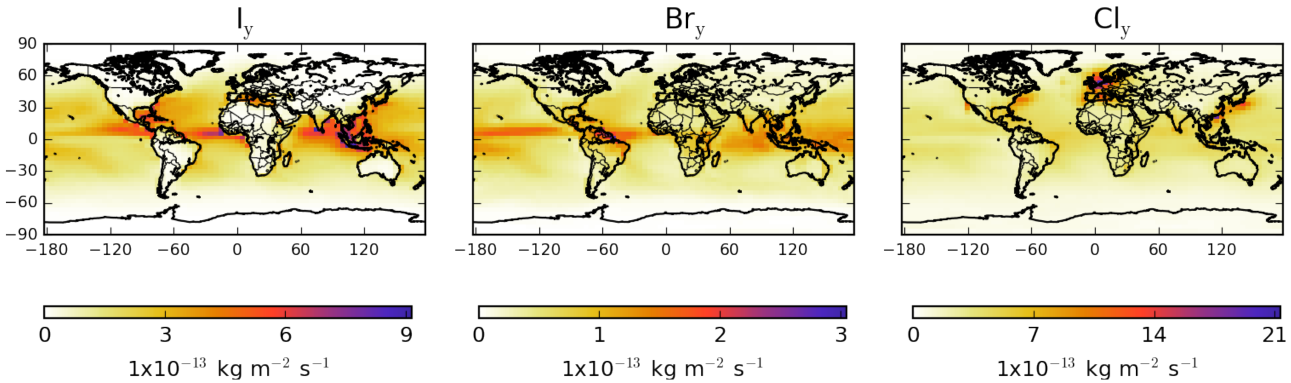

Figure 2. Annual global Xy (X=Cl, Br, I) deposition (defined in Footnote 1). Values are given in terms of mass of halogen deposited (kg X m^{-2} s^{-1}, X=Cl,Br,I).

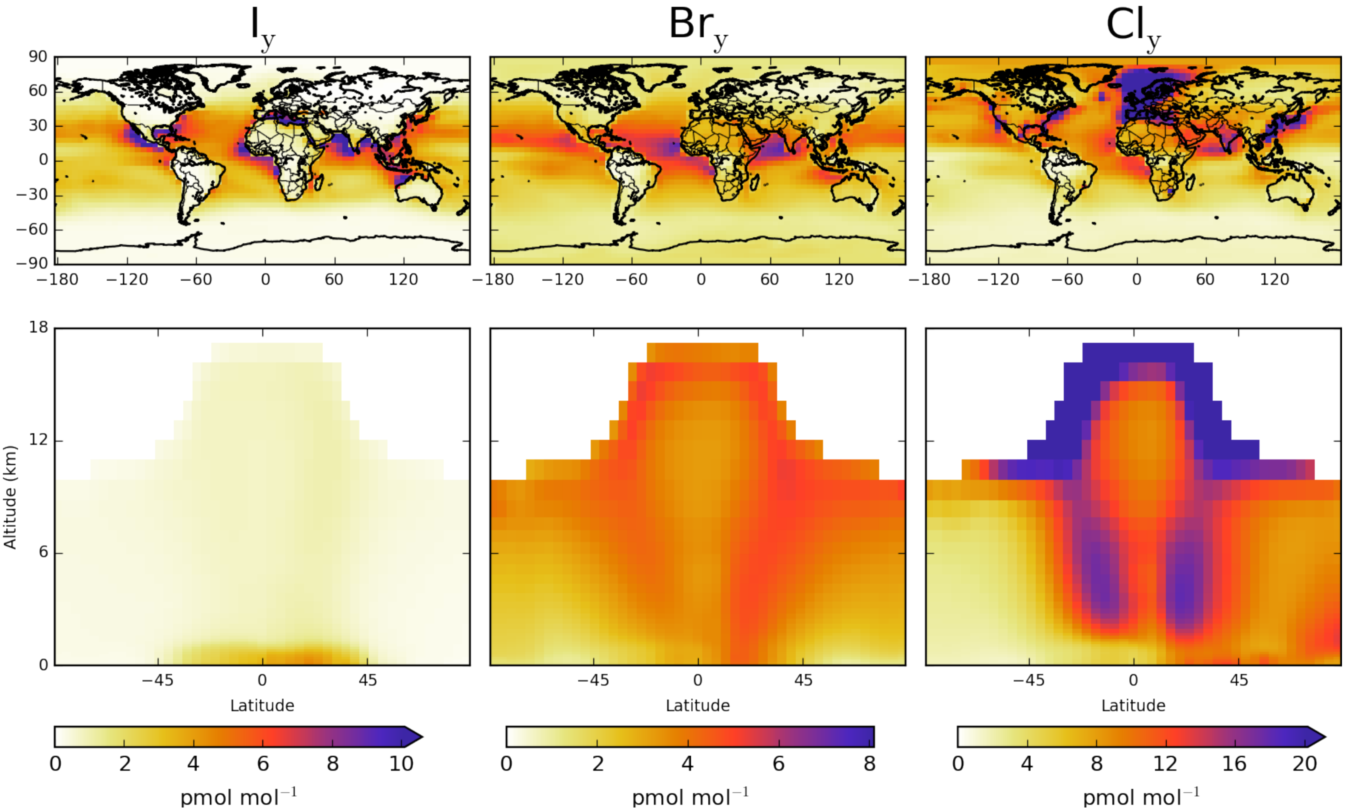

Figure 3. Tropospheric distribution of Cl_y, Br_y, and I_y (defined in Footnote 1) concentrations. Upper plots show surface and lower plots show zonal values. Only boxes that are entirely tropospheric are included in this plot. The Cl_y colourbar is capped at 20 pmol mol^{-1}, with a maximum plotted value of ~~118~~ 116 pmol mol^{-1} at the surface over the North Sea. The I_y ~~colorer~~ colourbar is capped at 10 pmol mol^{-1}, with a maximum plotted value of ~~17~~ 16.4 pmol mol^{-1} at the surface over the Red Sea.

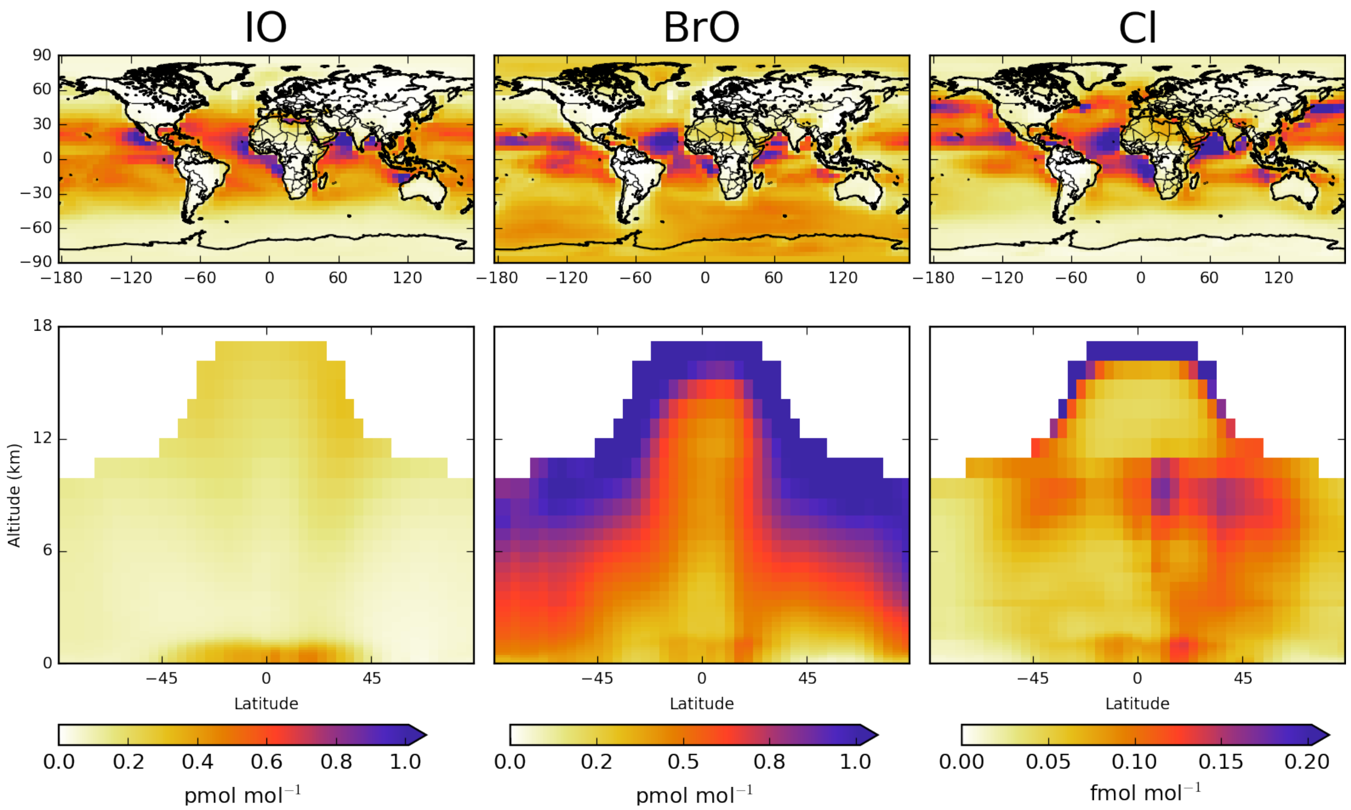

Figure 4. Tropospheric distribution of IO, BrO, and Cl concentrations. Upper plots show surface and lower plots show zonal values. Only boxes that are entirely tropospheric are included in this plot.

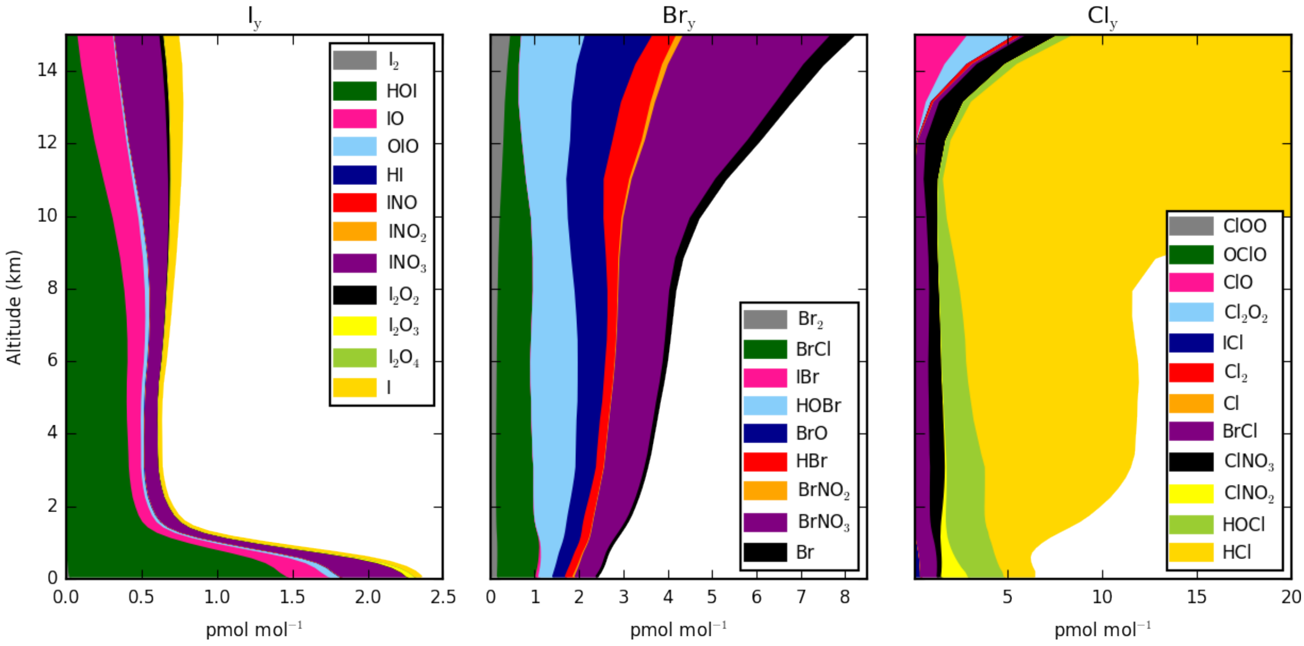

Figure 5. Modelled global average vertical Xy (X=Cl, Br, I) (defined in Footnote 1). Units are pmol mol^{-1} of X (where X=Cl, Br, I). For Cl_y the y-axis is capped at 20 pmol mol^{-1} to show speciation. A Cl_y maximum of 1062 pmol mol^{-1} is found within the altitudes shown due to additional HCl contributions increasing with altitude.

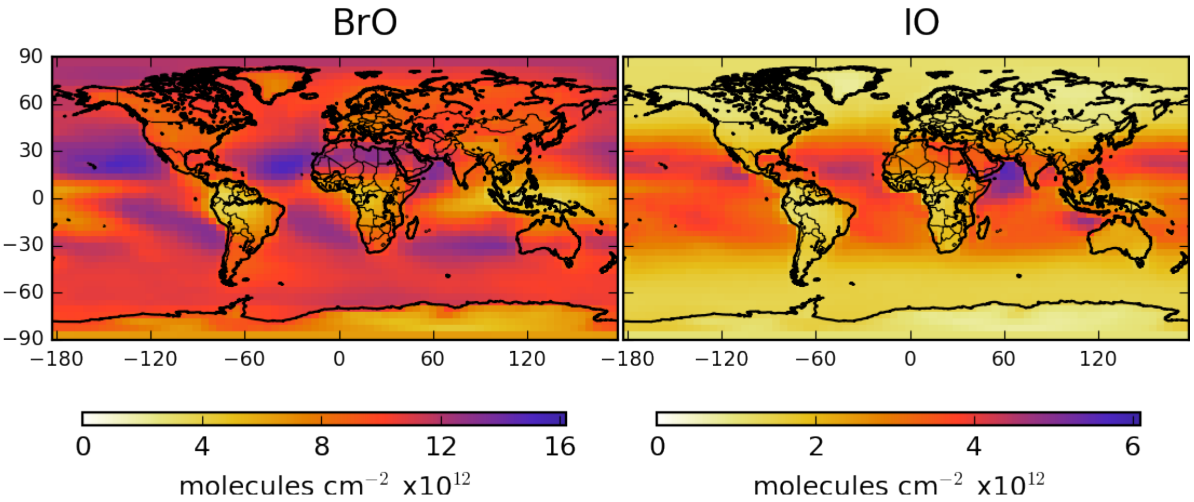

Figure 6. Annual mean integrated model tropospheric column for BrO and IO in molecules cm^{-2}.

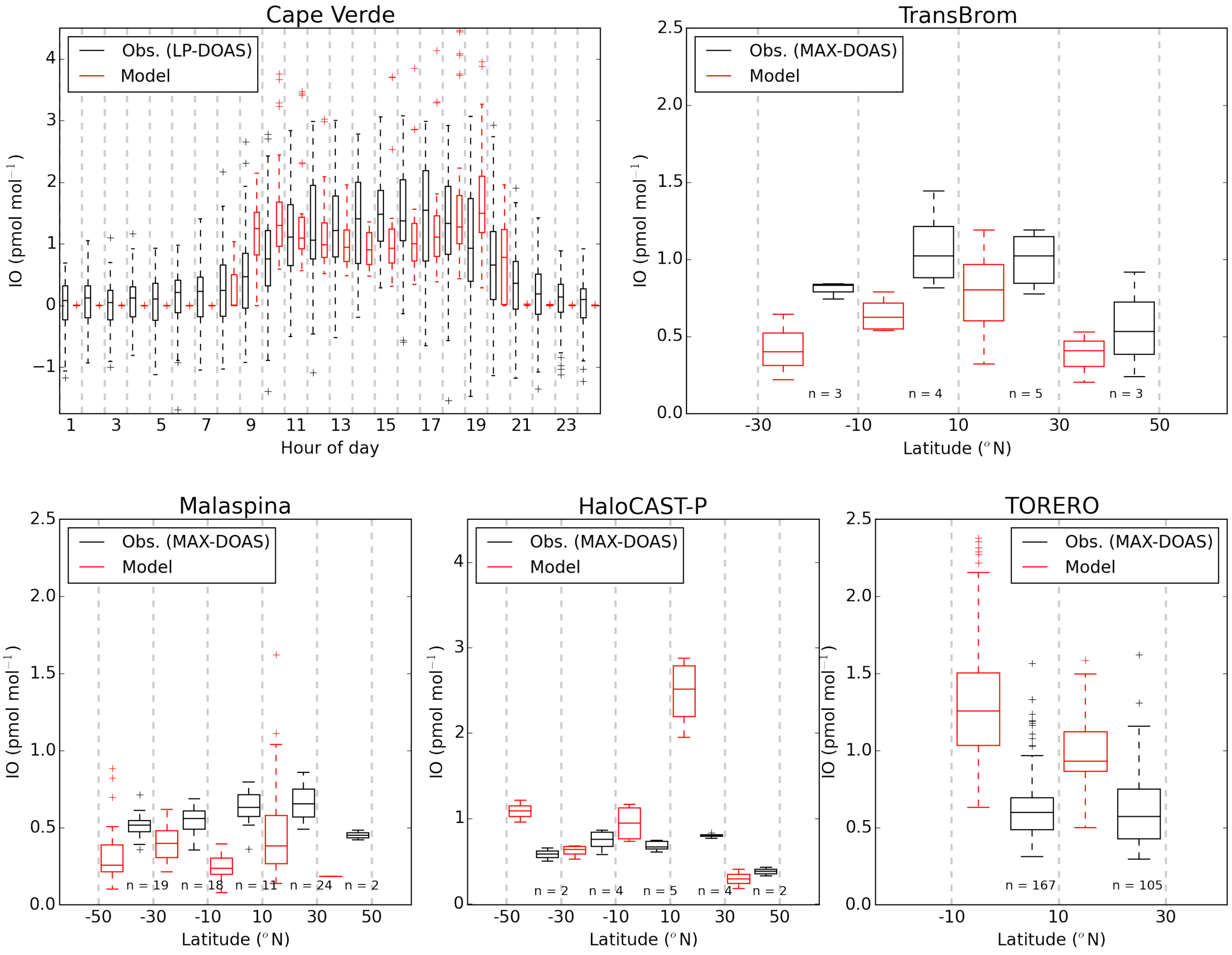

Figure 7. Iodine oxide (IO) surface observations (black) by campaign compared against the simulation with halogen chemistry ("Cl+Br+I", red). Cape Verde measurements are shown against hour of day and others are shown as a function of latitude. Values are considered in 20° bins, with observations and modelled values at the same location and time (as described in section 2) shown side-by-side around the mid point of each bin. The extent of the bins is highlighted with grey dashed lines. Observations are from Cape Verde (Tropical Atlantic, Mahajan et al. 2010; Read et al. 2008), TransBrom (West Pacific, Großmann et al. 2013), the Malaspina circumnavigation (Prados-Roman et al., 2015b), HaloCAST-P (East Pacific, Mahajan et al. 2012), and TORERO ship (East Pacific, Volkamer et al. 2015). The number of data points within latitudinal bin are shown as "n". The boxplot extents give the inter-quartile range, with the median shown within the box. The whiskers give the most extreme point within 1.5 times the inter-quartile range. Locations of observations are shown in Fig. 20.

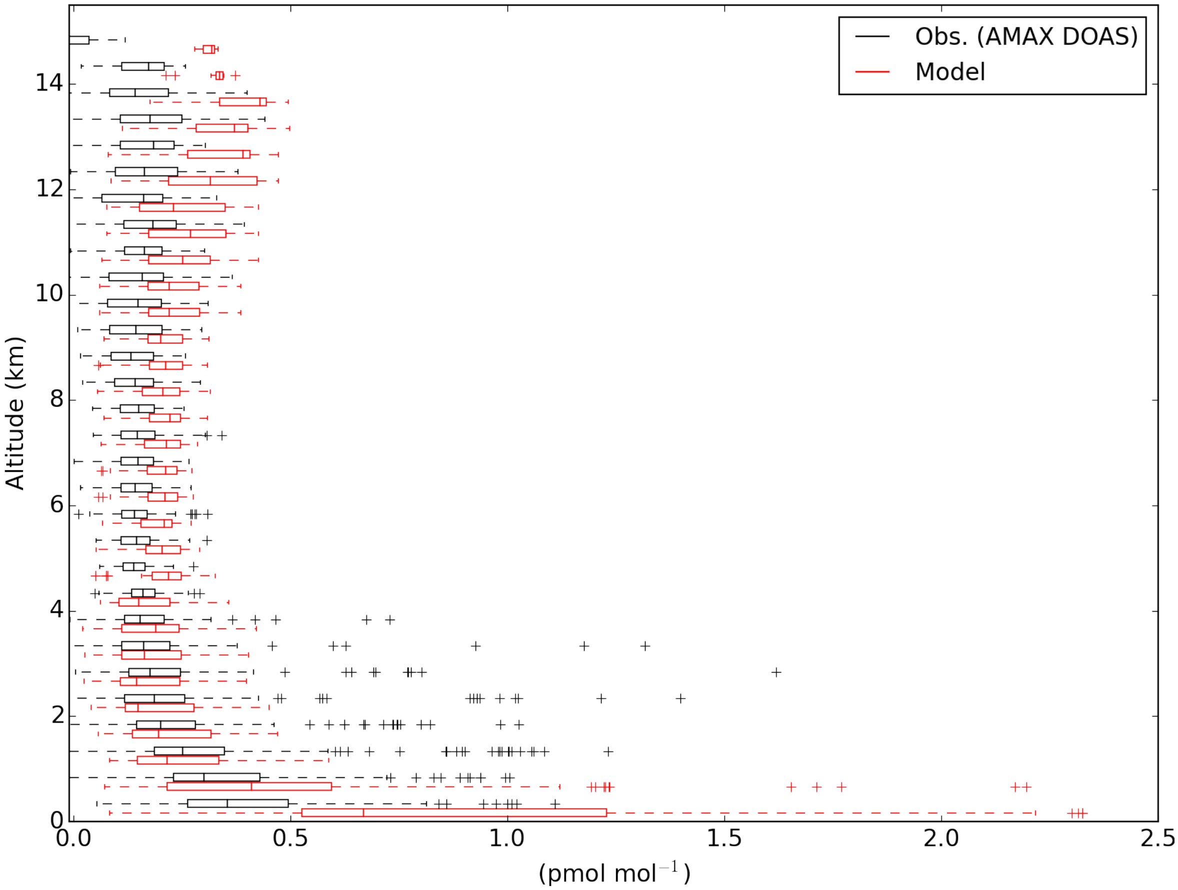

Figure 8. Vertical comparison of the model ("Cl+Br+I") and measured iodine oxide (IO) during TORERO aircraft campaign (Volkamer et al., 2015; Wang et al., 2015). Model and observations are in red and black respectively. Values are considered in 0.5 km bins, with observations and modelled values at the same location and time (as described in section 2) shown side-by-side around the mid point of each bin. Measurements were taken aboard the NSF/NCAR GV research aircraft by the University of Colorado airborne Multi-Axis DOAS instrument (CU AMAX-DOAS) in the eastern Pacific in January and February 2012 (Volkamer et al., 2015; Wang et al., 2015). The boxplot extents give the inter-quartile range, with the median shown within the box. The whiskers give the most extreme point within 1.5 times the inter-quartile range. Locations of observations are shown in Fig. 20.

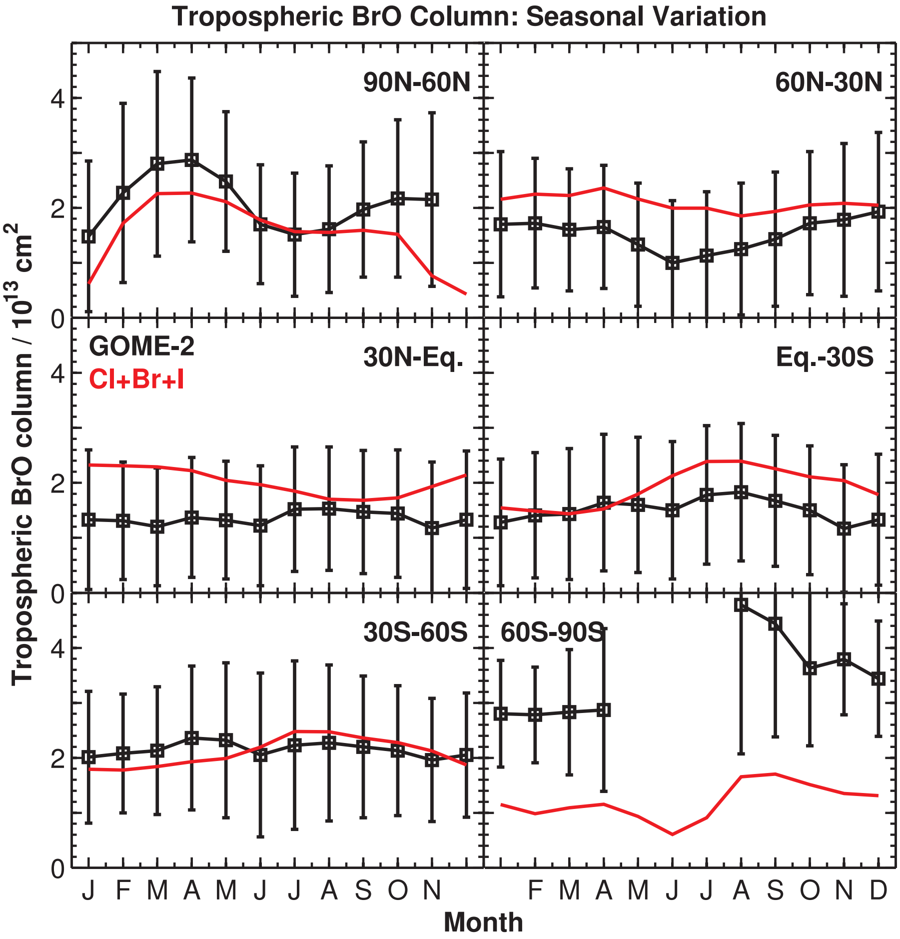

Figure 9. Seasonal variation of zonal mean tropospheric BrO columns in different latitudinal bands. 2007 observations from the GOME-2 satellite instrument (Theys et al., 2011) are compared to GEOS-Chem values at the GOME- 2 local overpass time (9:00-11:00).

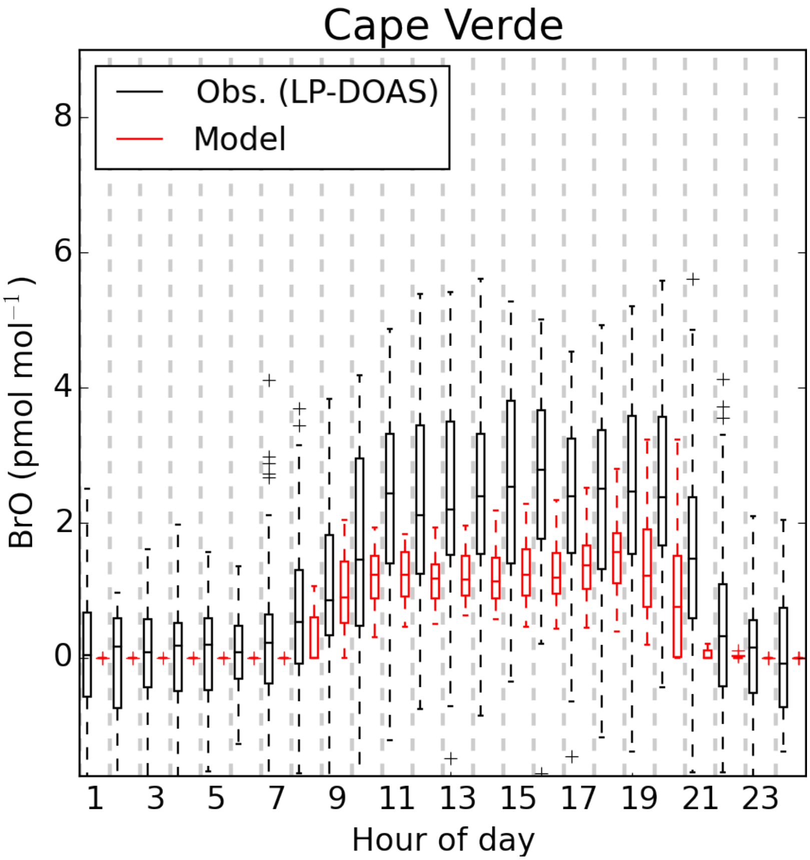

Figure 10. Bromine oxide (BrO) surface observations (black) at Cape Verde (Read et al., 2008; Mahajan et al., 2010) compared against the simulation with halogen chemistry ("Cl+Br+I", red). Values are binned by hour of day. Locations of observations are shown in Fig. 20.

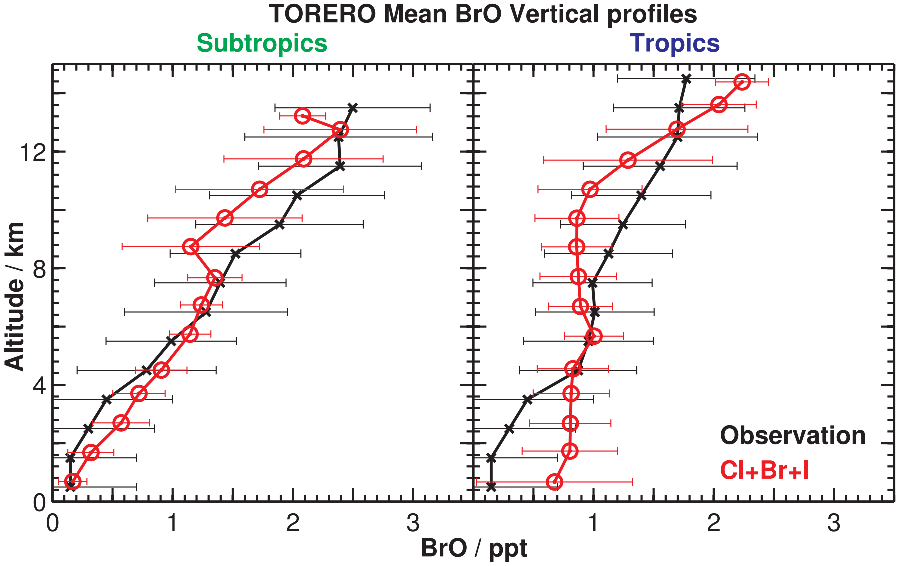

Figure 11. Vertical comparison of the model ("Cl+Br+I") and measured ~~iodine~~ bromine oxide (BrO) during TORERO aircraft campaign (Volkamer et al., 2015; Wang et al., 2015) in the Subtropics (left) and Tropics (right). ~~.~~Model and observations are in red and black, respectively. Observations and modelled values at the same location and time (as described in section 2) are shown side-by-side around the mid point of each bin. Measurements were taken aboard the NSF/NCAR GV research aircraft by the University of Colorado airborne Multi-Axis DOAS instrument (CU AMAX-DOAS) in the eastern Pacific in January and February 2012 (Volkamer et al., 2015; Wang et al., 2015). ~~Observations below 4 km were at or below the limit~~ Locations of ~~detection, which is illustrated with a dashed green line (∼0.5 pmol mol^{-1})~~observations are shown in Fig. 20.

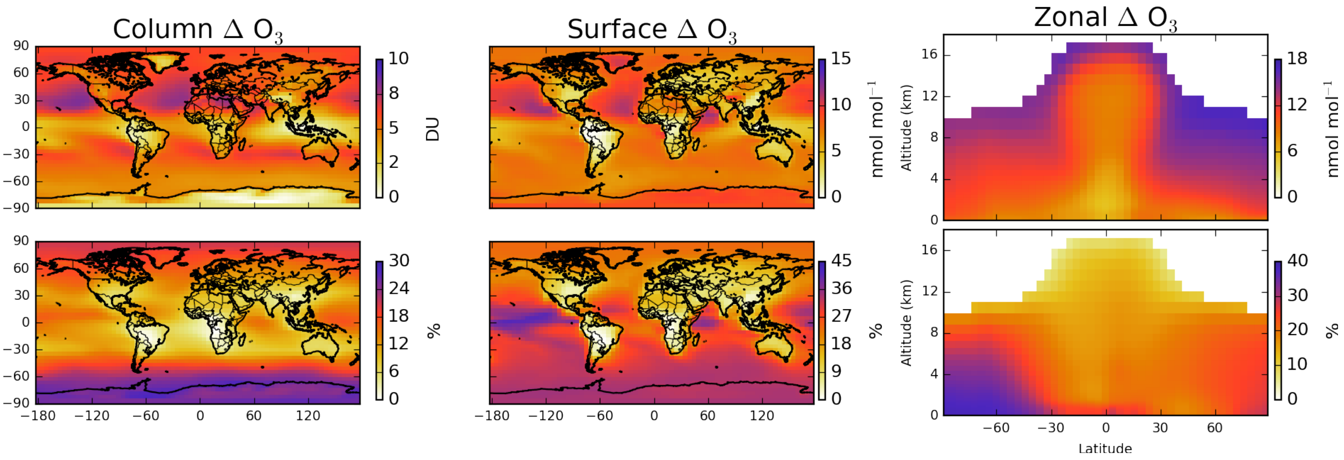

Figure 12. Change in tropospheric O_3 on inclusion of halogen chemistry. Column (left), surface (middle) and zonal (right) change are shown. Upper plots show absolute change and lower plots below give change in % terms ((“Cl+Br+I”-“NOHAL”)/“NOHAL”*100).

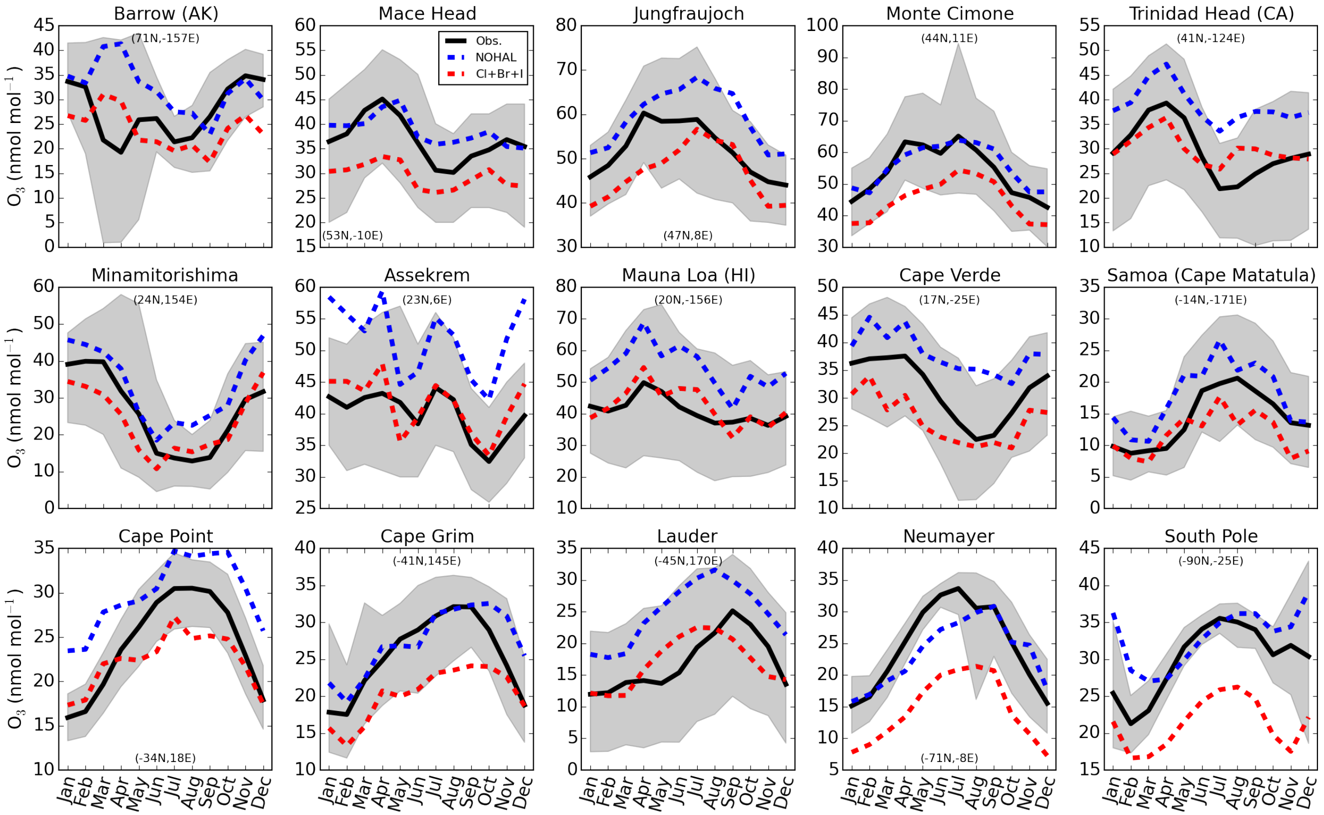

Figure 13. Seasonal cycle of near-surface O_3 at a range of Global Atmospheric Watch (GAW) sites. Observational data shown are 6 year monthly averages (2006-2012). Model data is for 2005. Data is from GAW compiled and processed as described in (Sofen et al., 2016). Blue and red lines represent simulations without halogens ("NOHAL") with halogens ("Cl+Br+I"), respectively. Grey shaded area gives 5^{th} and 95^{th} percentiles of the observations. Locations of observations are shown in Fig. 21.

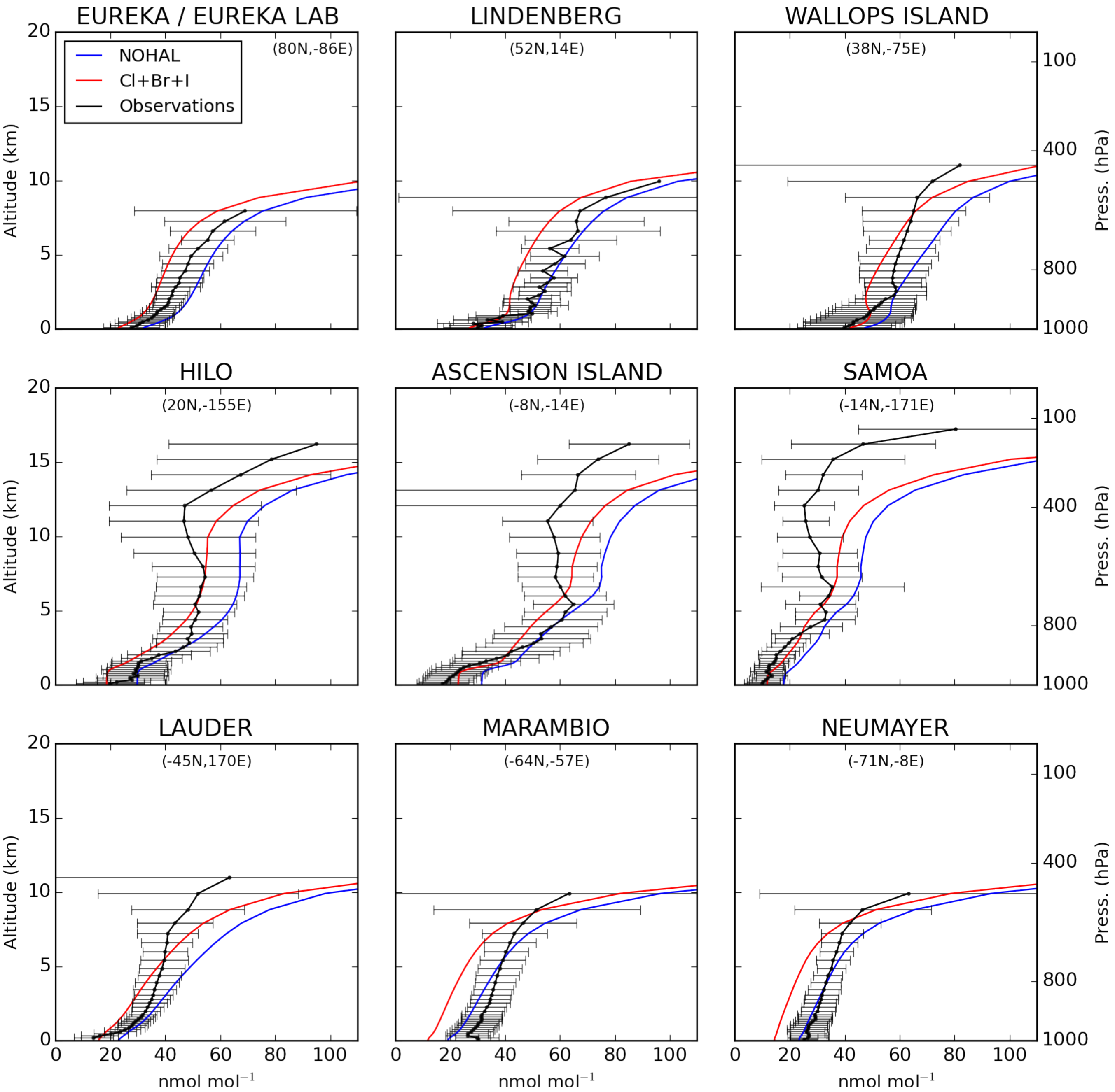

Figure 14. Comparison between annual modelled O_3 profiles and sonde data (2005). Profiles shown are the annual mean of available observations from World Ozone and Ultraviolet Radiation Data Centre (WOUDC, 2014) and model data for 2005 at given locations. Blue and red lines represent simulations without halogens ("NOHAL") with halogens ("Cl+Br+I"), respectively. Observations (in black) show mean concentrations with upper and lower quartiles given by whiskers. Locations of observations are shown in Fig. 21.

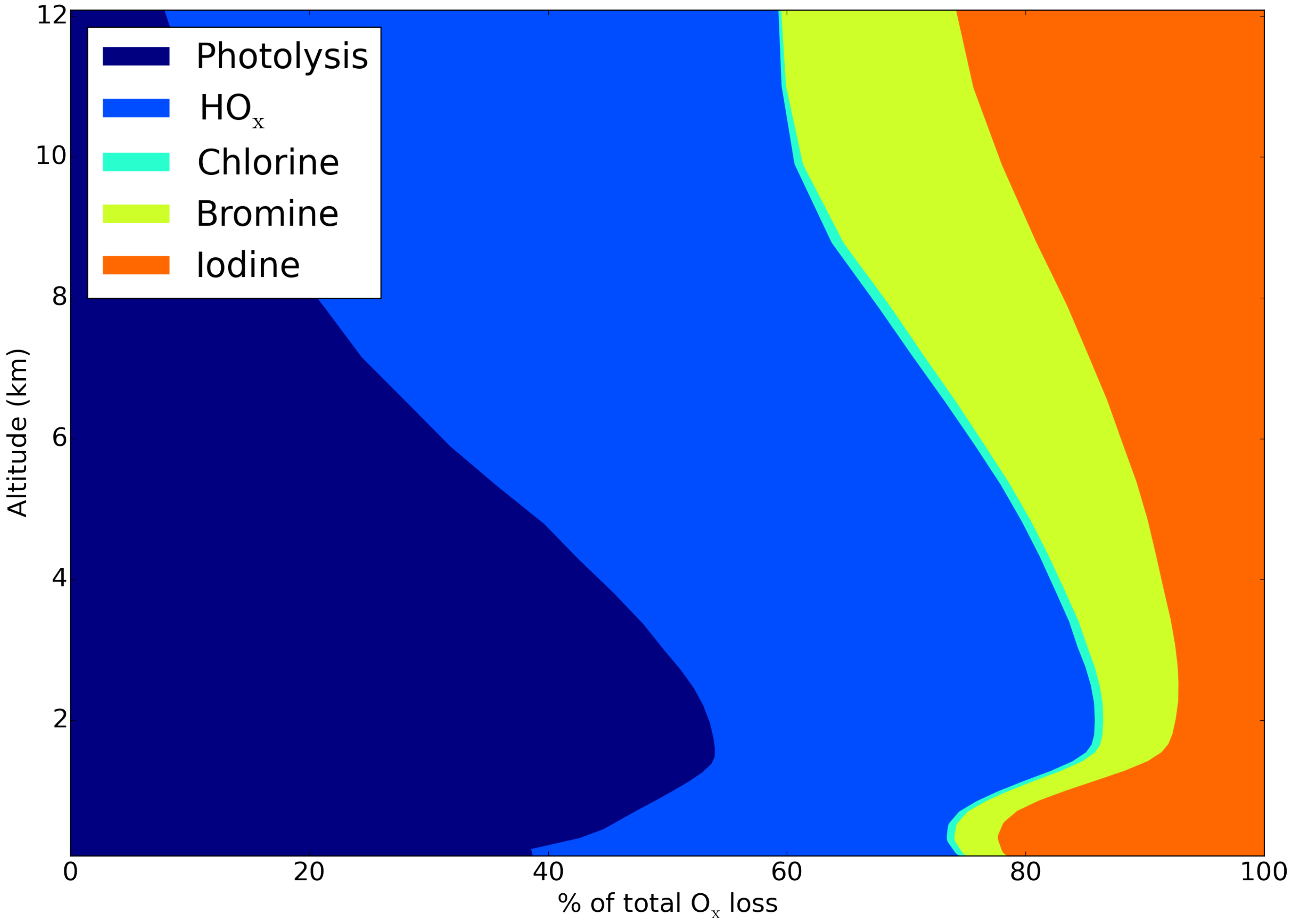

Figure 15. Global annual average tropospheric vertical odd oxygen loss (O_x) through different reaction routes (Photolysis, HO_x, IO_x, BrO_x, and ClO_x).

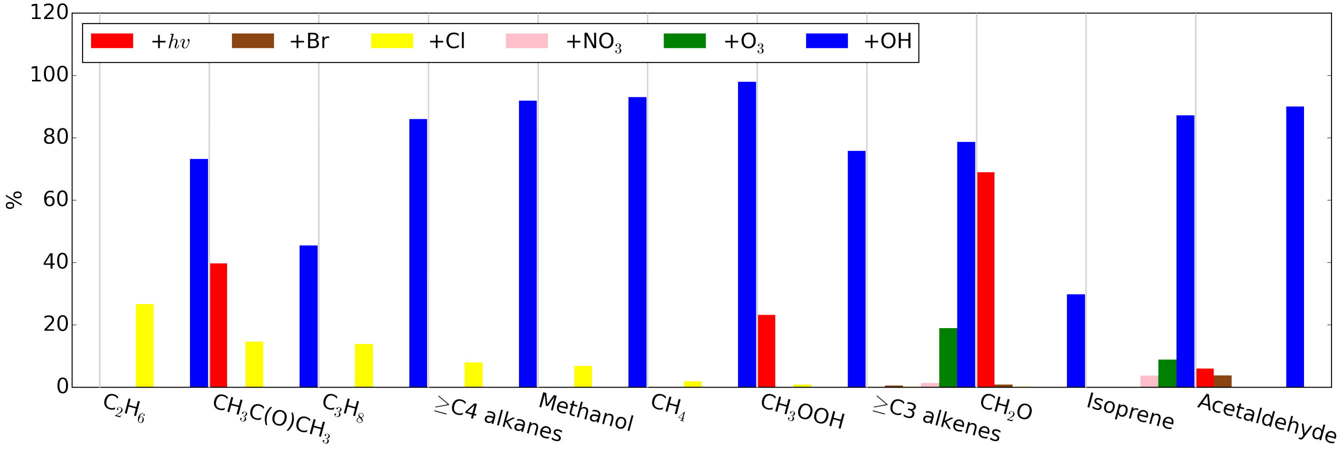

Figure 16. Global loss routes (+$h\nu$, +Br, +NO_3, +Cl, +OH) of organic compounds shown as % of total tropospheric losses.

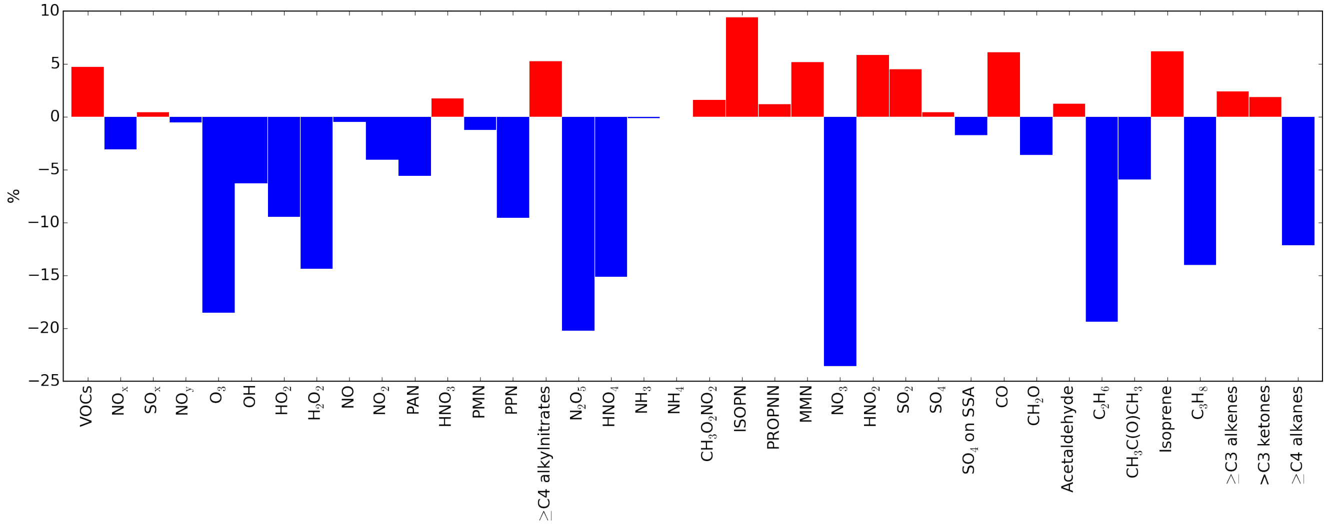

Figure 17. Changes in tropospheric burden of species and families on inclusion of halogens (“Cl+Br+I”) compared to no halogens (“NOHAL”). Burdens are considered in elemental terms (e.g Tg S/N/C) and species masses for OH, HO_2, H_2O_2 and O_3. The family denoted by “VOCs” in this plot is defined as the sum of carbon masses of CO, formaldehyde, acetaldehyde, ethane, acetone, isoprene, propane, ≥C4 alkanes, ≥C3 alkenes, and ≥~~3C~~ C3 ketones. Abbreviations for tracers are expanded in Footnote 3

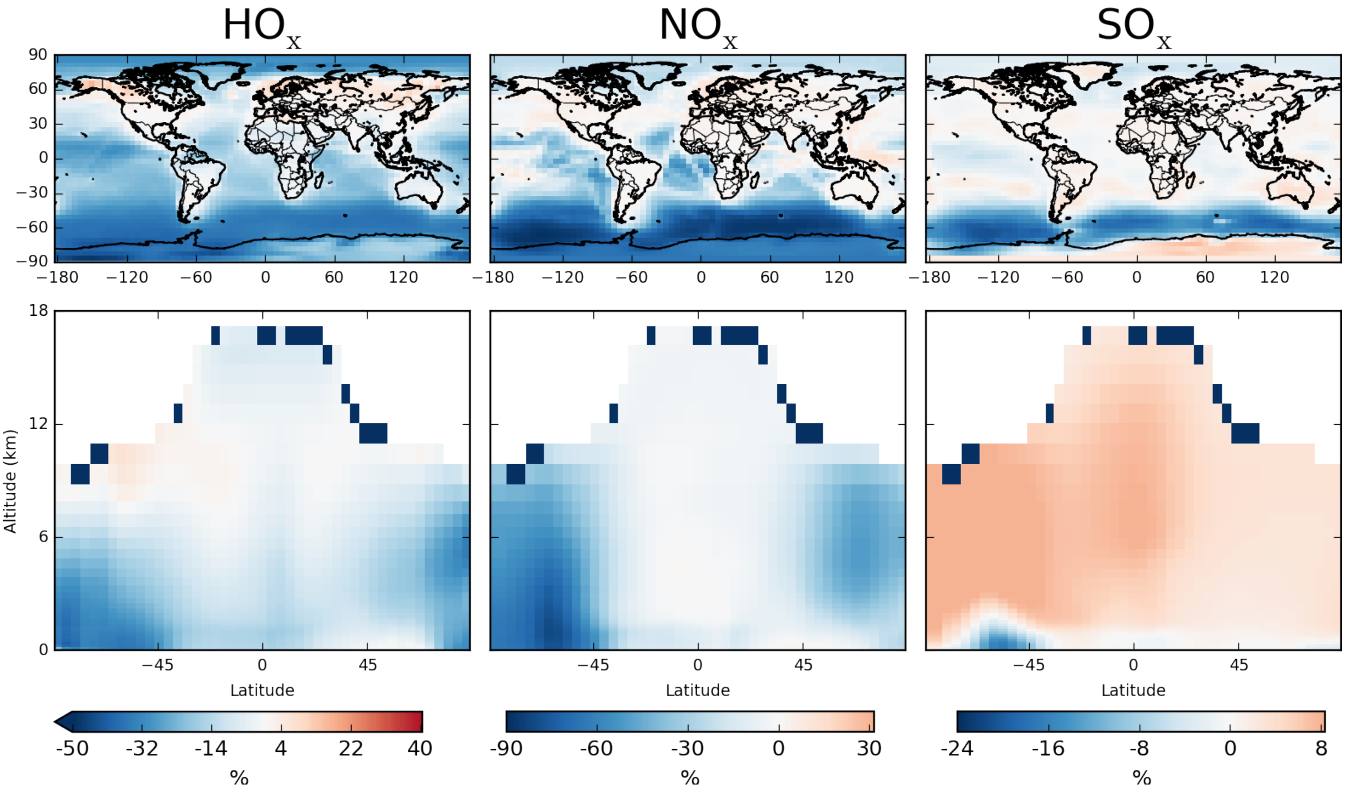

Figure 18. Global annual average surface and zonal change (%) in HO$_x$, NO$_x$ and SO$_x$ families (as defined in Footnote 4) on inclusion of halogens

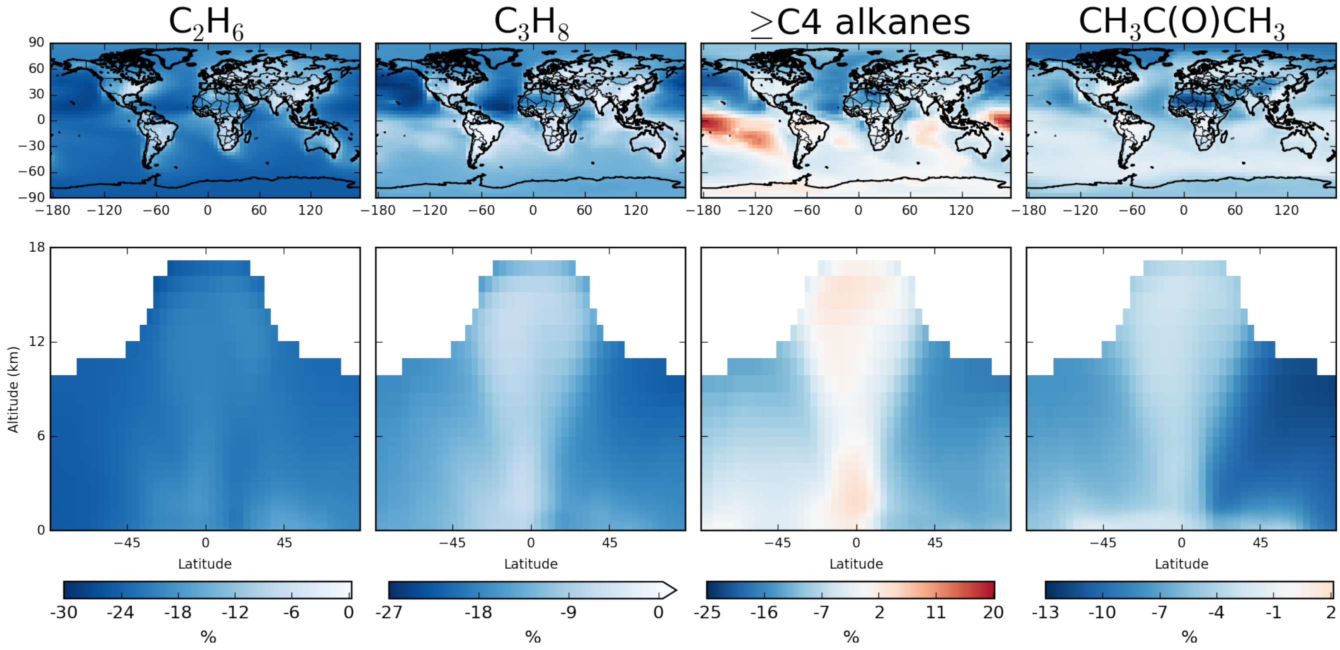

Figure 19. Global annual average surface and zonal change (%) in ethane (C_2H_6), propane (C_3H_8), ≥C4 alkanes, and acetone ($CH_3C(O)CH_3$) on inclusion of halogens. For species where all average changes are negative a continuous colourbar is used (C_3H_8 and C_2H_6) and for species where both negative and positive changes are present a divergent colourbar is used (≥C4 alkanes and $CH_3C(O)CH_3$).

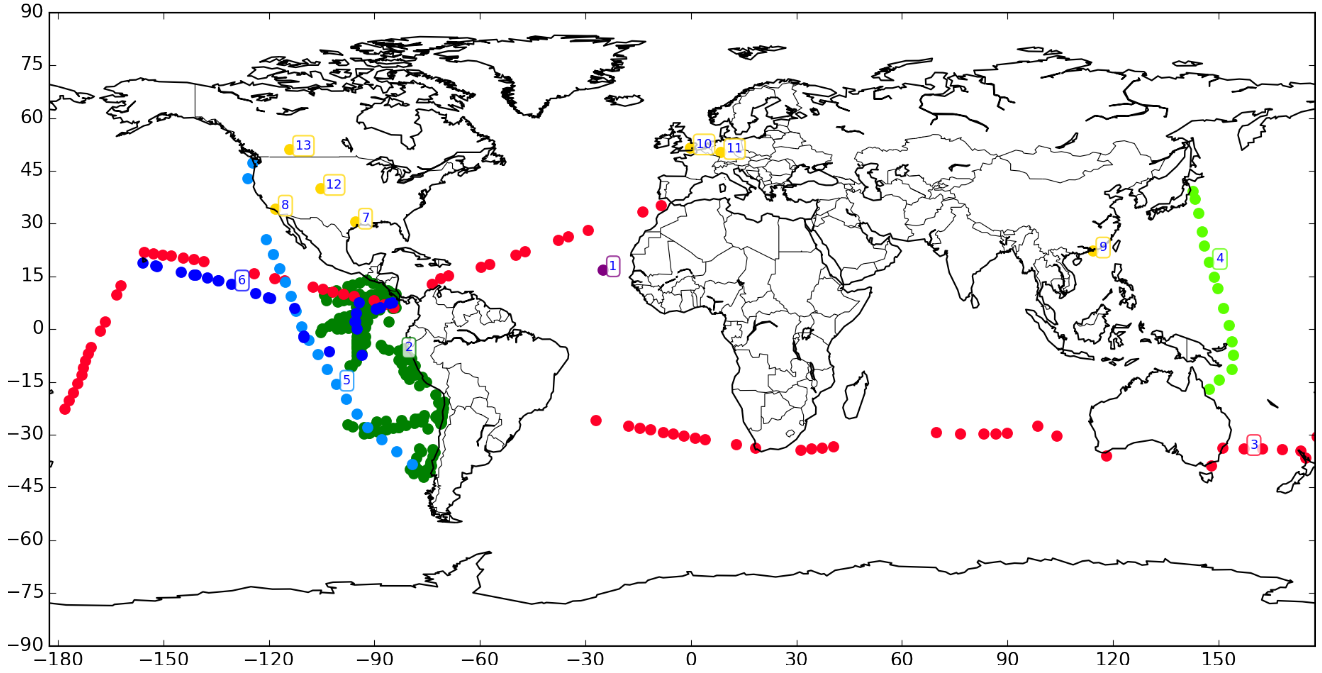

Figure 20. Locations of halogen observations the model is compared against. IO observations are shown in different colours (1=Cape Verde, CV (Read et al., 2008; Mahajan et al., 2010); 2=TORERO (aircraft-based, Volkamer et al. 2015; Wang et al. 2015); 3=Malasapina (Prados-Roman et al., 2015b); 4=TransBrom (Prados-Roman et al., 2015b); 5=HaloCAST-P (Mahajan et al., 2012); 6=TORERO (ship-based, Volkamer et al. 2015; Wang et al. 2015). BrO observations presented here were made at the same locations as IO observations (1=Cape Verde, CV (Read et al., 2008; Mahajan et al., 2010); 2=TORERO (aircraft-based, Volkamer et al. 2015; Wang et al. 2015). $ClNO_2$ observations are shown in gold (7=Texas, US (Faxon et al., 2015; Osthoff et al., 2008); 8=California, US (Riedel et al., 2012; Mielke et al., 2013); 9=Southern China, CN (Tham et al., 2014); 10= London, GB (Bannan et al., 2015); 11=Hessen, Germany (Phillips et al., 2012); 12=Colorado, US (Thornton et al., 2010; Riedel et al., 2013), 13=Calgary, CA (Mielke et al., 2011)).

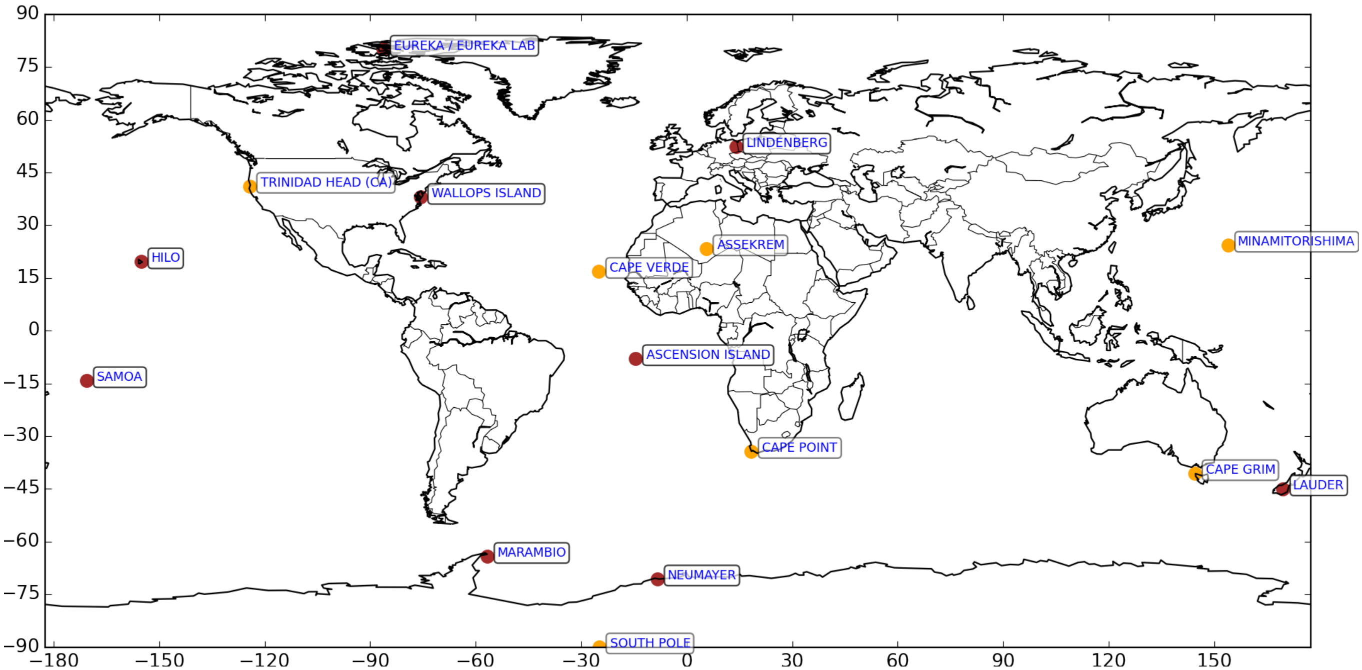

Figure 21. Locations of O_3 observations the model is compared against. Observations made by O_3 sonde are shown in brown, surface observations at GAW sites are shown in gold. Where a site is both a location of sonde release and surface O_3 observation it is shown in brown (Samoa, Neumayer, Lauder, and Milo).

Table 1. Additional halogen reactions included in this simulation that are not described in previous work ~~(Eastham et al., 2014; Schmidt et al., 2016; ?)~~(Eastham et al., 2014; Schmidt et al., 2016; Sherwen et al., 2016a). The full reaction scheme is given in the Appendix (Sections 6-9). The rate constant is calculated using a standard Arrhenius expression ~~$Ae^{-(Ea/RT)}$~~$A \cdot \exp(\frac{-Ea}{RT})$.

Rxn ID	Reaction	A cm^3 $molecules^{-1}$ s^{-1}	~~Ea/R~~ $-Ea/R$ K	Citation
M29	IO + ClO $\rightarrow$ I + OClO	2.59x10^{-12}	280	Atkinson et al. (2007)
M30	IO + ClO $\rightarrow$ I + Cl + O_2	1.18x10^{-12}	280	Atkinson et al. (2007)
M31	IO + ClO $\rightarrow$ ICl + O_2	9.40x10^{-13}	280	Atkinson et al. (2007)
M32	Cl + HCOOH $\rightarrow$ HCl + CO2 + H_2O	2.00x10^{-13}	-	Sander et al. (2011)
M33	Cl + CH_3O_2 $\rightarrow$ ClO + CH_2O + HO_2(●)	1.60x10^{-10}	-	Sander et al. (2011)
M34	Cl + CH_3OOH $\rightarrow$ HCl + CH_3O_2	5.70x10^{-11}	-	Sander et al. (2011)
M35	Cl + C_2H_6 $\rightarrow$ HCl + $C_2H_5O_2$	7.20x10^{-11}	-70	Sander et al. (2011)
M36	Cl + $C_2H_5O_2$ $\rightarrow$ ClO + HO_2+ ALD2 ($\star$)	7.40x10^{-11}	-	Sander et al. (2011)
M37	Cl + EOH $\rightarrow$ HCl + ALD2 ($\triangleleft$)	9.60x10^{-11}	-	Sander et al. (2011)
M38	Cl + $CH_3C(O)OH$ $\rightarrow$ HCl + CH_3O_2, + CO2	2.80x10^{-14}	-	Sander et al. (2011)
M39	Cl + C_3H_8 $\rightarrow$ HCl + A3O2	7.85x10^{-11}	-80	Sander et al. (2011)
M40	Cl + C_3H_8 $\rightarrow$ HCl + B3O2	6.54x10^{-11}	-	Sander et al. (2011)
M41	Cl + ACET $\rightarrow$ HCl + ATO2	7.70x10^{-11}	-1000	Sander et al. (2011)
M42	Cl + ISOP $\rightarrow$ HCl + RIO2	7.70x10^{-11}	500	Sander et al. (2011)
M43	Cl + MOH $\rightarrow$ HCl + CH_2O + HO_2	5.50x10^{-11}	-	Sander et al. (2011)
M61	Cl + ALK4 $\rightarrow$ HCl + R4O2	2.05x10^{-10}	-	Atkinson et al. (2006)
M62	Br + PRPE $\rightarrow$ ~~HCl~~HBr + PO2	3.60x10^{-12}	-	Atkinson et al. (2006)
M63	Cl + PRPE $\xrightarrow{M}$ HCl + PO2 ~~+ M~~	2.80x10^{-10}($)	-	Atkinson et al. (2006)
H1	N_2O_5 $\xrightarrow{\gamma}$ HNO_3+ $ClNO_2$(⊖)	-	-	(see table footnote)
H2	HOI $\xrightarrow{\gamma}$ 0.85ICl + 0.15IBr*	-	-	(see table footnote)
H3	INO_2 $\xrightarrow{\gamma}$ 0.85ICl +.015IBr*	-	-	(see table footnote)
H4	INO_3 $\xrightarrow{\gamma}$ 0.85ICl + 0.15IBr*	-	-	(see table footnote)
P1	ICl $\xrightarrow{h\nu}$ I + Cl	-	-	Sander et al. (2011)
P2	IBr $\xrightarrow{h\nu}$ I + Br	-	-	Sander et al. (2011)
P3	BrCl $\xrightarrow{h\nu}$ Cl + Br	-	-	Sander et al. (2011)

Table footnote: (●) Reaction from JPL, only considering the major channel (Dale and Poulet. 1996) and product of CH_3O reacts to form CH_2O + HO_2 (CH_3O +O_2 $\rightarrow$ CH_2O + HO_2). ($\star$) Only first channel from JPL considered. the 2nd channel forms a criegee (HCl + $C_2H_4O_2$) and therefore cannot be represented by reduced GEOS-Chem chemistry scheme.($\triangleleft$) Reaction defined by JPL and interpreted as proceeding via hydrogen abstraction, therefore the acetaldehyde product is assumed. ($) K(infinity) rate given in table, K(0) rate = 4.00x10^{-28} with Fc=0.6 as shown in Table 7). (⊖) Reaction only proceeds on sea-salt aerosol, with γ value as described in Evans and Jacob (2005). (*) Reactions which were included in previous work (Sherwen et al. (2016a)), but di-halogen products have been updated split between ICl and IBr (See Section 2) and only proceed on acidic sea-salt aerosol following McFiggans et al. (2000). Acidity of aerosol is calculated as described in Alexander (2005). γ values for uptake of halogen species are given in Table 8. Abbreviations for tracers are expanded in footnote 3.

Table 2. Global sources of reactive tropospheric inorganic halogens. Sources with fixed concentration in the model for Cl_y (CH_3Cl, CH_3Cl_2, $CHCl_3$) and Br_y ($CHBr_3$) are shown in terms of chemical release (e.g. +Cl, +OH, $+h\nu$) and are in bold. Inclusion of chlorine and bromine organic species has been reported before in GEOS-Chem (Eastham et al., 2014; Parrella et al., 2012; Schmidt et al., 2016). X_2 (I_2) and HOX (HOI) are the inorganic ocean source from (Carpenter et al., 2013), XNO_2 is the source from the uptake of N_2O_5 on sea-salt ($ClNO_2$).

Sources	I_y (Tg I yr^{-1})	Br_y (Tg Br yr^{-1})	Cl_y (Tg Cl yr^{-1})
CH_3X	0.26	**0.06**	**~~2.19~~2.10**
CH_2X_2	0.33	0.09	**~~0.59~~0.57**
CHX_3	-	0.41	**~~0.26~~0.25**
HOX	~~2.02~~ 1.97	-	-
X_2	0.14	-	-
IX	-	~~0.31~~0.30(*)	~~0.78~~0.73(*)
XNO_2	-	-	~~0.66~~ 0.65
stratosphere	0.00	0.06	0.43
total source(*)	~~2.75~~ 2.70	~~0.92~~ 0.91	~~4.90~~ 4.72

(*) Note: Acid catalysed sea-salt IX (X=Cl, Br) flux only stated for Cl_y and Br_y as it does not represent a net I_y source.

Table 3. Comparison between modelled and observed $ClNO_2$. Concentrations are shown as the maximum and average of the daily maximum value for the observational and equivalent model time period. Sites marked as (**) are considered continental sites. The model value are taken for the nearest time-step and location within the analysis year (2005).

			Obs.		"Cl+Br+I"		
Location	Lat.	Lon.	Max	Mean	Max	Mean	Reference
Coastal							
Pasedena, CA, US (2010)	34.2	-118.2	3.46	1.48	~~0.44~~ 0.43	0.20	Mielke et al. (2013)
Southern China, CN (2012)	22.2	114.3	2.00	0.31	~~0.61~~ 0.60	0.18	Tham et al. (2014)
Los Angeles, ~~California~~ CA, US (2010)	34.1	-118.2	1.83	0.50	~~0.44~~ 0.43	0.20	Riedel et al. (2012)
Houston, ~~Texas~~ TX, US (2006)	30.4	-95.4	1.15	0.80	0.19	0.04	Osthoff et al. (2008)
London, ~~UK~~ GB (2012)	51.5	-0.2	0.73	0.23	~~0.51~~ 0.50	0.17	Bannan et al. (2015)
~~Texas~~ TX, US (2013)	30.4	-95.4	0.14	0.08	0.19	0.04	Faxon et al. (2015)
Continental							
Hessen, ~~Germany~~ DE (2011)	50.2	8.5	0.85	0.20	0.16	0.02	Phillips et al. (2012)
Boulder, ~~Colorado~~ CO, US (2009)	40.0	-105.3	0.44	0.14	0.00	0.00	Thornton et al. (2010); Riedel et al. (2013)
Calgary, ~~CAN~~ CA, US (2010)	51.1	-114.1	0.24	0.22	0.02	0.01	Mielke et al. (2011)

Table 4. Comparison between global tropospheric ~~O~~O_x ~~$_x$~~ budgets of simulations “Cl+Br+I” (with halogen chemistry) and “NOHAL” (without halogen chemistry). Recent average model values from ACCENT (Young et al., 2013) are also shown for comparison. For the $X_1O + X_2O$ halogen crossover reactions where $X_1O \neq X_2O$ we split the O_3 loss equally between the two routes. Values are rounded to the nearest integer value.

	"Cl+Br+I"	"NOHAL"	ACCENT
O_3 burden (Tg)	~~355~~ 339	416	340 ± 40
O_x chemical sources (Tg yr ~~$^{-1}$~~)			
$NO + HO_2$	~~3526~~ 3436	3607	-
$NO + CH_3O_2$	~~1327~~ 1288	1316	-
$NO + RO_2$	~~524~~ 525	508	-
Total chemical ~~sources (~~O_x sources (PO_x)	~~5376~~ 5249	5431	5110 ± 606
O_x chemical sinks (Tg yr^{-1})			
$O_3 + H_2O \xrightarrow{h\nu} 2OH + O_2$	~~2102~~ 1997	2489	-
$O_3 + HO_2 \rightarrow OH + O_2$	~~1136~~ 1061	1432	-
$O_3 + OH \rightarrow HO_2 + O_2$	~~611~~ 562	737	-
$HOBr \xrightarrow{h\nu} Br + OH$	~~214~~ 285	-	-
$HOBr + HCl \rightarrow BrCl$	~~28~~ 54	-	-
$HOBr + HBr \rightarrow Br_2 + H_2O$ (aq. aerosol)	~~13~~ 22	-	-
$BrO + BrO \rightarrow 2Br + O_2$	~~8~~ 13	-	-
$BrO + BrO \rightarrow Br_2 + O_2$	~~3~~ 4	-	-
$BrO + OH \rightarrow Br + HO_2$	~~9~~ 12	-	-
$IO + BrO \rightarrow Br + I + O_2$	~~9~~ 11	-	-
$ClO + BrO \rightarrow Br + ClOO/OClO$	~~2~~ 4	-	-
Other bromine O_x sinks	0	-	-
Total bromine O_x sinks	~~284~~ 405	-	-
$HOI \xrightarrow{h\nu} I + OH$	~~457~~ 438	-	-
$OIO \xrightarrow{h\nu} I + O_2$	~~125~~ 140	-	-
$IO + BrO \rightarrow Br + I + O_2$	~~9~~ 11	-	-
$IO + ClO \rightarrow I + Cl + O_2/ ICl + O_2$	~~0~~ 1	-	-
Other iodine O_x sinks	2	-	-
Total iodine O_x sinks	~~593~~ 591	-	-
$HOCl \xrightarrow{h\nu} Cl + OH$	~~15~~ 27	-	-
$CH_3O_2 + ClO \rightarrow ClOO$	~~4~~ 6	-	-
$ClO + BrO \rightarrow Br + ClOO/OClO$	~~2~~ 4	-	-
$ClNO_3 + HBr \rightarrow BrCl$	~~1~~ 2	-	-
$IO + ClO \rightarrow I + Cl + O_2/ ICl + O_2$	~~0~~ 1	-	-
Other chlorine O_x sinks	1	-	-
Total chlorine O_x sinks	~~23~~ 40	-	-
Other O_x sinks	184	172	-
Total chem. ~~sinks (~~O_x sinks (LO_x)	~~4933~~ 4841	4829	4668 ± 727
O_3 PO_x-LO_x (Tg yr^{-1})	~~443~~ 408	602	618 ± 251
O_3 Dry deposition (Tg yr^{-1})	~~832~~ 799	980	1003 ± 200
O_3 Lifetime (days)	22	26	22 ± 2
O_3 STE (PO_x-LO_x-Dry dep.) (Tg yr^{-1})	~~389~~ 391	378	552 ± 168

Table 5. Photolysis reactions of halogens included in scheme. Photolysis is described in Eastham et al. (2014) ($ClNO_2$, $ClNO_3$, and ClOO), ~~?~~ Sherwen et al. (2016a) (I_2, HOI, IO, OIO, INO, INO_2, INO_3, I_2O_2, I_2O_3, I_2O_4, CH_3I, CH_2I_2, CH_2ICl, CH_2IBr), and Schmidt et al. (2016) (BrCl, Cl_2, ClO, HOCl, $ClNO_2$, $ClNO_3$, ClOO, Cl_2O_2, CH_3Cl, CH_3Cl_2, and $CHCl_3$.). As stated in Section 2, we have used the I_2O_2 cross-section for I_2O_4.

ID	Reaction	Cross-section reference
J1	$I_2 \xrightarrow{h\nu} 2I$	Sander et al. (2011)
J2	$HOI \xrightarrow{h\nu} I + OH$	Sander et al. (2011)
J3	$IO\ (+O_2) \xrightarrow{h\nu} I\ (+\ O_3)$	Sander et al. (2011)
J4	$OIO \xrightarrow{h\nu} I + O_2$	Sander et al. (2011)
J5	$INO \xrightarrow{h\nu} I + NO$	Sander et al. (2011)
J6	$INO_2 \xrightarrow{h\nu} I + NO_2$	Sander et al. (2011)
J7	$INO_3 \xrightarrow{h\nu} I + NO_3$	Sander et al. (2011)
J8	$I_2O_2 \xrightarrow{h\nu} I + OIO$	~~Gómez Martín et al. (2005), Spietz et al. (2005)~~ Gómez Martín et al. (2005); Spietz et al. (2005)
J9	$CH_3I \xrightarrow{h\nu} I$	Sander et al. (2011)
J10	$CH_2I_2 \xrightarrow{h\nu} 2I$	Sander et al. (2011)
J11	$CH_2ICl \xrightarrow{h\nu} I + Cl$	Sander et al. (2011)
J12	$CH_2IBr \xrightarrow{h\nu} I + Br$	Sander et al. (2011)
J13	$I_2O_4 \xrightarrow{h\nu} 2OIO$	see caption
J14	$I_2O_3 \xrightarrow{h\nu} OIO + IO$	~~Gómez Martín et al. (2005), Spietz et al. (2005)~~ Gómez Martín et al. (2005); Spietz et al. (2005)
J15	$CHBr_3 \xrightarrow{h\nu} 3Br$	Sander et al. (2011)
J16	$Br_2 \xrightarrow{h\nu} 2Br$	Sander et al. (2011)
J17	$BrO\ (+O_2) \xrightarrow{h\nu} Br\ (+O_3)$	Sander et al. (2011)
J18	$HOBr \xrightarrow{h\nu} Br + OH$	Sander et al. (2011)
J19	$BrNO_2 \xrightarrow{h\nu} Br + NO_2$	Sander et al. (2011)
J20	$BrNO_3 \xrightarrow{h\nu} Br + NO_3$	Sander et al. (2011)
J21	$BrNO_3 \xrightarrow{h\nu} BrO + NO_2$	Sander et al. (2011)
J22	$CH_2Br_2 \xrightarrow{h\nu} 2Br$	Sander et al. (2011)
J23	$BrCl \xrightarrow{h\nu} Br + Cl$	Sander et al. (2011)
J24	$Cl_2 \xrightarrow{h\nu} 2Cl$	Sander et al. (2011)
J25	$ClO\ (+O_2) \xrightarrow{h\nu} Cl\ (+O_3)$	Sander et al. (2011)
J26	$OClO\ (+O_2) \xrightarrow{h\nu} ClO\ (+O_3)$	Sander et al. (2011)
J27	$Cl_2O_2 \xrightarrow{h\nu} Cl + ClOO$	Sander et al. (2011)
J28	$ClNO_2 \xrightarrow{h\nu} Cl + NO_2$	Sander et al. (2011)
J29	$ClNO_3 \xrightarrow{h\nu} Cl + NO_3$	Sander et al. (2011)
J30	$ClNO_3 \xrightarrow{h\nu} ClO + NO_2$	Sander et al. (2011)
J31	$HOCl \xrightarrow{h\nu} Cl + OH$	Sander et al. (2011)
J32	$ClOO \xrightarrow{h\nu} Cl$	Sander et al. (2011)
J33	$CH_3Cl \xrightarrow{h\nu} Cl + CH_3O_2,$	Sander et al. (2011)
J34	$CH_3Cl_2 \xrightarrow{h\nu} 2Cl$	Sander et al. (2011)

Table 6. Bimolecular halogen reactions included in scheme. This includes reactions from previous updates to descriptions of halogen chemistry in GEOS-Chem ~~(Parrella et al. (2012); Eastham et al. (2014); Schmidt et al. (2016); ?)~~(Eastham et al., 2014; Parrella et al., 2012; Schmidt et al., 2016; Sherwen et al., 2016a), and those described in Section 2. These are given in the Arrhenius form with the rate equal to $A \cdot \exp\left(\frac{-Ea}{RT}\right)$. Unknown values are represented by a ~~–~~dash and these set to zero in the model, reducing the exponent to 1. The bi-molecular reactions with an M above the arrow represent termolecular reactions where the pressure dependence is not known or are uni-molecular decomposition reactions. Abbreviations for tracers are expanded in footnote 3.

Rxn ID	Reaction	A $\mathrm{cm^3\ molecules^{-1}\ s^{-1}}$	$-Ea/R$ K	Citation
M1	$I + O_3 \rightarrow IO + O_2$	$2.10\text{x}10^{-11}$	-830	Atkinson et al. (2007)
M2	$I + HO_2 \rightarrow HI + O_2$	$1.50\text{x}10^{-11}$	-1090	Sander et al. (2011)
M3	$I_2 + OH \rightarrow HOI + I$	$2.10\text{x}10^{-10}$	–	Atkinson et al. (2007)
M4	$HI + OH \rightarrow I + H_2O$	$1.60\text{x}10^{-11}$	440	Atkinson et al. (2007)
M5	$HOI + OH \rightarrow IO + H_2O$	$5.00\text{x}10^{-12}$	–	Riffault et al. (2005)
M6	$IO + HO_2 \rightarrow HOI + O_2$	$1.40\text{x}10^{-11}$	540	Atkinson et al. (2007)
M7	$IO + NO \rightarrow I + NO_2$	$7.15\text{x}10^{-12}$	300	Atkinson et al. (2007)
M8	$HO + CH_3I \rightarrow H_2O + I$	$4.30\text{x}10^{-12}$	-1120	Atkinson et al. (2008)
M9	$INO + INO \rightarrow I_2 + 2NO$	$8.40\text{x}10^{-11}$	-2620	Atkinson et al. (2007)
M10	$INO_2 + INO_2 \rightarrow I_2 + 2NO_2$	$4.70\text{x}10^{-12}$	-1670	Atkinson et al. (2007)
M11	$I_2 + NO_3 \rightarrow I + INO_3$	$1.50\text{x}10^{-12}$	–	Atkinson et al. (2007)
M12	$INO_3 + I \rightarrow I_2 + NO_3$	$9.10\text{x}10^{-11}$	-146	Kaltsoyannis and Plane (2008)
M13	$I + BrO \rightarrow IO + Br$	$1.20\text{x}10^{-11}$	–	Sander et al. (2011)
M14	$IO + Br \rightarrow I + BrO$	$2.70\text{x}10^{-11}$	–	Bedjanian et al. (1997)
M15	$IO + BrO \rightarrow Br + I + O_2$	$3.00\text{x}10^{-12}$	510	Atkinson et al. (2007)
M16	$IO + BrO \rightarrow Br + OIO$	$1.20\text{x}10^{-11}$	510	Atkinson et al. (2007)
M17	$OIO + OIO \rightarrow I_2O_4$	$1.50\text{x}10^{-10}$	–	Gómez Martín et al. (2007)
M18	$OIO + NO \rightarrow NO_2 + IO$	$1.10\text{x}10^{-12}$	542	Atkinson et al. (2007)
M19	$IO + IO \rightarrow I + OIO$	$2.16\text{x}10^{-11}$	180	Atkinson et al. (2007)
M20	$IO + IO \rightarrow I_2O_2$	$3.24\text{x}10^{-11}$	180	Atkinson et al. (2007)
M21	$IO + OIO \xrightarrow{M} I_2O_3$	$1.50\text{x}10^{-10}$	–	Gómez Martín et al. (2007)
M22	$I_2O_2 \xrightarrow{M} IO + IO$	$1.00\text{x}10^{12}$	-9770	Ordóñez et al. (2012)
M23	$I_2O_2 \xrightarrow{M} OIO + I$	$2.50\text{x}10^{14}$	-9770	Ordóñez et al. (2012)
M24	$I_2O_4 \xrightarrow{M} 2OIO$	$3.80\text{x}10^{-2}$	–	Kaltsoyannis and Plane (2008)
M25	$INO_2 \xrightarrow{M} I + NO_2$	$9.94\text{x}10^{17}$	-11859	~~(McFiggans et al., 2000)~~ McFiggans et al. (2000)
M26	$INO_3 \xrightarrow{M} IO + NO_2$	$2.10\text{x}10^{15}$	-13670	Kaltsoyannis and Plane (2008)
M27	$IO + ClO \rightarrow I + OClO$	$2.59\text{x}10^{-12}$	280	Atkinson et al. (2007)
M28	$IO + ClO \rightarrow I + Cl + O_2$	$1.18\text{x}10^{-12}$	280	Atkinson et al. (2007)
M29	$IO + ClO \rightarrow ICl + O_2$	$9.40\text{x}10^{-13}$	280	Atkinson et al. (2007)
M30	$Cl + HCOOH \rightarrow HCl + CO2 + H_2O$	$2.00\text{x}10^{-13}$	-	Sander et al. (2011)
M31	$Cl + CH_3O_2 \rightarrow ClO + CH_2O + HO_2(\star)$	$1.60\text{x}10^{-10}$	-	Sander et al. (2011)
M32	$Cl + CH_3OOH \rightarrow HCl + CH_3O_2$	$5.70\text{x}10^{-11}$	-	Sander et al. (2011)
M33	$Cl + C_2H_6 \rightarrow HCl + C_2H_5O_2$	$7.20\text{x}10^{-11}$	-70	Sander et al. (2011)

Table 6. Continued.

Rxn ID	Reaction	A cm^3 molecules^{-1} s^{-1}	$-Ea/R$ K	Citation
M42	$CHBr_3$ + OH → 3Br + CO	1.35x10^{-12}	-600	Sander et al. (2011)
M43	CH_2Br_2 + OH → 2Br + CO	2.00x10^{-12}	-840	Sander et al. (2011)
M44	CH_3Br + OH → 3Br + CO	2.35x10^{-12}	-1300	Sander et al. (2011)
M45	Br + O_3 → BrO + O_2	1.60x10^{-11}	-780	Sander et al. (2011)
M46	Br + CH_2O → HO_2 + CO	1.70x10^{-11}	-800	Sander et al. (2011)
M47	Br + HO_2 → HBr + O_2	4.80x10^{-12}	-310	Sander et al. (2011)
M48	Br + CH_3CHO → CH3CO$_3$	1.30x10^{-11}	-360	Atkinson et al. (2007)
M49	Br + $(CH_3)_2CO$ → CH3C(O)CH$_2$OO	1.66x10^{-10}	-7000	King et al. (1970)
M50	Br + C_2H_6 → C2H5OO	2.36x10^{-10}	-6411	Seakins et al. (1992)
M51	Br + C_3H_8 → C3H7OO	8.77x10^{-11}	-4330	Seakins et al. (1992)
M52	Br + $BrNO_3$ → Br_2 + NO_3	4.90x10^{-11}	0	Orlando and Tyndall (1996)
M53	Br + NO_3 → BrO + NO_2	1.60x10^{-11}	0	Sander et al. (2011)
M54	HBr + OH → Br + H_2O	5.50x10^{-12}	200	Sander et al. (2011)
M55	BrO + NO → Br + NO_2	8.80x10^{-12}	260	Sander et al. (2011)
M56	BrO + OH → Br + HO_2	1.70x10^{-11}	250	Sander et al. (2011)
M57	BrO + BrO → 2Br + O_2	2.40x10^{-12}	40	Sander et al. (2011)
M58	BrO + BrO → Br_2 + O_2	2.80x10^{-14}	860	Sander et al. (2011)
M59	BrO + HO_2 → HOBr + O_2	4.50x10^{-12}	460	Sander et al. (2011)
M60	Br_2 + OH → HOBr + Br	2.10x10^{-11}	240	Sander et al. (2011)
M61	Cl + ALK4 → HCl + R4O2	2.05x10^{-10}	-	Atkinson et al. (2006)
M62	Cl + PRPE → HCl + PO2	3.60x10^{-12}	-	Atkinson et al. (2006)
M63	CH_3Cl + Cl → CO + 2HCl + HO_2	2.17x10^{-11}	-1130	Sander et al. (2011)
M64	Cl + H_2O_2 → HO_2 + HCl	1.10x10^{-11}	-980	Sander et al. (2011)
M65	Cl + HO_2 → O_2 + HCl	1.40x10^{-11}	270	Sander et al. (2011)
M66	Cl + HO_2 → OH + ClO	3.60x10^{-11}	-375	Sander et al. (2011)
M67	Cl + O_3 → ClO + O_2	2.30x10^{-11}	-200	Sander et al. (2011)
M68	$ClNO_3$ + Cl → Cl_2 + NO_3	6.50x10^{-12}	135	Sander et al. (2011)
M69	ClO + ClO → Cl_2 + O_2	1.00x10^{-12}	-1590	Sander et al. (2011)
M70	ClO + ClO → OClO + Cl	3.50x10^{-13}	-1370	Sander et al. (2011)
M71	ClO + ClO → Cl + ClOO	3.00x10^{-11}	-2450	Sander et al. (2011)
M72	ClO + HO_2 → O_2 + HOCl	2.60x10^{-12}	290	Sander et al. (2011)
M73	ClO + NO → Cl + NO_2	6.40x10^{-12}	290	Sander et al. (2011)
M74	ClOO + Cl → 2ClO	1.20x10^{-11}	-	Sander et al. (2011)
M75	ClOO + Cl → Cl_2 + O_2	2.30x10^{-10}	-	Sander et al. (2011)
M76	MO2 + ClO → ClOO + HO_2 + CH2O	3.30x10^{-12}	-115	Sander et al. (2011)
M77	OH + CH_3Cl → Cl + HO_2 + H_2O	3.90x10^{-12}	-1411	Sander et al. (2011)
M78	OH + Cl_2 → HOCl + Cl	2.60x10^{-12}	-1100	Sander et al. (2011)
M79	OH + Cl_2O_2 → HOCl + ClOO	6.00x10^{-13}	670	Sander et al. (2011)
M80	OH + $ClNO_2$ → HOCl + NO_2	2.40x10^{-12}	-1250	Sander et al. (2011)
M81	OH + $ClNO_3$ → HOCl + NO_3	1.20x10^{-12}	-330	Sander et al. (2011)
M82	OH + ClO → HCl + O_2	6.00x10^{-13}	230	Sander et al. (2011)
M83	OH + ClO → HO_2 + Cl	7.40x10^{-12}	270	Sander et al. (2011)
M84	OH + HCl → H_2O + Cl	1.80x10^{-12}	-250	Sander et al. (2011)
M85	OH + HOCl → H_2O + ClO	3.00x10^{-12}	-500	Sander et al. (2011)
M86	OH + OClO → HOCl + O_2	1.50x10^{-12}	600	Sander et al. (2011)

Table 7. Termolecular halogen reactions included in the scheme. This includes reactions from previous updates to halogen chemistry in GEOS-Chem ~~(Eastham et al., 2014; Parrella et al., 2012; Schmidt et al., 2016; ?)~~(Eastham et al., 2014; Parrella et al., 2012; Schmidt et al., 2016; Sherwe and those detailed in section 2. The lower pressure limit rate (k_0) is given by: $A_0 \cdot (\frac{300}{T})^x$. The high pressure limit is given by k_∞. Fc characterises the fall off curve of the reaction as described by Atkinson et al. (2007).

Rxn ID	Reaction	A_0 cm^6 molecules^{-2} s^{-1}	x	k_∞ cm^3 molecules^{-1} s^{-1}	Fc	Citation
T1	$I + NO \xrightarrow{M} INO$	1.80x10^{-32}	1	1.70x10^{-11}	0.6	Atkinson et al. (2007)
T2	$I + NO_2 \xrightarrow{M} INO_2$	3.00x10^{-31}	1	6.60x10^{-11}	0.63	Atkinson et al. (2007)
T3	$IO + NO_2 \xrightarrow{M} INO_3$	7.70x10^{-31}	5	1.60x10^{-11}	0.4	Atkinson et al. (2007)
T4	$Br + NO_2 \xrightarrow{M} BrNO_2$	4.20x10^{-31}	2.4	2.70x10^{-11}	0.6	Sander et al. (2011)
T5	$BrO + NO_2 \xrightarrow{M} BrNO_3$	5.20x10^{-31}	3.2	6.90x10^{-12}	0.6	Sander et al. (2011)
T5	$BrO + NO_2 \xrightarrow{M} BrNO_3$	5.20x10^{-31}	3.2	6.90x10^{-12}	0.6	Sander et al. (2011)
T6	Cl + ~~ALK4~~ PRPE $\xrightarrow{M}$ HCl + R4O2	4.00x10^{-28}	0	2.80x10^{-10}	0.6	Atkinson et al. (2006)
T7	$Cl + O_2 \xrightarrow{M} ClOO$	2.20x10^{-33}	0	1.80x10^{-10}(*)	0.6	Sander et al. (2011)
T8	$Cl_2O_2 \xrightarrow{M} 2ClO$	9.30x10^{-6}	2	1.74x10^{15}(*)	0.6	Sander et al. (2011)
T9	$ClO + ClO \xrightarrow{M} Cl_2O_2$	1.60x10^{-21}	2	3.00x10^{-12}(*)	0.6	Sander et al. (2011)
T10	$ClO + NO_2 \xrightarrow{M} ClNO_3$	1.80x10^{-31}	1.9	1.50x10^{-11}(*)	0.6	Sander et al. (2011)
T11	$ClOO \xrightarrow{M} Cl + O_2$	3.30x10^{-9}	0	2.73x10^{14}(*)	0.6	Sander et al. (2011)

Table footnote: . (*) k_∞(T) for reactions T7-T11 have a form of $k_\infty(T) = k\infty(\frac{T}{300})^{-m}$, where m = 3.1, 4.5, 4.5, 3.4 and 3.1 respectively. Abbreviations for tracers are expanded in footnote 3.

Table 8. Halogen multiphase reactions and reactive uptake coefficients (γ).

ID	Reaction	Reactive uptake coefficient (γ)	Note	Reference
1	$\mathrm{HCl} \rightarrow \mathrm{Cl^-(SSA)}$	$4.4\times10^{-6}\,\exp(2989\,\mathrm{K}/T)$	Sea salt only	Ammann et al. (2013)
2	$\mathrm{HBr} \rightarrow \mathrm{Br^-(SSA)}$	$1.3\times10^{-8}\,\exp(4290\,\mathrm{K}/T)$	Sea salt only	Ammann et al. (2013)
3	$\mathrm{HI} \rightarrow \mathrm{I(aerosol)}$	0.1		
4	$\mathrm{ClNO_3} \rightarrow \mathrm{HOCl} + \mathrm{HNO_3}$	0.024	Hydrolysis	Deiber et al. (2004)
5	$\mathrm{BrNO_3} \rightarrow \mathrm{HOBr} + \mathrm{HNO_3}$	0.02	Hydrolysis	Deiber et al. (2004)
6	$\mathrm{INO_3} \rightarrow 0.85\mathrm{ICl} + 0.15\mathrm{IBr} + \mathrm{HNO_3}$	0.01	Sea salt only	
7	$\mathrm{INO_2} \rightarrow 0.85\mathrm{ICl} + 0.15\mathrm{IBr} + \mathrm{HNO_3}$	0.02	Sea salt only	
8	$\mathrm{HOBr} + \mathrm{Cl^-(aq)} \rightarrow \mathrm{BrCl}$	See ~~text~~ appendix section B3		Ammann et al. (2013)
9	$\mathrm{HOBr} + \mathrm{Br^-(aq)} \rightarrow \mathrm{Br_2}$	See ~~text~~ appendix section B3		Ammann et al. (2013)
10	$\mathrm{HOI} \rightarrow 0.85\mathrm{ICl} + 0.15\mathrm{IBr}$	0.01	Sea salt only	
11	$\mathrm{ClNO_3} + \mathrm{Br^-(aq)} \rightarrow \mathrm{BrCl} + \mathrm{HNO_3}$	See ~~text~~ appendix section B3		Ammann et al. (2013)
12	$\mathrm{O_3} + \mathrm{Br^-(aq)} \rightarrow \mathrm{HOBr}$	See ~~text~~ appendix section B3		Ammann et al. (2013)
13	$\mathrm{I_2O_2} \rightarrow \mathrm{I(aerosol)}$	0.02		
14	$\mathrm{I_2O_3} \rightarrow \mathrm{I(aerosol)}$	0.02		
15	$\mathrm{I_2O_4} \rightarrow \mathrm{I(aerosol)}$	0.02		

Table 9. Henry's law coefficients and molar heats of formation of iodine species. Where Henry's law constant equals infinity a very large values is used within the model ($1 \times 10^{20}\ \mathrm{M\,atm^{-1}}$). The $\mathrm{INO_2}$ Henry's law constant is assumed equal to that of $\mathrm{BrNO_3}$, from Sander (2015), by analogy. For $\mathrm{I_2O_X}$ (~~$x = 2,3,4$~~X=2,3,4) a Henry's law constant of infinity is assumed by analogy with $\mathrm{INO_3}$. ($*$) Effective Henry's law of HX is calculated for acid conditions through $K^*_H(T) = K_H(T) \times (1 + \frac{K_a}{[\mathrm{H}+]})$. A pH of 4.5 is assumed for a typical cloud droplet.

Species	Henry's Law Constant (H) at 298K $\mathrm{M\,atm^{-1}}$	Reference	$\frac{\mathrm{d(ln\,H)}}{\mathrm{d(1/T)}}$ K	Reference
HOBr	$6.1x10^{3}$	Frenzel et al. (1998)	$6.01x10^{3}$	McGrath and Rowland (1994)
HBr(*)	$7.1x10^{13}$	Frenzel et al. (1998)	$1.02x10^{4}$	Schweitzer et al. (2000)
$\mathrm{BrNO_2}$	0.3	Frenzel et al. (1998)	-	-
$\mathrm{BrNO_3}$	∞	Sander (2015)	-	-
$\mathrm{Br_2}$	0.76	Dean (1992)	$3.72x10^{3}$	Dean (1992)
HOCl	$6.5x10^{3}$	Sander (2015)	$5.9x10^{3}$	Sander (2015)
HCl(*)	$7.1x10^{15}$	Sander (2015)	$5.9x10^{3}$	Sander (2015)
$\mathrm{ClNO_3}$	∞	Sander (2015)	-	-
BrCl	0.97	Sander (2015)	-	-
ICl	$1.11x10^{2}$	Sander (2015)	$2.11x10^{3}$	Sander et al. (2006)
IBr	$2.43x10^{1}$	Sander (2015)	$4.92x10^{3}$	Sander et al. (2006)
HOI	$1.53x10^{4}$	Sander (2015)	$8.37x10^{3}$	Sander et al. (2006)
HI (*)	$7.43x10^{13}$	Sander (2015)	$3.19x10^{3}$	Sander et al. (2006)
$\mathrm{INO_3}$	∞	Vogt et al. (1999)	$3.98x10^{4}$	Kaltsoyannis and Plane (2008)
$\mathrm{I_2O_2}$	∞	see caption text	$1.89x10^{4}$	Kaltsoyannis and Plane (2008)
$\mathrm{I_2}$	2.63	Sander (2015)	$7.51x10^{3}$	Sander et al. (2006)
$\mathrm{INO_2}$	0.3	see caption text	$7.24x10^{3}$	Sander et al. (2006)
$\mathrm{I_2O_3}$	∞	see caption text	$7.70x10^{3}$	Kaltsoyannis and Plane (2008)
$\mathrm{I_2O_4}$	∞	see caption text	$1.34x10^{4}$	Kaltsoyannis and Plane (2008)

Table 10. Tropospheric burden of species and families with ("Cl+Br+I") and without halogens ("NOHAL"), and % change. Burdens are considered in elemental terms (e.g Gg S/N/C) and species masses for OH, HO_2, H_2O_2 and O_3 Families are defined in footnote 3.

	"NOHAL"	"Cl+Br+I"	% Δ
NO_3	~~1.23~~ 1.49	~~1.23~~ 1.14	~~-17.8~~ -23.57
~~O_3 415843.25 355123.69 -14.6~~ N_2O_5	9.38	~~8.02~~ 7.48	~~-14.5~~ -20.22
~~H_2O_2 3229.09 2828.80 -12.4~~ C_2H_6	3258.84	~~2855.31~~ 2628.05	~~-12.4~~ -19.36
O_3	415843.25	338708.23	-18.55
HNO_4	19.84	~~17.63~~ 16.84	~~-11.1~~ -15.14
H_2O_2	3229.09	2764.27	-14.39
C_3H_8	609.76	~~550.68~~ 524.31	~~-9.7~~ -14.01
≥C4 alkanes	488.35	~~441.96~~ 429.02	~~-9.5~~ -12.15
~~HO_2~~ PPN	~~27.55~~ 15.82	~~25.37~~ 14.31	~~-7.9~~ -9.55
~~PPN~~ HO_2	~~15.82~~ 27.55	~~14.65~~ 24.95	~~-7.4~~ -9.44
~~PAN~~ OH	~~202.89~~ 0.28	~~194.70~~ 0.26	~~-4.0~~ -6.31
$CH_3C(O)CH_3$	7533.51	~~7289.92~~ 7085.23	~~-3.2~~ -5.95
~~OH~~ PAN	~~0.28~~ 202.89	~~0.27~~ 191.57	~~-2.9~~ -5.58
NO_2	123.53	~~120.35~~ 118.52	~~-2.6~~ -4.06
CH_2O	389.55	~~380.88~~ 375.42	~~-2.2~~ -3.63
~~PMN~~ NO_x	~~0.68 0.67 -1.8 NO_X~~ 171.01	~~168.15~~ 165.75	~~-1.7~~ -3.07
SO_4 on SSA	1.97	1.94	~~-1.6~~ -1.74
~~NH_3~~ PMN	~~126.61~~ 0.68	~~126.28~~ 0.67	~~-0.3~~ -1.27
NO~~$_Y$~~$_y$	1374.56	~~1371.59~~ 1367.26	~~-0.2~~ -0.53
~~Acetaldehyde~~ NO	~~184.93~~ 47.48	~~184.59~~ 47.24	~~-0.2~~ -0.50
NH~~$_4$~~$_3$	~~270.93~~ 126.61	~~271.43~~ 126.42	~~0.2~~ -0.15
~~>C3 ketones~~ NH_4	~~186.99~~ 270.93	~~188.11~~ 270.88	~~0.6~~ -0.02
SO~~$_X$~~$_x$	398.98	~~401.59~~ 400.80	~~0.7~~ 0.46
SO_4	397.01	~~399.65~~ 398.86	~~0.7~~ 0.47
~~NO~~ PROPNN	~~47.48~~ 7.46	~~47.80~~ 7.55	~~0.7~~ 1.22
~~≥C3 alkenes~~ Acetaldehyde	~~97.93~~ 184.93	~~98.79~~ 187.23	~~0.9~~ 1.25
~~PROPNN~~ $CH_3O_2NO_2$	~~7.46~~ 13.80	~~7.55~~ 14.03	~~1.1~~ 1.63
HNO_3	463.49	~~470.69~~ 471.53	~~1.6~~ 1.74
~~VOCs~~ >C3 ketones	~~148193.29~~ 186.99	~~151283.71~~ 190.49	~~2.1~~ 1.87
≥~~C4 alkylnitrates~~ C3 alkenes	~~64.60~~ 97.93	~~65.99~~ 100.28	~~2.2~~ 2.40
SO_2	286.11	~~294.17~~ 298.96	~~2.8~~ 4.49
~~CO~~ VOCs	~~134654.88~~ 148193.29	~~138477.76~~ 155234.49	~~2.8~~ 4.75
MMN	3.15	~~3.26~~ 3.32	~~3.2~~ 5.17
~~CH_3NO~~ ≥C4 alkylnitrates	64.60	68.00	5.26
HNO_2	~~13.80~~ 2.76	~~14.25~~ 2.92	~~3.3~~ 5.84
~~Isoprene~~ CO	~~788.55~~ 134654.88	~~815.73~~ 142877.06	~~3.4~~ 6.11
~~HNO_2~~ Isoprene	~~2.76~~ 788.55	~~2.92~~ 837.40	~~5.5~~ 6.19
ISOPN	0.65	~~0.69~~ 0.71	~~6.2~~ 9.40